AD-A079 525 WASHINGTON UNIV SEATTLE DEPT OF OCEANOGRAPHY F/G 20/4
INITIAL-VALUE PROBLEMS IN STRATIFIED SHEAR FLOWS.(U)
1979 J E BRADT AFOSR-78-3655
UNCLASSIFIED AFOSR-TR-79-1358 NL

1 OF 2
AD
A079525

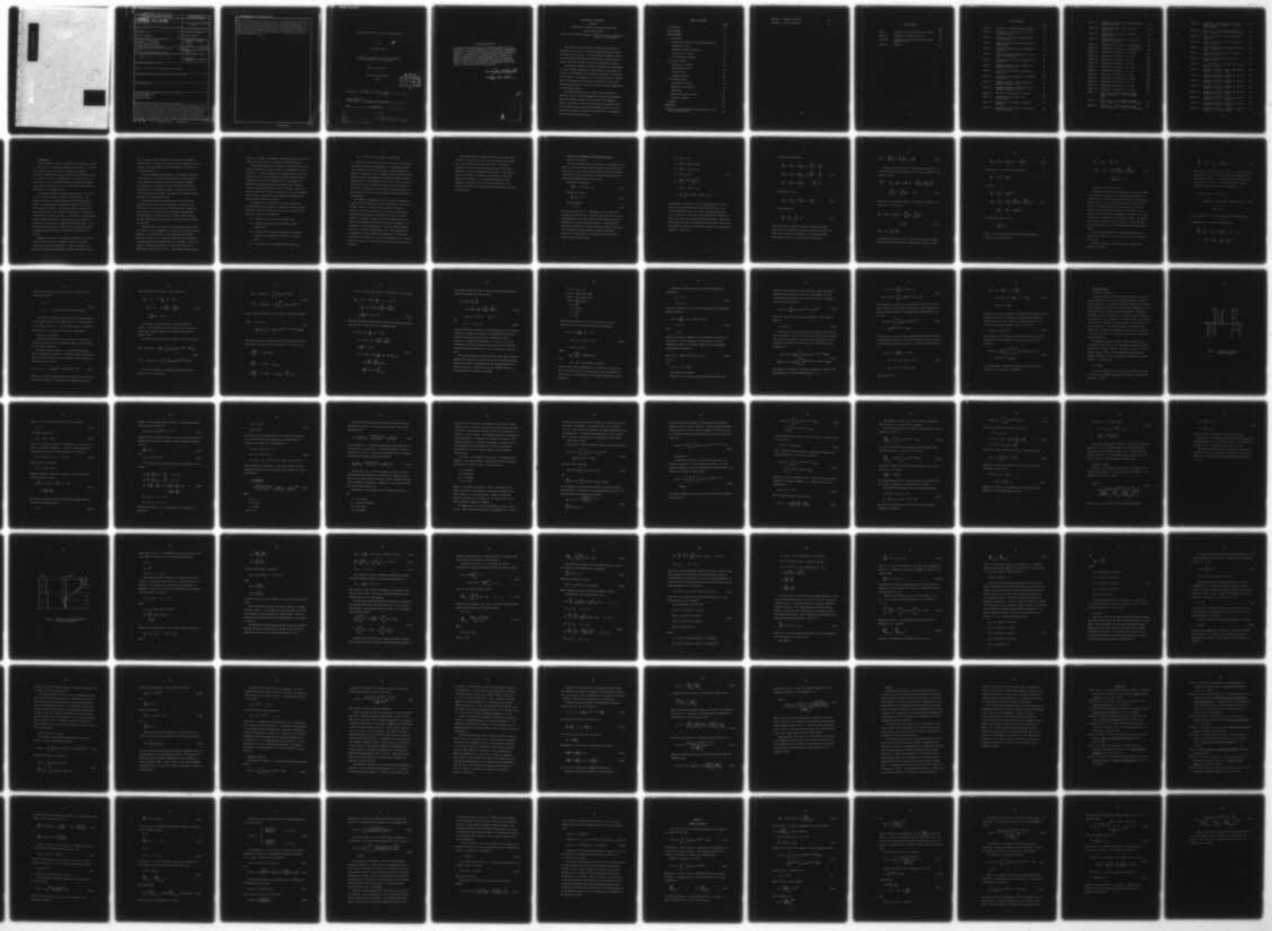

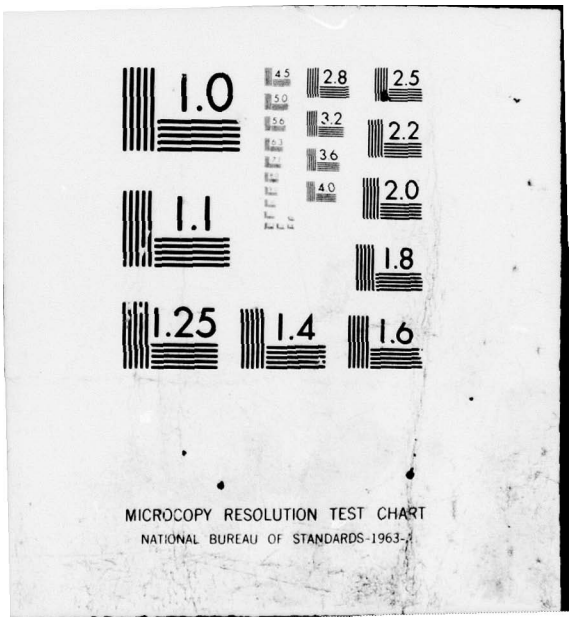
1.0
1.1
1.25
1.4
1.6
1.8
2.0
2.2
2.5
2.8
3.2
3.6
4.0
4.5
5.0
5.6
MICROCOPY RESOLUTION TEST CHART
NATIONAL BUREAU OF STANDARDS-1963-A

UNCLASSIFIED
SECURITY CLASSIFICATION OF THIS PAGE (When Data Entered)

REPORT DOCUMENTATION PAGE	READ INSTRUCTIONS BEFORE COMPLETING FORM
1. REPORT NUMBER: AFOSR-TR-79-1358	2. GOVT ACCESSION NO. / 3. RECIPIENT'S CATALOG NUMBER
4. TITLE (and Subtitle): INITIAL-VALUE PROBLEMS IN STRATIFIED SHEAR FLOWS	5. TYPE OF REPORT & PERIOD COVERED: INTERIM
	6. PERFORMING ORG. REPORT NUMBER
7. AUTHOR(s): JERRE EUGENE BRADT	8. CONTRACT OR GRANT NUMBER(s): AFOSR-78-3655
9. PERFORMING ORGANIZATION NAME AND ADDRESS: UNIVERSITY OF WASHINGTON, DEPARTMENT OF OCEANOGRAPHY, SEATTLE, WASHINGTON 98195	10. PROGRAM ELEMENT, PROJECT, TASK AREA & WORK UNIT NUMBERS: 2307A2, A2, 61102F
11. CONTROLLING OFFICE NAME AND ADDRESS: AIR FORCE OFFICE OF SCIENTIFIC RESEARCH/NA, BLDG 410, BOLLING AIR FORCE BASE, D C 20332	12. REPORT DATE: 1979 / 13. NUMBER OF PAGES: 146
14. MONITORING AGENCY NAME & ADDRESS(if different from Controlling Office): Doctoral thesis,	15. SECURITY CLASS. (of this report): UNCLASSIFIED / 15a. DECLASSIFICATION/DOWNGRADING SCHEDULE

16. DISTRIBUTION STATEMENT (of this Report)

Approved for public release; distribution unlimited.

17. DISTRIBUTION STATEMENT (of the abstract entered in Block 20, if different from Report)

18. SUPPLEMENTARY NOTES

19. KEY WORDS (Continue on reverse side if necessary and identify by block number)

STRATIFIED SHEAR FLOWS
STABILITY THEORY
EIGENVALUES PROBLEM

20. ABSTRACT (Continue on reverse side if necessary and identify by block number)

The question of the stability of steady state solutions in geophysical fluid flows is addressed through qualitative analysis and quantitative examples. The inviscid linear stability theory of stratified shear flows and the solution of the stability problem using normal modes and Fourier-Laplace transforms are discussed. Two numerical examples are used to illustrate the relationship of various physical parameters to the stability of the system and to trace the development of the instability of the instability for short, intermediate and long times. The examples are (1) are two layer fluid of infinite extent with

DD FORM 1 JAN 73 1473 EDITION OF 1 NOV 65 IS OBSOLETE

370 280

UNCLASSIFIED

application to the air-sea interface and (2) a two-layer fluid having a free surface and finite depth with application to a salt wedge estuary. The initial-value problem is solved using a power series expansion for short times, superposition of modes for intermediate times and asymptotic analysis for long times. The asymptotic expansion applicable in non-conservative systems is compared with the approximate solution using ray techniques, which are valid in conservative systems, and analytic continuation of the eigenvalues into the complex wavenumber plane.

Initial-Value Problems in Stratified Shear Flows

by

Jerre Eugene Bradt

A dissertation submitted in partial fulfillment
of the requirements for the degree of

Doctor of Philosophy

University of Washington

1979

Approved by _____

Program Authorized
to Offer Degree Department of Oceanography

Date 6 August 1979

Doctoral Dissertation

In presenting this dissertation in partial fulfillment of the requirements for the Doctoral degree at the University of Washington, I agree that the Library shall make its copies freely available for inspection. I further agree that extensive copying of this dissertation is allowable only for scholarly purposes. Requests for copying or reproduction of this dissertation may be referred to University Microfilms, 300 North Zeeb Road, Ann Arbor, Michigan 48106, to whom the author has granted "the right to reproduce and sell (a) copies of the manuscript in microform and/or (b) printed copies of the manuscript made from microform."

Signature Jerre E. Bradt

Date Aug 16, 1979

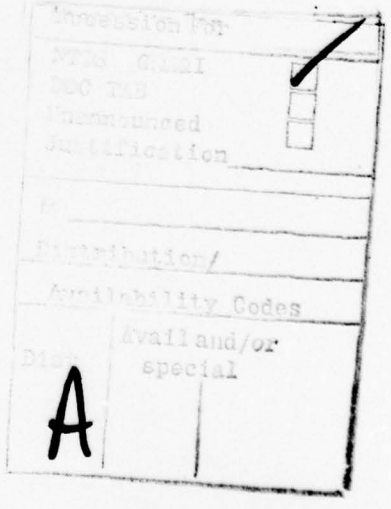

University of Washington

Abstract

Initial-Value Problems in Stratified Shear Flows

by Jerre Eugene Bradt

Chairperson of Supervisory Committee: Professor William O. Criminale, Jr.
Department of Oceanography

The question of the stability of steady state solutions in geophysical fluid flows is addressed through qualitative analysis and quantitative examples. The inviscid linear stability theory of stratified shear flows and the solution of the stability problem using normal modes and Fourier-Laplace transforms are discussed.

Two numerical examples are used to illustrate the relationship of various physical parameters to the stability of the system and to trace the development of the instability for short, intermediate and long times. The examples are (1) a two layer fluid of infinite extent with application to the air-sea interface and (2) a two-layer fluid having a free surface and finite depth with application to a salt wedge estuary.

The initial-value problem is solved using a power series expansion for short times, superposition of modes for intermediate times and asymptotic analysis for long times. The asymptotic expansion applicable in non-conservative systems is compared with the approximate solution using ray techniques, which are valid in conservative systems, and analytic continuation of the eigenvalues into the complex wavenumber plane.

TABLE OF CONTENTS

LIST OF TABLES

LIST OF FIGURES

Acknowledgements

I would like to express my sincere appreciation to Professor William O. Criminale, Jr. for the continued guidance, support and encouragement in bringing this work to successful completion.

I am also particularly grateful to my friends and fellow students who have offered suggestions, advice and encouragement throughout my studies.

This research was supported by the Air Force Office of Scientific Research under Grant AFSOR 74-2579.

1. Introduction

In the theoretical study of geophysical fluid flows an attempt is made to find a steady-state solution to the problem. The steady-state solution may be the result of solving the governing equations expressing the balance of forces in the physical problem or it may be the result of considering time averaged motion. In either case it is of considerable interest to know if the steady-state solution persists or if the flow is dynamically unstable and evolves into a time dependent flow.

The technique employed to answer this question is the linear theory of the hydrodynamic stability of parallel flows. The problem is posed as a combined boundary-value and initial-value problem. A time dependent perturbation expansion is made about the steady-state solution. The perturbations are assumed to be small compared to the mean flow and the equations are linearized. Traditionally the emphasis has been on the solution of the boundary-value or eigenvalue problem. The eigenvalues are evaluated to determine if the system has an exponentially growing mode. If an exponentially growing mode is found, then the system is unstable to small perturbations and the steady-state solution does not persist.

Completing the solution by solving the initial-value problem is more difficult because it requires solving for the eigen-functions as well as the eigenvalues. For some problems it is possible to determine the eigenvalues without being able to solve

for the eigenfunctions. However, the solution to the initial value problem is of interest because it not only indicates that the solution is time dependent, but also determines the structure of the time dependence.

For most geophysical fluid flows it is possible to formulate a very general set of equations describing the balance of forces and the applicable boundary conditions and initial conditions. The resulting set of equations forms a well-posed mathematical problem, but is analytically insoluble. To overcome this difficulty approximations are made at the expense of limiting the applicability of the resulting solution.

Justification for these approximations and the resulting limitations can be found in the literature. For example, the evaluation of the eigenvalues of a three-dimensional problem has been reduced to the solution of an equivalent two-dimensional problem through a transformation due to Squire (1933), however, the full three-dimensional structure of the initial-value problem is sacrificed.

Simplification of the systems to be considered is the result of the work of many investigators. The use of the linearized Euler equations as an approximation to the linearized Navier-Stokes equations for flows at high Reynolds number and small wavenumbers is demonstrated in work by Case (1961) and Lin (1967). This is an important simplification because it reduces the order of the differential equation to be solved. Drazin (1958, 1961) has shown

that it is possible to approximate continuous density and velocity profiles by discontinuous or piecewise continuous profiles.

The eigenfunctions of the boundary value problem form a set of normal modes which are used as a basis for expanding the initial conditions. In general, however, the eigenfunctions do not form a complete set and it is not possible to expand arbitrary initial conditions as a sum of the eigenfunctions. Case (1960) and Pedlosky (1963) demonstrated that in addition to the discrete spectrum of normal modes there are also continuous spectra of modes arising from the singular solutions of the inviscid differential equations. Evaluation of the initial-value problem must include these solutions to be valid.

Following this it was pointed out by Banks, Drazin and Zaturska (1976) that the modes of a parallel inviscid stratified fluid fall into five classes, some of which may be absent for a given flow. These five classes are:

(1) a finite set of non-singular unstable modes

(2) a conjugate finite set of non-singular damped stable modes

(3) a finite set of singular stable modes, each having a branch point and being the limit of an unstable mode

(4) a discrete set of non-singular stable modes, and

(5) a continuous set of singular stable modes.

The complex nature of stratified shear flows is indicated by the findings of several investigators. It is generally agreed that increasing the stable stratification and the presence of boundaries stabilize the flow. However, Maslowe and Kelly (1971) showed that under some conditions increasing the stable stratification leads to destabilization of the flow. Hazel (1972) and Lalas, Einaudi and Fua (1976) have demonstrated the destabilizing effects of boundaries. Davey (1977) showed that increasing the curvature of the mean velocity profile increases the range of unstable modes.

Two different mathematical models are used to demonstrate features of the stability and initial-value problems. The choice of these examples is dictated by the existence of analytic solutions to demonstrate features of the initial-value problem while maintaining relevance to geophysical flows. The first system is an infinite two-layer flow with uniform velocity and density in each layer and surface tension at the interface. The eigenvalues for this system exhibit a limited range of unstable modes with a definite maximum growth rate. This system is used to demonstrate the three-dimensional development of an initial Gaussian pulse for short time and in the asymptotic limit. Results from this example have application to disturbances of the air-sea interface.

The second system is modeled on features of the salt-wedge estuary. The fluid is of finite vertical extent; bounded above by a free surface and below by a solid wall. The density structure is two layers and the continuous velocity profile is approximated by three piecewise-linear segments. This model is used to investigate the effects of stratification, shear and boundaries on stability. The difference between a correct asymptotic exapnsion of the initial-value problem of a non-conservative system and the approximate ray-mathematics expansion is demonstrated.

2. Initial-Value Problems in Stratified-Shear Flows

Equations of Motion

The initial-value problem corresponds to a description of the motion of the fluid derived from the physical laws governing the motion and the constraints on that motion in the form of boundary conditions and initial conditions. The governing equations for inviscid and incompressible fluid flow are:

Conservation of momentum -

$$\frac{\partial \vec{u}}{\partial t} + \vec{u} \cdot \nabla \vec{u} = \frac{-1}{\rho} \nabla \underline{p} - \nabla \underline{G} \tag{2.1}$$

Conservation of mass -

$$\frac{\partial \rho}{\partial t} + \vec{u} \cdot \nabla \rho = 0 \tag{2.2}$$

Incompressibility -

$$\nabla \cdot \vec{u} = 0 \tag{2.3}$$

The motion is described as a combination of a mean flow plus a perturbation about the mean. The mean quantities of the flow are time independent and for the purpose of this analysis are only a function of the vertical spatial dimension. The perturbation quantities are functions of time and the three spatial dimensions. It is assumed that the mean motion is entirely horizontal. Utilizing these restrictions the variables in the equations of motion take the following form:

$$\vec{u} = (\underline{u}', \underline{v}', \underline{w}')$$

$$\underline{u}' = \bar{\underline{U}}(\underline{z}) + \underline{u}(\underline{x}, \underline{y}, \underline{z}, \underline{t})$$

$$\underline{v}' = \bar{\underline{V}}(\underline{z}) + \underline{v}(\underline{x}, \underline{y}, \underline{z}, \underline{t})$$

$$\underline{w}' = w(\underline{x}, \underline{y}, \underline{z}, \underline{t}) \qquad (2.4)$$

$$\underline{\theta}' = \frac{\bar{\rho}(\underline{z})}{\rho_o} + \frac{\rho(\underline{x}, \underline{y}, \underline{z}, \underline{t})}{\rho_o}$$

$$= \bar{\Theta}(\underline{z}) + \theta(\underline{x}, \underline{y}, \underline{z}, \underline{t})$$

$$p' = \underline{g}/\rho_o \int_{\underline{z}}^{o} \bar{\rho}(\underline{z}')d\underline{z}' + \underline{p}(\underline{x}, \underline{y}, \underline{z}, \underline{t})$$

The equations of motion for the small perturbations on the mean flow are obtained by substituting the functional form of the variables indicated in eq. (2.4) into the governing equations (2.1, 2.2 and 2.3). The terms in the equations are collected by order; the zeroth order terms govern the mean motion. These terms are subtracted to obtain the equations for the higher order terms. The remaining equations are linearized in terms of the perturbation variables. These are:

Conservation of momentum -

$$\left(\frac{\partial}{\partial \underline{t}} + \bar{\underline{U}}\frac{\partial}{\partial \underline{x}} + \bar{\underline{V}}\frac{\partial}{\partial \underline{y}}\right)\underline{u} + \underline{w}\frac{d\bar{\underline{U}}}{d\underline{z}} = -\frac{\partial \underline{p}}{\partial \underline{x}}$$

$$\left(\frac{\partial}{\partial \underline{t}} + \bar{\underline{U}}\frac{\partial}{\partial \underline{x}} + \bar{\underline{V}}\frac{\partial}{\partial \underline{y}}\right)\underline{v} + \underline{w}\frac{d\bar{\underline{V}}}{d\underline{z}} = -\frac{\partial \underline{p}}{\partial \underline{y}} \qquad (2.5)$$

$$\left(\frac{\partial}{\partial \underline{t}} + \bar{\underline{U}}\frac{\partial}{\partial \underline{x}} + \bar{\underline{V}}\frac{\partial}{\partial \underline{y}}\right)\underline{w} = -\frac{\partial \underline{p}}{\partial \underline{z}} - \underline{g}\theta$$

Conservation of mass -

$$\left(\frac{\partial}{\partial \underline{t}} + \bar{\underline{U}}\frac{\partial}{\partial \underline{x}} + \bar{\underline{V}}\frac{\partial}{\partial \underline{y}}\right)\theta + \underline{w}\frac{d\bar{\Theta}}{d\underline{z}} = 0 \qquad (2.6)$$

Incompressibility -

$$\frac{\partial \underline{u}}{\partial \underline{x}} + \frac{\partial \underline{v}}{\partial \underline{y}} + \frac{\partial \underline{w}}{\partial \underline{z}} = 0 \qquad (2.7)$$

These equations are combined to obtain a single differential equation for the vertical perturbation velocity $\underline{w}(\underline{x},\underline{y},\underline{z},\underline{t})$. The first step is to take the divergence of the vector momentum equation which reduces to an equation for the pressure.

$$\nabla^2 \underline{p} = -2\left(\frac{d\bar{\underline{U}}}{d\underline{z}} \frac{\partial}{\partial \underline{x}} + \frac{d\bar{\underline{V}}}{d\underline{z}} \frac{\partial}{\partial \underline{y}}\right) \underline{w} - \underline{g} \frac{\partial \theta}{\partial \underline{z}} \tag{2.8}$$

Another equation involving the Laplacian of the pressure can be derived by taking the Laplacian of the vertical component of the momentum equation.

$$\nabla^2 \frac{\partial \underline{p}}{\partial \underline{z}} = -\left(\frac{\partial}{\partial \underline{t}} + \bar{\underline{U}} \frac{\partial}{\partial \underline{x}} + \bar{\underline{V}} \frac{\partial}{\partial \underline{y}}\right) \nabla^2 \underline{w} - 2\left(\frac{d\bar{\underline{U}}}{d\underline{z}} \frac{\partial}{\partial \underline{x}} + \frac{d\bar{\underline{V}}}{d\underline{z}} \frac{\partial}{\partial \underline{y}}\right) \frac{\partial \underline{w}}{\partial \underline{z}}$$

$$- \left(\frac{d^2\bar{\underline{U}}}{d\underline{z}^2} \frac{\partial}{\partial \underline{x}} + \frac{d^2\bar{\underline{V}}}{d\underline{z}^2} \frac{\partial}{\partial \underline{y}}\right) \underline{w} + \underline{g} \nabla^2 \theta \tag{2.9}$$

Elimination of the pressure between the vertical derivative of eq. (2.8) and eq. (2.9) yields

$$\left(\frac{\partial}{\partial \underline{t}} + \bar{\underline{U}} \frac{\partial}{\partial \underline{x}} + \bar{\underline{V}} \frac{\partial}{\partial \underline{y}}\right) \nabla^2 \underline{w} - \left(\frac{d^2\bar{\underline{U}}}{d\underline{z}^2} \frac{\partial}{\partial \underline{x}} + \frac{d^2\bar{\underline{V}}}{d\underline{z}^2} \frac{\partial}{\partial \underline{y}}\right) \underline{w}$$

$$= - \underline{g} \nabla_h^2 \theta \tag{2.10}$$

Where $\nabla_h^2 = \frac{\partial^2}{\partial \underline{x}^2} + \frac{\partial^2}{\partial \underline{y}^2}$.

To eliminate the density from eq. (2.10) first take the horizontal Laplacian of the equation for the conservation of mass, eq. (2.6)

$$\left(\frac{\partial}{\partial \underline{t}} + \bar{\underline{U}} \frac{\partial}{\partial \underline{x}} + \bar{\underline{V}} \frac{\partial}{\partial \underline{y}}\right) \nabla_h^2 \theta = - \frac{d\bar{\Theta}}{d\underline{z}} \nabla_h^2 \underline{w} \tag{2.11}$$

Next operate on eq. (2.10) with the operator

$$\left(\frac{\partial}{\partial \underline{t}} + \bar{\underline{U}} \frac{\partial}{\partial \underline{x}} + \bar{\underline{V}} \frac{\partial}{\partial \underline{y}}\right)$$

to obtain

$$\left(\frac{\partial}{\partial \underline{t}} + \bar{\underline{U}} \frac{\partial}{\partial \underline{x}} + \bar{\underline{V}} \frac{\partial}{\partial \underline{y}}\right)^2 \nabla^2 \underline{w}$$

$$- \left(\frac{\partial}{\partial \underline{t}} + \bar{\underline{U}} \frac{\partial}{\partial \underline{x}} + \bar{\underline{V}} \frac{\partial}{\partial \underline{y}}\right) \left(\frac{d^2 \bar{\underline{U}}}{d\underline{z}^2} \frac{\partial}{\partial \underline{x}} + \frac{d^2 \bar{\underline{V}}}{d\underline{z}^2} \frac{\partial}{\partial \underline{y}}\right) \underline{w} \tag{2.12}$$

$$= \underline{g} \left(\frac{\partial}{\partial \underline{t}} + \bar{\underline{U}} \frac{\partial}{\partial \underline{x}} + \bar{\underline{V}} \frac{\partial}{\partial \underline{y}}\right) \nabla_h^2 \theta$$

or substituting from eq. (2.11),

$$= g \frac{d\bar{\Theta}}{d\underline{z}} \nabla_h^2 \underline{w}$$

which is the desired equation in the vertical perturbation velocity and can be written as

$$\left(\frac{\partial}{\partial \underline{t}} + \bar{\underline{U}}\frac{\partial}{\partial \underline{x}} + \bar{\underline{V}}\frac{\partial}{\partial \underline{y}}\right)^2 \nabla^2 \underline{w}$$

$$- \left(\frac{\partial}{\partial \underline{t}} + \bar{\underline{U}}\frac{\partial}{\partial \underline{x}} + \bar{\underline{V}}\frac{\partial}{\partial \underline{y}}\right)\left(\frac{d^2\bar{\underline{U}}}{d\underline{z}^2}\frac{\partial}{\partial \underline{x}} + \frac{d^2\bar{\underline{V}}}{d\underline{z}^2}\frac{\partial}{\partial \underline{y}}\right)\underline{w} \qquad (2.13)$$

$$- \underline{g}\frac{d\bar{\underline{\theta}}}{d\underline{z}} \nabla_h^2 \underline{w} = 0$$

Boundary and Initial Conditions

The boundary conditions to be applied in solving the differential equation are determined by the physical problem under consideration. For the salt wedge estuary problem it is assumed that the horizontal extent is much greater than the vertical extent. Because of the great difference in the horizontal to vertical length scales, the side boundaries have little effect on the motion at the scales under investigation. Therefore, the $\underline{x}$ and $\underline{y}$ coordinates are considered to be infinite in extent. The appropriate boundary conditions at $\underline{x} \rightarrow \pm\infty$ and $\underline{y} \rightarrow \pm\infty$ are that $\underline{w}$ and the first derivatives of $\underline{w}$ in the horizontal directions remain finite.

The boundary conditions in the vertical direction are the free surface condition at the surface and a no flux condition at the bottom.

The free surface is a constant pressure surface and the boundary condition is

$$\frac{D\underline{p}'}{D\underline{t}} = \left(\frac{\partial}{\partial \underline{t}} + \underline{\bar{U}} \frac{\partial}{\partial \underline{x}} + \underline{\bar{V}} \frac{\partial}{\partial \underline{y}}\right) \underline{p} = 0 \qquad (2.14)$$

This condition can be expressed in terms of the vertical velocity. The pressure is expressed as the sum of three components; the atmospheric pressure, th hydrostatic pressure and the perturbation pressure. The functi al dependence of each of these components is indicated in the following equation.

$$\underline{p}'(\underline{x}, \underline{y}, \underline{z}, \underline{t}) = \underline{P}_a(\underline{x}, \underline{y}, \underline{t})$$

$$+ \underline{g}[\bar{\theta}(\underline{z}) + \theta(\underline{x}, \underline{y}, \underline{z}, \underline{t})] \cdot [\underline{\eta}(\underline{x}, \underline{y}, \underline{t}) - \underline{z}] \qquad (2.15)$$

$$+ \underline{p}(\underline{x}, \underline{y}, \underline{z}, \underline{t})$$

where $\underline{\eta}(\underline{x},\underline{y},\underline{t}) - \underline{z} = 0$ is the equation of the free surface.

Expanding the free surface condition yields

$$\frac{D\underline{p}'}{D\underline{t}} = \left(\frac{\partial}{\partial \underline{t}} + \underline{\bar{U}} \frac{\partial}{\partial \underline{x}} + \underline{\bar{V}} \frac{\partial}{\partial \underline{y}}\right) \underline{P}_a - \underline{g}(\bar{\theta} + \theta)\, \underline{w}$$

$$+ \underline{g}(\bar{\theta} + \theta) \left(\frac{\partial}{\partial \underline{t}} + \underline{\bar{U}} \frac{\partial}{\partial \underline{x}} + \underline{\bar{V}} \frac{\partial}{\partial \underline{y}}\right) \underline{\eta}$$

$$+ \underline{g}(\underline{\eta} - \underline{z}) \left(\frac{\partial}{\partial \underline{t}} + \bar{\underline{U}}\frac{\partial}{\partial \underline{x}} + \bar{\underline{V}}\frac{\partial}{\partial \underline{y}}\right) \theta$$

$$+ \underline{g}\,\frac{\partial \bar{\Theta}}{\partial \underline{z}}\,(\underline{\eta} - \underline{z})\underline{w} + \underline{g}(\underline{\eta} - \underline{z})\,\underline{w}\,\frac{\partial \theta}{\partial \underline{z}} \qquad (2.16)$$

$$+ \left(\frac{\partial}{\partial \underline{t}} + \bar{\underline{U}}\,\frac{\partial}{\partial \underline{x}} + \bar{\underline{V}}\,\frac{\partial}{\partial \underline{y}}\right) \underline{p} + \underline{w}\,\frac{\partial \underline{p}}{\partial \underline{z}} = 0$$

Let the free surface be defined as

$$\left(\frac{\partial}{\partial \underline{t}} + \bar{\underline{U}}\,\frac{\partial}{\partial \underline{x}} + \bar{\underline{V}}\,\frac{\partial}{\partial \underline{y}}\right) (\underline{P}_a + \underline{g}\bar{\Theta}\underline{\eta}) = 0 \qquad (2.17)$$

This is the zeroth order surface boundary condition and is subtracted from eq. (2.16). The remaining terms are linearized and rewritten utilizing conservation of mass and the definition of a material surface at $\underline{z} = \underline{\eta}$. The linearized surface boundary condition becomes

$$\left(\frac{\partial}{\partial \underline{t}} + \bar{\underline{U}}\,\frac{\partial}{\partial \underline{x}} + \bar{\underline{V}}\,\frac{\partial}{\partial \underline{y}}\right) \underline{p} - \underline{g}\bar{\Theta}\underline{w} = 0 \qquad (2.18)$$

To the same order of approximation this condition is applied at $\underline{z} = 0$, rather than at the perturbed surface $\underline{z} = \underline{\eta}$.

The required form of the boundary condition is an equation in $\underline{w}$ only. To eliminate the pressure from the above equation, use the horizontal momentum equations and continuity. This is accomplished

by operating on the $\underline{x}$-component of the momentum equations by

$$\left(\frac{\partial}{\partial \underline{t}} + \bar{\underline{U}} \frac{\partial}{\partial \underline{x}} + \bar{\underline{V}} \frac{\partial}{\partial \underline{y}}\right) \frac{\partial}{\partial \underline{x}}$$

and the $\underline{y}$-component by

$$\left(\frac{\partial}{\partial \underline{t}} + \bar{\underline{U}} \frac{\partial}{\partial \underline{x}} + \bar{\underline{V}} \frac{\partial}{\partial \underline{y}}\right) \frac{\partial}{\partial \underline{y}}$$

Add the resulting equations and solve for

$$\left(\frac{\partial}{\partial \underline{t}} + \bar{\underline{U}} \frac{\partial}{\partial \underline{x}} + \bar{\underline{V}} \frac{\partial}{\partial \underline{y}}\right) \nabla_h^2 \underline{p} \quad .$$

This is substituted into eq. (2.18) after taking the horizontal Laplacian. The resulting boundary condition is

$$\left(\frac{\partial}{\partial \underline{t}} + \bar{\underline{U}} \frac{\partial}{\partial \underline{x}} + \bar{\underline{V}} \frac{\partial}{\partial \underline{y}}\right) \frac{\partial \underline{w}}{\partial \underline{z}}$$

$$- \left(\frac{\partial}{\partial \underline{t}} + \bar{\underline{U}} \frac{\partial}{\partial \underline{x}} + \bar{\underline{V}} \frac{\partial}{\partial \underline{y}}\right) \left(\frac{d\bar{\underline{U}}}{d\underline{z}} \frac{\partial}{\partial \underline{x}} + \frac{d\bar{\underline{V}}}{d\underline{z}} \frac{\partial}{\partial \underline{y}}\right) \underline{w}$$

$$- \underline{g}\, \bar{\theta}\, \nabla_h^2\, \underline{w} = 0 \qquad (2.19)$$

at $\underline{z} = 0$.

The boundary condition at the solid bottom is simply no flow through the bottom or

$$\underline{w} = 0 \qquad (2.20)$$

at $\underline{z} = -H$, the depth of the bottom boundary.

The initial conditions for the problem are the specification of the values of $\underline{w}(\underline{x},\underline{y},\underline{z},0)$ and $\frac{\partial \underline{w}}{\partial \underline{t}}(\underline{x},\underline{y},\underline{z},0)$, or some combination of $\underline{w}$ and $\frac{\partial \underline{w}}{\partial \underline{t}}$ at time $\underline{t} = 0$. Such conditions will be considered in greater detail in conjunction with specific applications.

Solution of the Problem

Two methods of solution for the differential equation specified in eq. (2.13) are to be considered, namely, normal modes and Fourier-Laplace transforms.

The first method considered is the normal modes solution. This is essentially a separation of variables method which assumes that the horizontal space and time dependence of the solution is wave-like and has the form:

$$\underline{w}(\underline{x}, \underline{y}, \underline{z}, \underline{t}) = \hat{\underline{w}}(\underline{z})[Ae^{-i\sigma\underline{t}} + Be^{-i\sigma\underline{t}}]e^{i(k\underline{x} + \ell\underline{y})} \qquad (2.21)$$

Substitution of this assumed form for the solution into the partial differential equation (2.13) results in an ordinary second order

differential equation for $\hat{\underline{w}}(\underline{z})$. This equation is

$$(k\bar{\underline{U}} + \ell\bar{\underline{V}} - \sigma)^2 \left(\frac{d^2}{d\underline{z}^2} - k^2 - \ell^2\right) \hat{\underline{w}}$$

$$- (k\bar{\underline{U}} + \ell\bar{\underline{V}} - \sigma) \left(k\frac{d^2\bar{\underline{U}}}{d\underline{z}^2} + \ell\frac{d^2\bar{\underline{V}}}{d\underline{z}^2}\right) \hat{\underline{w}} \qquad (2.22)$$

$$- \underline{g}\frac{d\bar{\underline{\theta}}}{d\underline{z}} (k^2 + \ell^2)\hat{\underline{w}} = 0$$

Now consider the Fourier-Laplace transform method of solution. This technique utilizes a double Fourier transform in $\underline{x}$ and $\underline{y}$ and a Laplace transform of the partial differential equation (2.13).

The double Fourier transform is defined by the transform pair

$$F(\underline{w}) = \tilde{\underline{w}}(k,\ell,\underline{z},\underline{t}) = \frac{1}{(2\pi)^2} \int_{-\infty}^{\infty}\int_{-\infty}^{\infty} \underline{w}(\underline{x},\underline{y},\underline{z},\underline{t})e^{-i(k\underline{x} + \ell\underline{y})}d\underline{x}d\underline{y}$$

(2.23)

$$F^{-1}(\tilde{w}) = \underline{w}(\underline{x},\underline{y},\underline{z},\underline{t}) = \int_{-\infty}^{\infty}\int_{-\infty}^{\infty} \tilde{\underline{w}}(\underline{k},\underline{\ell},\underline{z},\underline{t})e^{i(k\underline{x} + \ell\underline{y})}\, dkd\ell$$

The Laplace transform of Fourier-transformed function is defined by the transform pair

$$L(\tilde{w}) = \hat{w}(k,\ell,\underline{z},s) = \int_0^{\infty} \tilde{w}\,(k,\ell,\underline{z},\underline{t})e^{-s\underline{t}}\,d\underline{t}$$

$$L^{-1}(\hat{w}) = \tilde{w}(k,\ell,\underline{z},\underline{t}) = \frac{1}{2\pi i}\int_{\varepsilon-i\infty}^{\varepsilon+i\infty} \hat{w}(k,\ell,\underline{z},s)e^{s\underline{t}}\,ds \qquad (2.24)$$

Hence, the function $\hat{w}(k,\ell,\underline{z},s)$ is defined by the triple integral

$$FL(w) = \hat{w}(k,\ell,\underline{z},s)$$

$$= \frac{1}{(2\pi)^2}\int_0^{\infty}\int_{-\infty}^{\infty}\int_{-\infty}^{\infty} w(\underline{x},\underline{y},\underline{z},\underline{t})e^{-i(k\underline{x}+\ell\underline{y})}\,e^{-s\underline{t}}\,d\underline{x}d\underline{y}d\underline{t} \qquad (2.25)$$

The known properties of Laplace and Fourier transforms of derivatives which are necessary for the transform of eq. (2.13) are:

$$F\left(\frac{\partial^{\eta}\underline{w}}{\partial\underline{x}^{\eta}}\right) = (-ik)^{\eta}\,F(\underline{w})$$

$$L\left(\frac{\partial\underline{w}}{\partial\underline{t}}\right) = s\,L\,(\underline{w}) - \underline{w}\,|_{\underline{t}=0+}$$

$$L\left(\frac{\partial^2\underline{w}}{\partial\underline{t}^2}\right) = s^2\,L\,(\underline{w}) - s\,\underline{w}\,|_{\underline{t}=0+} - \frac{\partial\underline{w}}{\partial\underline{t}}\,|_{\underline{t}=0+}$$

First taking the double Fourier transform of eq. (2.13) gives

$$\left(\frac{\partial}{\partial \underline{t}} + ik\,\underline{\bar{U}} + i\ell\underline{\bar{V}}\right)^2 \left(\frac{d^2}{d\underline{z}^2} - k^2 - \ell^2\right) \underline{\tilde{w}}$$

$$- \left(\frac{\partial}{\partial \underline{t}} + ik\underline{\bar{U}} + i\ell\underline{\bar{V}}\right) \left(ik\,\frac{d^2\underline{\bar{U}}}{d\underline{z}^2} + i\ell\,\frac{d^2\underline{\bar{V}}}{d\underline{z}^2}\right) \underline{\tilde{w}}$$

$$+ \underline{g}\,\frac{d\underline{\bar{\Theta}}}{d\underline{z}}\,(k^2 + \ell^2)\,\underline{\tilde{w}} = 0 \qquad (2.26)$$

Now take the Laplace transforms and rewrite the transformed equation with the initial conditions on the right-hand side.

$$(s + ik\underline{\bar{U}} + i\ell\underline{\bar{V}}) \left(\frac{d^2}{d\underline{z}^2} - k^2 - \ell^2\right) \underline{\hat{w}}$$

$$- (s + ik\underline{\bar{U}} + i\ell\underline{\bar{V}}) \left(ik\,\frac{d^2\underline{\bar{U}}}{d\underline{z}^2} + i\ell\frac{d^2\underline{\bar{V}}}{d\underline{z}^2}\right) \underline{\hat{w}}$$

$$+ \underline{g}\,\frac{d\underline{\bar{\Theta}}}{d\underline{z}}\,(k^2 + \ell^2)\,\underline{\hat{w}}$$

$$= [s + 2i\,(k\underline{\bar{U}} + \ell\underline{\bar{V}})] \left(\frac{d^2}{d\underline{z}^2} - k^2 - \ell^2\right) \underline{\tilde{w}}\Big|_{\underline{t}=0^+} \qquad (2.27)$$

$$- i\left(k\,\frac{d^2\underline{\bar{U}}}{d\underline{z}^2} + \ell\frac{d^2\underline{\bar{V}}}{d\underline{z}^2}\right) \underline{\tilde{w}}\Big|_{\underline{t}=0^+}$$

$$+ \left(\frac{d^2}{d\underline{z}^2} - k^2 - \ell^2\right) \frac{\partial \underline{\tilde{w}}}{\partial \underline{t}}\Big|_{\underline{t}=0^+}$$

The boundary conditions, eqs. (2.19) and (2.20) are also Fourier-Laplace transformed and take the form:

$$(s + ik\underline{\bar{U}} + i\ell\underline{\bar{V}})^2 \frac{d\hat{\underline{w}}}{d\underline{z}}$$

$$- (s + ik\underline{\bar{U}} + i\ell\underline{\bar{V}}) \left(ik \frac{d\underline{\bar{U}}}{d\underline{z}} + i \frac{d\underline{\bar{V}}}{d\underline{z}}\right) \hat{\underline{w}} \tag{2.28}$$

$$+ g\underline{\bar{\Theta}} (k^2 + \ell^2) \hat{\underline{w}} = 0 \qquad \text{at } \underline{z} = 0$$

and

$$\hat{\underline{w}} = 0 \qquad \text{at } \underline{z} = -H \tag{2.29}$$

It can be seen that the Fourier Laplace transformation of the partial differential equation in $\underline{w}$ leads to an inhomogeneous second order, ordinary differential equation in the transformed variable $\hat{\underline{w}}\ (k,\ell,\underline{z},s)$. Making the substitution $s = -i\sigma$ in eq. (2.27) and comparing the homogeneous part with eq. (2.22) it can be seen that the derived governing equation for the two methods is of the same form.

Since the differential equation is of the same form for the two methods, that given in eq. (2.22) will be used to formulate the non-dimensional problem. The equation will be non-dimensionalized on a velocity scale, u_o, a length scale, h_o, and a density scale, ρ_o. The non-dimensional variables are defined:

$$(\alpha,\gamma) = (kh_o,\ \ell h_o)$$

$$(x,y,z) = (\underline{x}/h_o,\ \underline{y}/h_o,\ \underline{z}/h_o)$$

$$(u,v,w) = (\underline{u}/u_o,\ \underline{v}/u_o,\ \underline{w}/u_o)$$

$$(U,V) = (\underline{\bar{U}}/u_o,\ \underline{\bar{V}}/u_o)$$

$$p = \underline{p}/u_o^2$$

$$\omega = \sigma\, h_o/u_o$$

$$\theta = \rho/\rho_o$$

$$\bar{\Theta} = \bar{\rho}/\rho_o$$

Making the substitutions into eq. (2.13) produces the non-dimensional form of the governing differential equation:

$$(\alpha U + \gamma V - \omega)^2 \left(\frac{d^2}{dz^2} - \alpha^2 - \gamma^2\right) \hat{w}$$

$$- (\alpha U + \gamma V - \omega)\ (\alpha U'' + \gamma V'')\ \hat{w} \qquad (2.30)$$

$$+ J\ (\alpha^2 + \gamma^2)\ \hat{w} = 0$$

where

$$J^2_{(z)} = \frac{N^2 h_o^{\,2}}{u_o^{\,2}} \equiv \text{Richardson No.}$$

and

$$N^2 = -g\,\bar{\Theta}' \equiv \text{Brunt-Väisälä frequency.}$$

Utilizing the Squire transformation it can be shown that the solution to the three-dimensional problem posed above is equivalent to the solution of a two-dimensional problem with appropriately scaled parameters.

The Squire transformation is defined by the following two definitions.

$$\tilde{\alpha}^2 = \alpha^2 + \gamma^2$$

$$\tilde{\alpha}\tilde{U} = \alpha U + \gamma V \tag{2.31}$$

Using these definitions in eq. (2.30) the equivalent two-dimensional problem is given by

$$(\tilde{\alpha}\tilde{U} - \omega)^2 \left(\frac{d^2}{dz^2} - \tilde{\alpha}^2\right) \hat{w} - \tilde{\alpha}(\tilde{\alpha}\tilde{U} - \omega)\, \tilde{U}''\, \hat{w}$$

$$+ \tilde{J}\hat{w} = 0 \tag{2.32}$$

where

$$\tilde{J} = \tilde{\alpha}^2 J$$

Applying the Squire transformation to the boundary conditions, eq. (2.19) and eq. (2.20), completes the specification of the two-dimensional problem. The boundary conditions for the equivalent two-dimensional problem are

$$(\tilde{\alpha}\tilde{U} - \omega)^2\, \hat{w}' - [\tilde{\alpha}^2 g\bar{\Theta} + \tilde{\alpha}\tilde{U}'\, (\tilde{\alpha}\tilde{U} - \omega)]\, \hat{w} = 0 \tag{2.33}$$

at $z = 0$

and

$$\hat{w} = 0 \qquad \text{at } z = -H/h_o$$

The Initial-Value Problem

Solution of the initial-value problem using the normal modes

approach requires solution of the eigenvalue problem specified by the differential equation for $\hat{w}(z)$, eq. (2.22), subject to the boundary conditions given by eqs. (2.19) and (2.20). The eigenfunctions can be written as

$$\hat{w}(\alpha,\gamma,z,t) = \sum_{n=1}^{N} \hat{w}_n(\alpha,\gamma,z)[A_n e^{-i\omega_n t} + B_n e^{i\omega_n t}] \tag{2.34}$$

where the n specifies the mode and corresponds to the eigenvalue given by

$$\omega_n = \omega_n(\alpha,\gamma,J) \tag{2.35}$$

To apply the initial conditions to the problem, first take the Fourier transform or find the Fourier series of the initial vertical velocity and acceleration. Let $w_o(x,y,z,0)$ and $\frac{\partial}{\partial t} w_o(x,y,z,0)$ be the initial conditions and define the Fourier transforms of these conditions as

$$\begin{aligned} \tilde{w}_o(\alpha,\gamma,z,0) &= \frac{1}{(2\pi)^2} \int_{-\infty}^{\infty}\int_{-\infty}^{\infty} w_o(x,y,z,0)\ e^{-i(\alpha x + \gamma y)} dxdy \\ \frac{\partial}{\partial t}\tilde{w}_o(\alpha,\gamma,z,0) &= \frac{1}{(2\pi)^2} \int_{-\infty}^{\infty}\int_{-\infty}^{\infty} \frac{\partial w_o}{\partial t}(x,y,z,0)\ e^{-i(\alpha x + \gamma y)} dxdy \end{aligned} \tag{2.36}$$

Now expand the transforms of the initial conditions in terms of the eigenfunctions of the normal modes solution, i.e.,

$$\tilde{w}_o(\alpha,\gamma,z,0) = \sum_{n=1}^{N} \tilde{w}_n(\alpha,\gamma,z)[A_n + B_n]$$

$$\frac{\partial}{\partial t}\tilde{w}_o(\alpha,\gamma,z,0) = \sum_{n=1}^{N} - i\omega_n \tilde{w}_n(\alpha,\gamma,z)[A_n - B_n] \tag{2.37}$$

The coefficients A_n and B_n are determined from eqs. (2.37) and the final solution to the initial-value problem is found by taking the inverse Fourier transform of the normal modes solution which is of the form

$$w(x,y,z,t) = \int_{-\infty}^{\infty}\int_{-\infty}^{\infty} \sum_{n=1}^{N} \hat{w}_n(\alpha,\gamma,z)[A_n e^{-i\omega_n t} + B_n e^{i\omega_n t}]\, e^{i(\alpha x + \gamma y)} d\alpha d\gamma \tag{2.38}$$

The solution to the initial-value problem using the Fourier-Laplace transform method begins by solving for the Green's function solution of the differential equation given by eq. (2.27) which is rewritten as

$$(s + i\alpha U + i\gamma V)^2 \left(\frac{d^2}{dz^2} - \alpha^2 - \gamma^2\right) \hat{w}$$

$$- (s + i\alpha U + i\gamma V)\ (i\alpha U'' + i\gamma V'')\ \hat{w} \tag{2.39}$$

$$+ g\bar{\Theta}'\ (\alpha^2 + \gamma^2)\ \hat{w} = W(\alpha,\gamma,z;s)$$

where the function

$$W(\alpha,\gamma,z;s) = \left(\frac{d^2}{dz^2} - \alpha^2 - \gamma^2\right) \left.\frac{\partial \tilde{w}}{\partial t}\right|_{o+}$$

$$+ [s + 2i(\alpha U + \gamma V)] \left[\frac{d^2}{dz^2} - \alpha^2 - \gamma^2\right] \left.\tilde{w}\right|_{o+} \qquad (2.40)$$

$$- i(\alpha U'' + \gamma V'') \left.\tilde{w}\right|_{o+}$$

specifies the initial conditions. The functions $\tilde{w}$ and $\partial\tilde{w}/\partial t$ are the Fourier transforms of the vertical velocity and acceleration as specified in eqs. (2.36). The Green's function solution to eq. (2.39) is discussed in Appendix A and is of the form

$$G(z,z_o) = G(z,z_o;s,\alpha,\gamma) \qquad (2.41)$$

The solution to the initial-value problem in terms of the Green's function is specified formally by the inverse Fourier-Laplace transform:

$$w(x,y,z,t) = \frac{1}{2\pi i} \int_{-\infty}^{\infty} \int_{-\infty}^{\infty} \int_{\varepsilon-i\infty}^{\varepsilon+i\infty} \int_{-h}^{o} G(z,z_o)\, W(\alpha,\gamma,z_o;s)\, dz_o \cdot e^{st}\, e^{i(\alpha x + \gamma y)}\, ds d\alpha d\gamma \qquad (2.42)$$

The correspondence between this solution and the normal modes solution is also discussed in Appendix A.

3. Two-Layer Problem

Description of Problem

The first example of an initial-value problem is a two layer system consisting of two fluids of different density in uniform motion relative to each other with surface tension at the interface. It is assumed that the fluids are inviscid and incompressible. The illustration (Fig. 1) shows the general features of the system. The density of the bottom layer, ρ_2, is greater than the density of the upper layer, ρ_1. The system is statically stable. The analysis assumes that the velocity of the upper layer is $+\bar{U}$ and that of the bottom layer is $-\bar{U}$. The essential feature is the velocity difference $2\bar{U}$. A Galilean transformation could be made to place the zero of the velocity at any appropriate value without changing the following analysis.

The scaling parameters for this problem are based on the magnitude of the velocity $\bar{U}$, the gravitational constant g and the density of pure water, 1 gm/cm^3. The velocity scale $u_o = \bar{U}$ and the length scale $h_o = \bar{U}^2/g$. The non-dimensional variables are as defined in Section 2. The non-dimensional coefficient of surface tension, τ, is defined as:

$$\tau = \underline{\tau}\, u_o^2 h_o .$$

In the preceding section the differential equation governing the motion of an inviscid incompressible stratified, shear flow is given by eq. (2.8)

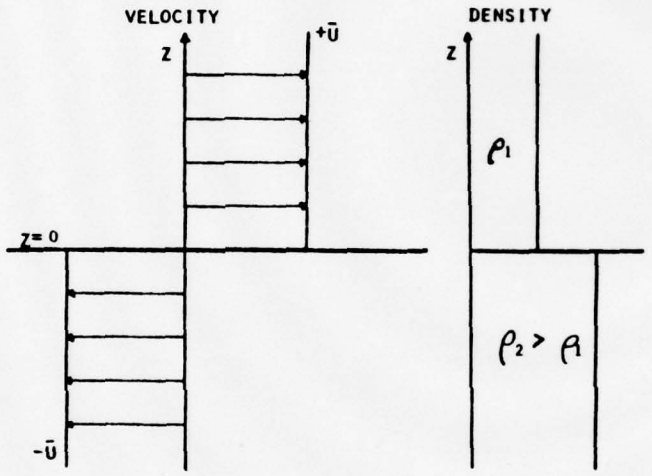

Figure 1. Schematic of unbounded two-layer example.

$$(\alpha U + \gamma V - \omega)^2 \left(\frac{d^2}{dz^2} - \alpha^2 - \gamma^2\right) \hat{w}$$

$$- (\alpha U + \gamma V - \omega)\ (\alpha U'' + \gamma V'')\ \hat{w} \qquad (3.1)$$

$$+ J\ (\alpha^2 + \gamma^2)\ \hat{w} = 0$$

For this example the differential equation can be greatly simplified - the horizontal velocity in the y-direction is zero and the velocity in the x-direction is constant in each of the layers. Also, the density is constant in each of the two layers. This means that the derivatives of U with respect to z are zero and $J = 0$. The differential equation for $\hat{w}$ in each of the layers is simply

$$\frac{d^2\hat{w}}{dz^2} - (\alpha^2 + \gamma^2)\ \hat{w} = 0 \qquad (3.2)$$

or

$$\frac{d^2\hat{w}}{dz^2} - \tilde{\alpha}^2\hat{w} = 0$$

which has as solutions

$$\hat{w}(z) = Ae^{\tilde{\alpha}z} + Be^{-\tilde{\alpha}z}$$

The solution in each region will be designated by a subscript 1 or 2.

It is assumed that the fluid is of infinite extent and the boundary conditions are applied at $z \to \pm \infty$ rather than at $z = 0$ and $z = -h$. The interface between the two fluids at $z = 0$ is an

internal boundary which divides the solution into two regions. Matching conditions to be applied to the solutions in the two regions must be derived.

The two conditions which are to be applied are the kinematic and dynamic boundary conditions. The kinematic condition is that the interface is a material surface specified by

$$z = \eta = d\, e^{i(\alpha x + \gamma y - \omega t)} \tag{3.4}$$

and is subject to the conditions that

$$\frac{D\eta}{Dt} = w \tag{3.5}$$

The linearized form of the kinematic condition is

$$\frac{\partial \eta}{\partial t} + U\frac{\partial \eta}{\partial x} = w_+ \qquad \text{at } z = 0^+ \tag{3.6}$$

and

$$\frac{\partial \eta}{\partial t} - U\frac{\partial \eta}{\partial x} = w_- \qquad \text{at } z = 0^-$$

where 0^+ and 0^- indicates the value at 0 approached from above and below respectively.

The dynamic condition is that the difference in pressure across the interface is sustained by surface tension.

Brenoulli's equation for the pressure can be written as

$$p = \frac{\partial \phi}{\partial t} - gz - \frac{1}{2}\vec{u} \cdot \vec{u} \tag{3.7}$$

where ϕ is the velocity potential of the flow defined by

$$\vec{u} = -\nabla\phi \tag{3.8}$$

The boundary condition is

$$\Theta_2 p_2 - \Theta_1 p_1 = -\tau \nabla_h^2 \eta \tag{3.9}$$

where τ is the surface tension. The expression for pressure given by eq. (3.7) must be linearized. In terms of a mean velocity and perturbation velocities the kinetic energy term is given by

$$\frac{1}{2}\vec{u}\cdot\vec{u} = \frac{1}{2}\left[U^2 + 2uU + u^2 + v^2 + w^2\right] \tag{3.10}$$

which becomes on linearizing

$$\frac{1}{2}\vec{u}\cdot\vec{u} \simeq \frac{1}{2}\left[U^2 + 2uU\right]$$

Making the necessary substitutions into eq. (3.9) the linearized boundary condition becomes

$$\Theta_2\left(\frac{\partial\phi_2}{\partial t} - g\eta + Uu_2\right) - \Theta_1\left(\frac{\partial\phi_1}{\partial t} - g\eta - Uu_1\right) = -\tau\left(\frac{\partial^2\eta}{\partial x^2} + \frac{\partial^2\eta}{\partial y^2}\right) \tag{3.11}$$

The continuity equation gives the differential equation which the velocity potential must satisfy.

$$\nabla^2\phi = 0 \tag{3.12}$$

However, from the normal modes assumption, the velocity potential must have the following form

$$\phi(x,y,z,t) = \hat{\phi}(z)\, e^{i(\alpha x + \gamma y - \omega t)} \tag{3.13}$$

Substituting the functional form of ϕ into the partial differential equation (3.12) gives the following ordinary differntial equation for $\hat{\phi}(z)$:

$$\frac{d^2\hat{\phi}}{dz^2} - \tilde{\alpha}^2\hat{\phi} = 0 \tag{3.14}$$

and

$$\hat{\phi}(z) = a\, e^{\tilde{\alpha}z} + b\, e^{-\tilde{\alpha}z} \tag{3.15}$$

The following set of equations defines the eigenvalues of the problem.

$$\text{(a)}\quad \frac{\partial \eta}{\partial t} + U\frac{\partial \eta}{\partial x} = w_1 = -\frac{\partial \phi_1}{\partial z} \qquad \text{at } z = 0^+$$

$$\text{(b)}\quad \frac{\partial \eta}{\partial t} - U\frac{\partial \eta}{\partial x} = w_2 = -\frac{\partial \phi_2}{\partial z} \qquad \text{at } z = 0^-$$

$$\text{(c)}\quad \Theta_2\left(\frac{\partial \phi_2}{\partial t} - U\frac{\partial \phi_2}{\partial x} - g\eta\right) - \Theta_1\left(\frac{\partial \phi_1}{\partial t} + U\frac{\partial \phi_1}{\partial x} - g\eta\right) = -\tau\left(\frac{\partial^2 \eta}{\partial x^2} + \frac{\partial^2 \eta}{\partial y^2}\right) \tag{3.16}$$

$$\text{(d)}\quad \hat{\phi}_1 \longrightarrow 0 \quad \text{as} \quad z \longrightarrow +\infty$$

$$\text{(e)}\quad \hat{\phi}_2 \longrightarrow 0 \quad \text{as} \quad z \longrightarrow -\infty$$

Condition (d) requires $a_1 = 0$ and condition (e) requires $b_2 = 0$ which gives

$$\hat{\phi}_1(z) = b_1 e^{-\tilde{\alpha}z}$$

$$\hat{\phi}_2(z) = a_2 e^{\tilde{\alpha}z} \tag{3.17}$$

Substituting the functional form of ϕ and η into the conditions (a), (b) and (c) gives the following set of linear algebraic equations to be solved for the eigenvalues, ω.

$$\text{(a)} \quad i(\omega - \alpha U)d + \tilde{\alpha} b_1 = 0$$

$$\text{(b)} \quad i(\omega + \alpha U)d - \tilde{\alpha} a_2 = 0 \tag{3.18}$$

$$\text{(c)} \quad [g(\Theta_1 - \Theta_2) - \tau\tilde{\alpha}^2]d + i\Theta_1(\omega - \alpha U)b_1 - i\Theta_2(\omega + \alpha U)a_2 = 0$$

The determinant of coefficients of these three equations is the eigenvalue relation and can be written as the solution of a quadratic equation:

$$\omega = \frac{-\tilde{\alpha}\cos\psi\, U\Delta\Theta}{(\Theta_1 + \Theta_2)} \pm \left[\frac{-4\tilde{\alpha}^2 \cos^2\psi\, U^2\Theta_1\Theta_2}{(\Theta_1 + \Theta_2)^2} + \frac{\tilde{\alpha} g\Delta\Theta}{(\Theta_1 + \Theta_2)} + \frac{\tilde{\alpha}^3\tau}{(\Theta_1 + \Theta_2)}\right]^{1/2} \tag{3.19}$$

where

$$\Delta\Theta = \Theta_2 - \Theta_1$$

$$\alpha = \tilde{\alpha}\cos\psi$$

$$\gamma = \tilde{\alpha}\sin\psi$$

$$\tan\psi = \gamma/\alpha$$

The stability boundary for this problem is obtained from considering the argument of the radical in eq. (3.19). Let this be represented by Q,

$$Q = \tilde{\alpha}\left[\frac{\tilde{\alpha}^2\tau}{(\theta_1+\theta_2)} - \frac{4\tilde{\alpha}\cos^2\psi\, U^2\theta_1\theta_2}{(\theta_1+\theta_2)^2} + \frac{g\Delta\theta}{(\theta_1+\theta_2)}\right] \tag{3.20}$$

If Q is negative, ω is complex and the flow can be unstable, but if Q is positive ω is always real. The stability boundary is determined by the locus $Q = 0$. The range of instability can be determined by solving the quadratic equation in brackets.

$$\left[\frac{\tilde{\alpha}^2\tau}{(\theta_1+\theta_2)} - \frac{4\tilde{\alpha}\cos^2\psi\, U^2\theta_1\theta_2}{(\theta_1+\theta_2)^2} + \frac{g\Delta\theta}{(\theta_1+\theta_2)}\right] = 0 \tag{3.21}$$

If the roots of eq. (3.21) are complex, the flow is stable or unstable everywhere depending on the sign of Q. However, if the roots are real, they specify the points at which Q changes sign and thus the regions of instability. Figures 5, 7 and 8 show the values of (-Q) for two different cases.

The values of the parameters used in evaluating Q for Fig. 5 are:

$\underline{\tau} = 74.\ \text{cm}^3/\text{sec}^2$

$\underline{\rho_1} = 1.293 \times 10^{-3}\ \text{gm/cm}^3$

$\underline{\rho_2} = 1.02\ \text{gm/cm}^3$

$\underline{U} = 100.\ \text{cm/sec}$

The parameters for this case correspond to an air-water interface. The roots of eq. (3.21) for this case are complex and the value of Q is positive. The two-layer problem with this set of parameters is stable for all wave-numbers. The threshold velocity for instability is 324.405 cm/sec at a wavenumber of 3.673/cm. The value of the threshold velocity as a function of wavenumber is shown in Fig. 6. The wavenumber range for instability is given by the points of intersection of a line of constant velocity and the threshold velocity curve.

The second case corresponds more closely to an internal fluid boundary. The surface tension is small and the density difference between the two fluids is small. The parameters are

$$\underline{\tau} = 1.0 \text{ cm}^3/\text{sec}^2$$

$$\underline{\rho_1} = 1.0 \text{ gm/cm}^3$$

$$\underline{\rho_2} = 1.02 \text{ gm/cm}^3$$

$$\underline{U} = 10. \text{ cm/sec}$$

Figure 7 is a graph of the value of (-Q) as a function of wavenumber and indicates the regions of instability for waves at different angles, ψ, to the mean velocity. Figure 8 is the same function, but indicates the stable ($-Q < \theta$) region of the flow at small wavenumbers (large wave lengths).

The eigenvalues for this set of parameters are shown in Figs. 9 and 10. Figure 9 shows the real part of the eigenvalue ω. It can

be seen that the real part of the frequency is nearly constant over the range of instability. The imaginary part of ω is shown in Fig. 10. As in all inviscid problems, the complex eigenvalues occur in complex pairs. For every growing mode there is also a damped mode. The range of instability is clearly shown in this graph.

Initial-Value Problem

The solution to the initial-value problem is given by (2.38) as

$$w(x,y,z,t) = \int_{-\infty}^{\infty}\int_{-\infty}^{\infty} \sum_{n=1}^{N} \hat{w}_n(\alpha,\gamma,z)\ [A_n e^{-i\omega_n t} + B_n e^{i\omega_n t}]\ e^{i(\alpha x + \gamma y)} d\alpha d\gamma \tag{3.22}$$

with the initial conditions

$$\tilde{w}_o(\alpha,\gamma,z,0) = \sum_{n=1}^{N} \hat{w}_n(\alpha,\gamma,z)\ [A_n + B_n] \tag{3.23}$$

and

$$\frac{\partial \tilde{w}_o}{\partial t}(\alpha,\gamma,z,0) = \sum_{n=1}^{N} \hat{w}_n(\alpha,\gamma,z)\ [-i\omega_n A_n + i\omega_n B_n]$$

As an example of an initial-value problem, the flow described by the second set of parameters in the preceding section is used. The initial conditions prescribed are chosen as

$$\tilde{w}_o(\alpha,\gamma,z,0) = \frac{e^{-\frac{\lambda^2(\alpha^2+\gamma^2)}{2}}}{(2\pi)^2}\ e^{-\lambda^2 z^2}$$

$$\frac{\partial \tilde{w}_o}{\partial t}(\alpha,\gamma,z,0) = 0 \tag{3.24}$$

This is the Fourier transform of a Gaussian pulse in amplitude centered around the density interface. Substituting the prescribed initial conditions into eq. (3.23) determines the value of A_n and B_n. Solving and making the substitution into eq. (3.22) gives the result that

$$w(x,y,z,t) = \mathrm{Re} \sum_{n=1}^{N} \int_{-\infty}^{\infty} \int_{-\infty}^{\infty} A_n \tilde{w}_o(\alpha,\gamma,z,0)\, e^{i(\alpha x + \gamma y - \omega t)}\, d\alpha d\gamma \tag{3.25}$$

Initial Period

To determine the motion of the pulse for small times, the function is expanded in a Taylor series about time t = 0. The following technique follows that described by Criminale (1960). The Taylor series expansion takes the form

$$w(x,y,z,t) = \sum_{k=0}^{K} \frac{t^k}{k!} \frac{\partial^k}{\partial t^k} \int_{-\infty}^{\infty} \int_{-\infty}^{\infty} \tilde{w}_o(\alpha,\gamma,z) e^{i(\alpha x + \gamma y - \omega t)} \cdot d\alpha d\gamma \Big|_{t=0} \tag{3.26}$$

The Fourier integral in eq. (3.25) can be broken into two integrals and rewritten as

$$w(x,y,z,t) = \int_{0}^{\infty}\int_{-\infty}^{\infty} \tilde{w}_o \, e^{-i\omega t} \, e^{i(\alpha x + \gamma y)} d\alpha d\gamma \tag{3.27}$$

$$+ \int_{-\infty}^{0}\int_{-\infty}^{\infty} \tilde{w}_o \, e^{-i\omega t} \, e^{i(\alpha x + \gamma y)} d\alpha d\gamma$$

In the second integral change α and γ to $-\alpha$ and $-\gamma$. From eq. (3.19) it is noted that

$$\omega(\alpha,\gamma^2) = -\omega^*(-\alpha,(-\gamma)^2) \tag{3.28}$$

where * indicates complex conjugate. Making these changes in the second integral eq. (3.27) can be rewritten as

$$w(x,y,z,t) = \int_{0}^{\infty}\int_{-\infty}^{\infty} \tilde{w}_o \, e^{-i\omega t} \, e^{i(\alpha x + \gamma y)} d\alpha d\gamma$$

$$+ \int_{0}^{\infty}\int_{-\infty}^{\infty} \tilde{w}_o \, e^{i\omega^* t} \, e^{-i(\alpha x + \gamma y)} d\alpha d\gamma \tag{3.29}$$

Represent the first integral by W and it can be seen that the second integral is the complex conjugate of W. Equation (3.29) can be represented by

$$w(x,y,z,t) = W + W^* \tag{3.30}$$

and the Taylor's series can be written as

$$w(x,y,z,t) = \mathrm{Re} \sum_{k=0}^{K} \frac{t^k}{k!} \left[\frac{\partial^k W}{\partial t^k} + \frac{\partial^k W^*}{\partial t^k}\right]_{t=0} \tag{3.31}$$

The evaluation of only one of these integrals is necessary since the other is just the complex conjugate.

The information needed is the form of the time derivative of W evaluated at time t = 0.

$$\left.\frac{\partial^k W}{\partial t^k}\right|_{t=0} = \int_{-o}^{\infty}\int_{-\infty}^{\infty} \tilde{w}_o (-i\omega)^k \, e^{i(\alpha x + \gamma y)} d\alpha d\gamma \tag{3.32}$$

If ω can be approximated by a polynomial these integrals can be evaluated explicitly. Each term is of the form

$$\left.\frac{\partial^k W}{\partial t^k}\right|_{t=0} = (-i\underline{\omega})^k \int_{-o}^{\infty}\int_{-\infty}^{\infty} \tilde{w}_o \, e^{i(\alpha x + \gamma y)} d\alpha d\gamma \tag{3.33}$$

This form is obtained by recalling the expression for the Fourier transform of a derivative

$$F\left(\frac{\partial^k w}{\partial x^k}\right) = (-i\alpha)^k F(w)$$

The linear operator $\underline{\omega}$ in eq. (3.33) has the same functional form as $\omega(\alpha,\gamma)$ with α replaced by $(-i\ \partial/\partial x)$ and γ by $(-i\ \partial/\partial y)$.

Approximate the eigenvalues ω by the following polynomials:

$$\begin{aligned} \omega_r &= Re(\omega) = \omega_{ro} + a_1\alpha + a_2\gamma^2 \\ \omega_i &= Im(\omega) = \omega_{io} - b_1(\alpha - \alpha_o)^2 - b_2\gamma^2 \end{aligned} \tag{3.34}$$

Also note that the integral in eq. (3.33) is half the initial condition in real space

$$\frac{1}{2} w_o(x,y,z) = \int_0^\infty \int_{-\infty}^{\infty} \tilde{w}_o \, e^{i(\alpha x + \gamma y)} d\alpha d\gamma \tag{3.35}$$

Define the complex linear operator L such that

$$L = -i\underline{\omega} = L_r + iL_i$$

$$L_r = (\omega_{io} - b_1\alpha_o^2) - a_1 \frac{\partial}{\partial x} + b_1 \frac{\partial^2}{\partial x^2} + b_2 \frac{\partial^2}{\partial y^2} \tag{3.36}$$

$$L_i = -i[\omega_{ro} + 2\alpha_o b_1 \frac{\partial}{\partial x} - a_2 \frac{\partial^2}{\partial y^2}]$$

Substituting into the Taylor series eq. (3.31) takes the form

$$w(x,y,z,t) = \sum_{k=0}^{K} \frac{t^k}{k!} [L^k + L^{*k}] \frac{w_o}{2} \tag{3.37}$$

Expanding this series and keeping only real terms the initial disturbance takes the form

$$w(x,y,z,t) = w_o + t_r(w_o)$$

$$+ t^2[L_r^2 - L_i^2] \frac{w_o}{4} + \ldots \tag{3.38}$$

Expanding the operator L and keeping only the linear term, the expansion valid for small time is given by

$$w(x,y,z,t) \tilde{=} \{1 + t[(\omega_{io} - b_1\alpha_o^2) + a_1\, x/\lambda^2 - b_1/\lambda^2 + \frac{b_1 x^2}{\lambda^4} - b_2/\lambda^2 + \frac{b_2 y^2}{\lambda^4}]\} \frac{e^{-(x^2 + y^2)/\lambda^2}}{4\pi\lambda^2} \tag{3.39}$$

The initial spreading and distortion of the initial conditions given by eq. (3.24) are shown in Fig. 11. The initial Gaussian pulse has a standard deviation equal to 0.1. Fig. 11a shows the initial pulse at t = 0. The distorted pulse is shown at t = 0.05 and t = 0.75 in Fig. 11b and Fig. 11c, respectively.

Asymptotic Analysis

The form of the asymptotic expansion of the solution to the initial-value problem, eq. (3.25), is derived in Appendix B. This expansion is given by eq. (B.19)

$$w(x,y,z,t) \sim \mathrm{Re}\left[\frac{w_o(\alpha_*,\gamma_*,z,o)\; e^{i(\alpha_* x + \gamma_* y - \omega_* t)}}{t\left[\left.\frac{\partial^2\omega}{\partial\alpha^2}\right|_{\alpha_*,\gamma_*} \cdot \left.\frac{\partial^2\omega}{\partial\gamma^2}\right|_{\alpha_*,\gamma_*} - \left(\left.\frac{\partial^2\omega}{\partial\alpha\partial\gamma}\right|_{\alpha_*,\gamma_*}\right)^2\right]^{1/2}}\right] \tag{3.40}$$

where α_* and γ_* are solutions of the simultaneous equations:

$$x/t - \frac{\partial \omega}{\partial \alpha}(\alpha_*, \gamma_*) = 0$$

$$y/t - \frac{\partial \omega}{\partial \gamma}(\alpha_*, \gamma_*) = 0 \qquad (3.41)$$

where ω, α and γ are considered to be complex variables.

Evaluation of the expansion for the same Gaussian pulse with standard deviation $\lambda = 0.1$ is shown in Fig. 12. The expansion in Fig. 12a is at $t = 20$ and that in Fig. 12b at $t = 60$.

The continued spreading and distortion of the pulse and the appearance of dominant wavelengths are apparent in the series of figures 11 and 12 showing the development of the pulse from $t = 0$ to $t = 60$.

4. Salt Wedge Estuary

Description of Problem

A salt wedge estuary is used as the second physical example in this analysis.

A salt wedge estuary is a highly stratified estuary consisting of nearly homogeneous upper and lower layers separated by a strong halocline. The brackish upper layer is primarily river runoff. The "salt wedge" is the layer below the density interface consisting of a saltwater intrusion from the ocean. Salt wedges occur in shallow estuaries with high river discharge and relatively weak tidal currents.

The general profile of a salt wedge is depicted in Fig. 2 and a general velocity profile in Fig. 3. The velocity profile is such that there is no net flow in a stationary salt wedge. Three regions are indicated on the schematic of the wedge profile. These are defined by the depth of the halocline. The outer region has the density interface near the surface. The inner regime is defined by a halocline near the bottom with the central region having a halocline near the center of the water column.

The velocity profile is nearly two-dimensional and is treated as such in the following analysis. In addition, the scale of perturbations to be considered are such that the x-dependence (downstream) of the velocity and density structure is considered only in terms of the inner, central and outer regime. At each cross-section the velocity and density profile will be similar to

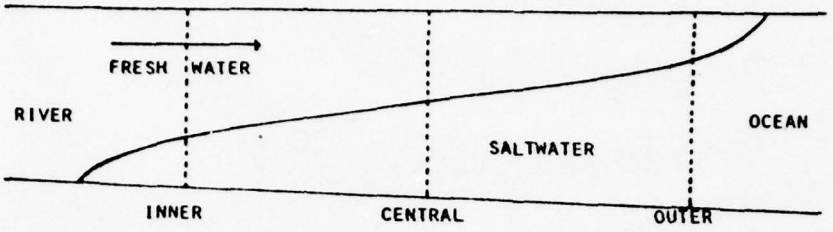

Figure 2. Schematic of a longitudinal section of a salt-wedge estuary.

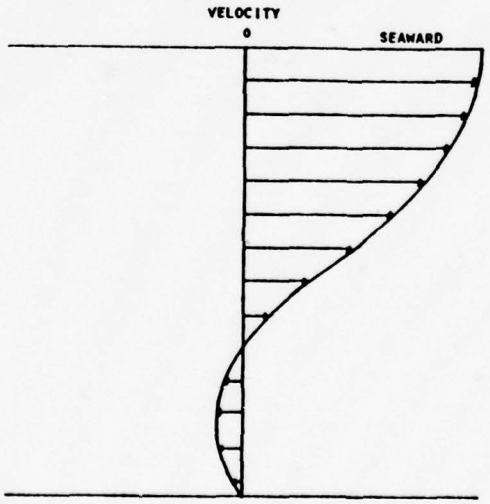

Figure 3. Schematic of downstream velocity profile in a salt-wedge.

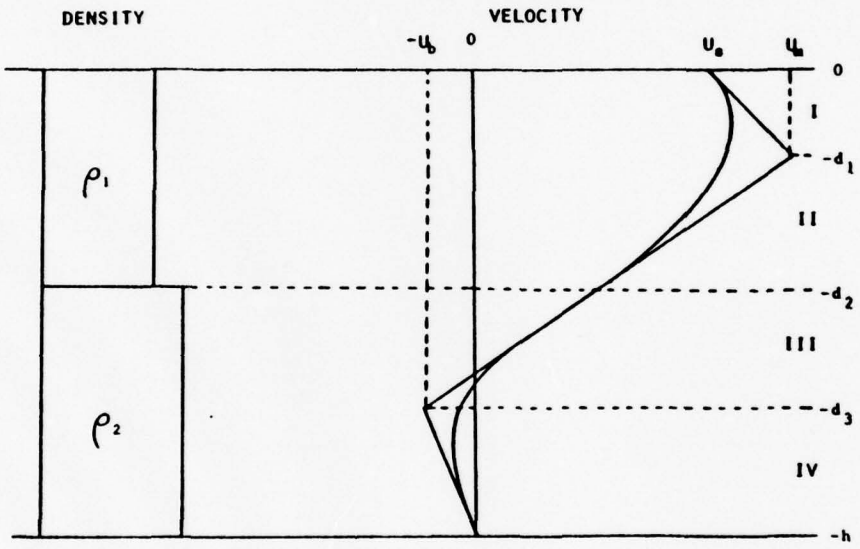

Figure 4. Schematic of linearized profiles for salt-wedge example.

those shown in Fig. 4. The parameters h_o and u_o are scaled on the total depth of the fluid and the gravitational constant g.

$$h_o = H$$

$$u_o = \sqrt{gH}$$

Mathematical Description

The density structure is modeled as a two-layer system with density ρ_1 in the upper layer of depth d_2. The lower layer is of density ρ_2 of thickness $h-d_2$. The smooth velocity profile is modeled by a piecewise linear profile consisting of three segments. The first segment is given by

$$\bar{u}_I = u_I + u'_I z \quad ; \quad 0 \geq z \geq -d_1$$

where

$u_I = u_s$ = velocity at the surface

$$u'_I = \frac{d\bar{u}_I}{dz} = \text{shear in layer I}$$

$$= \frac{u_s - u_m}{d_1}$$

Similarly, the middle segment of the velocity profile is given by

$$\bar{u}_{II} = u_{II} + u'_{II} z \quad ; \quad -d_1 \geq z \geq -d_3$$

where

$$u_{II} = \frac{u_m d_3 - u_b d_1}{(d_3 - d_1)}$$

$$u'_{II} = \frac{u_m - u_b}{(d_3 - d_1)}$$

and the bottom segment is given by

$$\bar{u}_{III} = u_{III} + u'_{III}\, z \quad ; \quad -d_3 \geq z \geq -h$$

where

$$u_{III} = \frac{u_b h}{(h - d_3)}$$

$$u'_{III} = \frac{u_b}{(h - d_3)}$$

A restriction on the velocity profile is that it goes to zero at the bottom.

These approximations divide the vertical extent of the model into four regions. In each region the mean properties of the flow are described by constant density and constant shear. There are three internal boundaries defined by discontinuities in the density or velocity.

The differential equation governing the flow and the external boundary conditions are given by eqs. (2.30), (2.31) and (2.32). Repeating the equations and using the definition of J gives

$$(\tilde{\alpha}\tilde{U} - \omega)^2 \left(\frac{d^2}{dz^2} - \tilde{\alpha}^2\right) \hat{w} - (\tilde{\alpha}\tilde{U} - \omega)\, \tilde{\alpha}\tilde{U}'' \hat{w} - g\Theta' \tilde{\alpha}\hat{w} = 0 \qquad (4.1)$$

$$\frac{d\hat{w}}{dz} - \left[\frac{\tilde{\alpha}^2 g\Theta}{(\tilde{\alpha}\tilde{U} - \omega)^2} + \frac{\tilde{\alpha}\tilde{U}'}{(\tilde{\alpha}\tilde{U} - \omega)}\right] \hat{w} = 0 \quad \text{at } z = 0 \qquad (4.2)$$

$$\hat{w} = 0 \qquad \text{at } z = -h \qquad (4.3)$$

The differential equation simplifies immediately on substituting the assumed profiles of mean velocity and density to

$$(\tilde{\alpha}\tilde{U} - \omega)^2 \left(\frac{d^2}{dz^2} - \tilde{\alpha}^2\right) \hat{w} = 0$$

The solutions of this equation are subject to the boundary conditions eq. (4.2) and eq. (4.3) and to matching conditions at the discontinuities of the mean profiles.

The applicable matching conditions are derived by integrating the complete differential equation given by eq. (4.1) across the discontinuity. The matching condition at depth z = -d is given by the following equation.

$$\lim_{\varepsilon \to 0} \left[\int_{-d-\varepsilon}^{-d+\varepsilon} (\tilde{\alpha}\tilde{U} - \omega)^2 \frac{d^2\hat{w}}{dz^2}\, dz - \tilde{\alpha}^2 \int_{-d-\varepsilon}^{-d+\varepsilon} (\tilde{\alpha}\tilde{U} - \omega)^2\, \hat{w} dz \right. \qquad (4.4)$$

$$\left. - \tilde{\alpha} \int_{-d-\varepsilon}^{-d+\varepsilon} \hat{w}(\tilde{\alpha}\tilde{U} - \omega)\, \tilde{U}'' dz - \tilde{\alpha} g \int_{-d-\varepsilon}^{-d+\varepsilon} \hat{w}\Theta' dz \right] = 0$$

Evaluation of the integrals at a given depth will be simplified by requiring that the vertical perturbation velocity, $\hat{w}(z)$, be

continuous and noting that the mean velocity is a continuous function of depth, but the shear is discontinuous.

Evaluating eq. (4.4) at $z = d_1$, proceeds as follows. Evaluating the integrals and taking the limit of small ϵ produces

$$(\tilde{\alpha}\tilde{U}_m - \omega)^2 [\frac{\hat{dw}}{dz}]_{-d_1^-}^{-d_1^+} - 0$$
$$- \tilde{\alpha}\hat{w}(-d_1)(\tilde{\alpha}U_m - \omega)[\frac{\tilde{dU}}{dz}]_{-d_1^-}^{-d_1^+} - 0 = 0 \qquad (4.5)$$

which can be solved for $\hat{dw}/dz$ to give

$$[\frac{\hat{dw}}{dz}]_{-d_1} = \frac{\tilde{\alpha}\hat{w}(-d_1)}{(\tilde{\alpha}U_m - \omega)} (u_I' - u_{II}') \qquad \text{at } z = -d_1 \qquad (4.6)$$

Evaluating the integrals in eq. (4.4) at the other discontinuities leads to the remaining two matching conditions.

At $z = -d_2$

$$[\frac{\hat{dw}}{dz}]_{-d_2} = \frac{-\tilde{\alpha}g(\Theta_2 - \Theta_1)\,\hat{w}(-d_2)}{(\tilde{\alpha}\,U\rho - \omega)^2} \qquad (4.7)$$

where

$$U\rho = u_{II} - u_{II}'\,d_2$$

and at $z = -d_3$

$$[\frac{\hat{dw}}{dz}]_{-d_3} = \frac{\tilde{\alpha}\,\hat{w}(-d_3)}{(\tilde{\alpha}U_b - \omega)}\,(u'_{II} - u'_{III}) \tag{4.8}$$

The eigenvalue problem for the salt wedge estuary is given by the solution to the following set of equations:

$$\frac{d^2\hat{w}_j}{dz^2} - \tilde{\alpha}^2\,\hat{w}_j = 0 \tag{4.9}$$

which has solutions of the form

$$\hat{w}_j(z) = a_j \sinh(\tilde{\alpha}z) + b_j \cosh(\tilde{\alpha}z) \tag{4.10}$$

where i indicates the layer in which the solution is valid.

The conditions on the solutions $\hat{w}_j(z)$ are:

$$\text{(a)}\quad \frac{\hat{dw}_1}{dz} - [\frac{\tilde{\alpha}g\Theta}{(\tilde{\alpha}U_s - \omega)^2} + \frac{u'_I}{(\tilde{\alpha}U_s - \omega)}]\,\hat{w}_1 = 0 \qquad \text{at } z = 0$$

$$\text{(b)}\quad \hat{w}_1 = \hat{w}_2 \qquad \text{at } z = -d_1$$

$$\text{(c)}\quad \frac{\hat{dw}_1}{dz} - \frac{\hat{dw}_2}{dz} = \frac{\tilde{\alpha}\,\hat{w}}{(\tilde{\alpha}U_m - \omega)}\,(u'_I - u'_{II}) \qquad \text{at } z = -d_1$$

$$\text{(d)}\quad \hat{w}_2 = \hat{w}_3 \qquad \text{at } z = -d_2 \tag{4.11}$$

$$\text{(e)}\quad \frac{\hat{dw}_2}{dz} - \frac{\hat{dw}_3}{dz} = -\frac{\tilde{\alpha}g(\Theta_2 - \Theta_1)\,\hat{w}_2}{(\tilde{\alpha}\,U\rho - \omega)} \qquad \text{at } z = -d_2$$

$$\text{(f)}\quad \hat{w}_3 = \hat{w}_4 \qquad \text{at } z = -d_3$$

$$(g)\quad \frac{d\hat{w}_3}{dz} - \frac{d\hat{w}_4}{dz} = \frac{\tilde{\alpha}\hat{w}_4}{(\tilde{\alpha}U_b - \omega)}\,(u'_{II} - u'_{III}) \qquad \text{at } z = -d_3$$

$$(h)\quad \hat{w}_4 = 0 \qquad \text{at } z = -h$$

The result of substituting the solution $\hat{w}_j$ into eqs. (4.11) is a set of six linear equations in the unknown coefficients a_j and b_j. The determinant of coefficients of this set of linear equations is the dispersion relation for the system and can be written as a sixth degree polynomial in the frequency, ω.

$$\Phi_6\omega^6 + \Phi_5\omega^5 + \Phi_4\omega^4 + \Phi_3\omega^3 + \Phi_2\omega^2 + \Phi_1\omega + \Phi_0 = 0 \tag{4.12}$$

where the Φ_j are complicated transcendental functions of $\tilde{\alpha}$, the mean velocity, shear and density.

The eigenfunctions take the form:

$$\begin{aligned}
\hat{w}_1(z) &= a_1\,(\Gamma \sinh \tilde{\alpha}z + \tilde{\alpha} \cosh \tilde{\alpha}z)\\
\hat{w}_2(z) &= a_2 \sinh \tilde{\alpha}z + b_2 \cosh \tilde{\alpha}z\\
\hat{w}_3(z) &= a_3 \sinh \tilde{\alpha}z + b_3 \cosh \tilde{\alpha}z\\
\hat{w}_4(z) &= a_4 \sinh \tilde{\alpha}(z + h)
\end{aligned} \tag{4.13}$$

where

$$a_2 = a_1[\Gamma + \psi \cosh \tilde{\alpha}d_1(\Gamma \sinh \tilde{\alpha}d_1 - \tilde{\alpha} \cosh \tilde{\alpha}d_1)]$$

$$b_2 = a_1[\tilde{\alpha} + \psi \sinh \tilde{\alpha}d\,(\Gamma \sinh \tilde{\alpha}d_1 - \tilde{\alpha} \cosh \tilde{\alpha}d_1)]$$

$$a_3 = a_2[1 + \phi \sinh \tilde{\alpha} d_2 \cosh \tilde{\alpha} d_2] - b_2 \phi \cosh^2 \tilde{\alpha} d_2$$

$$b_3 = a_2 \phi \sinh^2 \tilde{\alpha} d_2 + b_2[1 - \phi \sinh \tilde{\alpha} d_2 \cosh \tilde{\alpha} d_2]$$

$$a_4 = [-a_3 \sinh \tilde{\alpha} d_3 + b_3 \cosh \tilde{\alpha} d_3]/\sinh \tilde{\alpha}(h - d_3)$$

$$\Gamma = \frac{\tilde{\alpha} g \Theta}{(\tilde{\alpha} U_s - \omega)^2} + \frac{\tilde{\alpha} u_I'}{(\tilde{\alpha} U_s - \omega)}$$

$$\psi = \frac{(u_I' - u_2')}{(\tilde{\alpha} U_m - \omega)}$$

$$\phi = \frac{\tilde{\alpha} g(\Theta_2 - \Theta_1)}{(\tilde{\alpha} U\rho - \omega)^2}$$

The next step in the solution of the problem posed in eq. (4.4) is to evaluate the solution for the values of $\omega = \tilde{\alpha}\tilde{U}$. Because the coefficient $(\tilde{\alpha}\tilde{U} - \omega)$ is squared there are two separate solutions possible for each $\omega = \tilde{\alpha}\tilde{U}$. These solutions form the continuous spectra of modes which Case (1960) showed are necessary to solve the initial value problem. They are given by the solutions to the following differential equations. The first is

$$\frac{d^2 \hat{w}_a}{dz^2} - \tilde{\alpha}^2 \hat{w}_a = \delta(z + z_o) \tag{4.14}$$

where $\delta(z + z_o)$ is the Dirac delta function and $-z_o$ is the depth at which the velocity $\tilde{U}$ is equal to $\omega/\tilde{\alpha}$.

The second is

$$\frac{d^2\hat{w}_b}{dz^2} - \tilde{\alpha}^2 \hat{w}_b = \delta'(z + z_o) \tag{4.15}$$

where $\delta'(z + z_o)$ is the derivative of the Dirac delta function with respect to z. Making the substitution $\hat{w}_b = \frac{dq}{dz}$, the equation to be solved becomes

$$\frac{d^2q}{dz^2} - \tilde{\alpha}^2 q = \delta(z + z_o) \tag{4.16}$$

The solution of these two equations proceed in the same manner as solution of eq. (4.9) except that there is an additional condition to be applied at $z = -z_o$.

Integrating the equation for $\hat{w}_a$, eq. (4.14) from $z = -z_o - \varepsilon$ to $z = -z_o + \varepsilon$ gives the following condition to be applied at $z = -z_o$:

$$\int_{-z_o-\varepsilon}^{-z_o+\varepsilon} \frac{d^2\hat{w}_a}{dz^2}\, dz - \int_{-z_o-\varepsilon}^{-z_o+\varepsilon} \tilde{\alpha}^2 \hat{w}_a\, dz = \int_{-z_o-\varepsilon}^{-z_o+\varepsilon} \delta(z + z_o)\, dz \tag{4.17}$$

Taking the limit as $\varepsilon \to 0$ and requiring the function $\hat{w}_a$ to be continuous at $z = -z_o$ gives

$$\left.\frac{d\hat{w}_a}{dz}\right|_{z=-z_o^+} - \left.\frac{d\hat{w}_a}{dz}\right|_{z=-z_o^-} = 1 \tag{4.18}$$

Similarly, the condition to be applied to q(z) at $-z_o$ is

$$\left.\frac{dq}{dz}\right|_{z=-z_o^+} - \left.\frac{dq}{dz}\right|_{z=-z_o^-} = 1 \tag{4.19}$$

where the requirement is that q be continuous at $-z_o$. However, from the definition $\hat{w}_b = \frac{dq}{dz}$ it can be seen that the jump condition eq. (4.19) is actually a jump in $\hat{w}_b$ given by

$$\hat{w}_b(-z_o^+) - \hat{w}_b(-z_o^-) = 1$$

The solution of the homogeneous equation (4.4) for the salt wedge is divided into four regions with boundary conditions at the surface (4.11a) and the bottom (4.11h) and matching and jump conditions given by eq. (4.11b-g). The solution $\hat{w}_a$ and $\hat{w}_b$ to the two auxiliary equations (4.14) and (4.15) must also satisfy the conditions given by eqs. (4.11a-h). However, the region is divided into five layers for the solutions of $\hat{w}_a(z)$ and $\hat{w}_b(z)$. The position of the additional internal boundary depends on the depth $z = -z_o$ which is defined by $\tilde{U}(-z_o) = \omega/\tilde{\alpha}$ and can occur anywhere in the region $0 \geq z \geq -h$. The solutions have the form

$$\begin{aligned}
\hat{w}_{a_1} &= A[\Gamma \sinh \tilde{\alpha}z + \tilde{\alpha} \cosh \tilde{\alpha}z] \\
\hat{w}_{a_2} &= a_2 \sinh \tilde{\alpha}z + b_2 \cosh \tilde{\alpha}z \\
\hat{w}_{a_3} &= a_3 \sinh \tilde{\alpha}z + b_3 \cosh \tilde{\alpha}z \\
\hat{w}_{a_4} &= a_4 \sinh \tilde{\alpha}z + b_4 \cosh \tilde{\alpha}z \\
\hat{w}_{a_5} &= a_5 \sinh \tilde{\alpha}(h + z)
\end{aligned} \tag{4.21}$$

and

$$\hat{w}_{bj}(z) = \frac{dq_j}{dz}$$

where

$$\begin{aligned} q_1 &= A'[\tilde{\alpha} \sinh \tilde{\alpha}z + \Gamma \cosh \tilde{\alpha}z] \\ q_2 &= a_2' \cosh \tilde{\alpha}z + b_2' \sinh \tilde{\alpha}z \\ q_3 &= a_3' \cosh \tilde{\alpha}z + b_3' \sinh \tilde{\alpha}z \\ q_4 &= a_4' \cosh \tilde{\alpha}z + b_4' \sinh \tilde{\alpha}z \\ q_5 &= a_5' \cosh \tilde{\alpha}(h + z) \end{aligned} \qquad (4.22)$$

The relationships among the coefficients A, a_j and b_j and A', a_j' and b_j' depend on the depth $-z_o$ relative to $-d_1$, $-d_2$ and $-d_3$ and are different for $-z_o$ in each layer.

Eigenvalues

The value of $\omega(\tilde{\alpha})$ for the auxiliary functions $\hat{w}_a(z)$ and $\hat{w}_b(z)$ are given by $\omega(\tilde{\alpha}) = \tilde{\alpha}\tilde{U}(z_o)$ and form a continuous spectrum of neutral modes. These correspond to the continuous spectrum of neutral modes which arise in the solution of the initial-value problem using Laplace transforms. In the normal mode solutions of the initial-value problem these provide additional modes for fitting arbitrary initial conditions (cf. Chimonas, 1977).

The eigenvalue problem specified by the differential eq. (4.9) and the conditions (4.11a-h) lead to the sixth degree polynomial given by eq. (4.12),

$$F(\tilde{\alpha},\omega) = \sum_{j=0}^{6} \Phi_j(\tilde{\alpha})\ \omega^j \tag{4.23}$$

$\Phi_j(\tilde{\alpha})$ = transcendental functions of $\tilde{\alpha}$.

In general $F(\tilde{\alpha},\omega)$ is a complex function of two complex variables $\tilde{\alpha}$ and ω. However, the stability problem is usually solved as a temporal problem by considering $\tilde{\alpha}$ real or as a spatial problem in which ω is real. Solution of the temporal problem results in ω being given as a function of $\tilde{\alpha}$ as in

$$\omega = f(\tilde{\alpha}) \tag{4.24}$$

For this specific example the temporal problem results in a discrete spectrum of six eigenmodes which are the solutions of the polynomial given in eq. (4.12).

The spatial problem has an eigenvalue relation of the form

$$\tilde{\alpha} = g(\omega) \tag{4.25}$$

which for this example is the solution of a non-linear transcendental equation. As a result of this nothing can be said in general about the number of modes, except that the spectrum is discrete.

The temporal eigenvalues of the salt-wedge problem are investigated to determine the effects of stratification, surface shear, top and bottom boundaries and transport of the water column. The numerical parameters for this study are given in Table II.

The eigenvalues for parameter set A shown in Fig. 13 shows the stable modes associated with the two-layer density profile with no mean motion. The unstable mode in the homogeneous fluid with the velocity profile of set B is shown in Fig. 14. This profile has no shear at the surface. The eigenvalues for parameter set C, which is a combination of A and B, shows the interaction of the two profiles resulting in four unstable modes (Fig. 15).

The effect of the top boundary on the eigenvalues is shown in set D which moves the top boundary far from the density interface. This suppresses two modes as shown in Fig. 16. Reversing the procedure and moving the bottom boundary far from the density interface is given by set E (Fig. 17). Comparing this case with set C (Fig. 15) shows that one mode is suppressed by removing the effect of the bottom boundary. A small positive shear at the surface (Set F, Fig. 18) alters the relative position of the four unstable modes and tends to decrease the magnitude of the two modes associated with the surface. The effect of a positive shear at the surface is to decrease the curvature of the velocity profile. Data Set G (Fig. 19) represents a negative shear at the surface. This

effect is to increase the curvature of the velocity profile and increase the amplitude of the two unstable surface modes.

Moving the density interface to a position near the bottom as in Set H (Fig. 20) has the effect of suppressing all but one mode.

Comparing Data Sets I and J (Figs. 21 and 22) shows that increasing the transport and consequently increasing the shear causes an increase in the value of the unstable mode and introduces an additional unstable mode.

The parameters of the profiles representing salt-wedge estuaries are given in Table III. Profiles 1, 2 and 3 represent the outer region with no surface shear, positive surface shear and negative surface shear, respectively. Profile 4 represents the central regime and Number 5 the inner regime.

The series of Figs. 14, 23, 24 and 25 show the effect on the eigenvalues of increasing the density difference between the layers. For the homogeneous fluid there is one unstable mode. Two unstable modes are added with the two-layer structure. As the density difference becomes greater, the strength of the instability increases as well as the frequency. Figures 23, 24 and 25 show that the scale length of the instability decreases as the density difference increases.

Profile 2 which has a positive surface shear exhibits only one unstable mode over the range of density differences evaluated. Figures 26, 27 and 28 show that with the decreased curvature of the

profile, the increased density appears to stabilize the profile and decrease the scale of instabilities.

The negative shear of Profile 3 not only increases the curvature, but also effectively introduces a second inflection point. This profile has two unstable modes for the homogeneous fluid as shown by the eigenvalues in Fig. 29. Introducing a density difference adds one unstable mode at the scales under consideration as shown in Fig. 30. Further, increasing the density difference either suppresses that unstable mode or moves it to a much smaller scale as shown in Fig. 31. Profiles 4 and 5 each exhibit two unstable modes for the scales being considered as shown in Figs. 32 and 33, respectively.

Finite Time Series Analysis

The solution to the initial-value problem is given by eq. (2.36) or for the two-dimensional problem,

$$w(x,z,t) = \int_{-\infty}^{\infty} \sum_{n=1}^{N} \hat{w}_n(\tilde{\alpha},z) \left[A_n e^{-i\omega_n t} + B_n e^{i\omega_n t}\right] e^{i\tilde{\alpha}x} d\tilde{\alpha} \qquad (4.46)$$

with initial conditions specified by

$$\begin{aligned} \tilde{w}_o(\tilde{\alpha},z) &= \sum_{n=1}^{N} \hat{w}_n(\tilde{\alpha},z) \left[A_n + B_n\right] \\ \frac{\partial \tilde{w}_o}{\partial t}(\tilde{\alpha},z) &= \sum_{n=1}^{N} -i\omega_n \hat{w}_n(\tilde{\alpha},z) \left[A_n - B_n\right] \end{aligned} \qquad (4.47)$$

The initial conditions to be considered are of the form

$$w_o(x,z) = f(z)e^{i\tilde{\alpha}_o x} \tag{4.48}$$

and

$$\frac{\partial w_o}{\partial t}(x,z) = 0$$

which have transforms

$$\tilde{w}_o(\tilde{\alpha},z) = f(z)\ \delta(\tilde{\alpha} - \tilde{\alpha}_o) \tag{4.49}$$

and

$$\frac{\partial \tilde{w}_o}{\partial t}(\tilde{\alpha},z) = 0$$

Substituting the initial conditions eq. (4.49) into (4.47) results in a set of linear equations in the coefficients A_n and B_n.

$$f(z) = \sum_{n=1}^{N} 2A_n \hat{w}_n(\tilde{\alpha}_o,z) \tag{4.50}$$

The salt-wedge estuary problem has six discrete eigenmodes plus two continuous spectra from the singular solutions. The solution is formed from the six discrete eigenmodes and a fixed number, N_1, of the continuous modes. A least squares fit at $(2N_1 + 6)$ equally spaced positions z_n is made to eq. (4.50) to determine the $(2N_1 + 6)$ coefficients A_n.

Two forms of the function f(z) are considered. One is an exponential decaying from the surface and the other is a Gaussian pulse centered at the density interface. The exponential function is of the form

$$f(z) = e^{2\pi z/\lambda} \quad , \quad \lambda = 0.1$$

and the form of the Gaussian pulse is

$$f(z) = e^{-(z + d_2)^2/\lambda^2} \quad , \quad \lambda = 0.1$$

Figure 34 is an expansion of the exponential at $\tilde{\alpha} = 0.5$ using only the six discrete modes from Profile 1. Including 21 modes from each of the singular solutions produces Fig. 35 which has a difference in phase and amplitude at a given time. Figures 36 and 37 show the difference between the exponential and Gaussian z-dependence for an expansion at $\tilde{\alpha} = 0.5$ using eigenvalues from Profile 2. At this wavelength there are no growing modes included in the expansion. An expansion of the exponential at $\tilde{\alpha} = 0.5$ for Profile 3 is shown in Fig. 38.

Asymptotic Analysis

The asymptotic evaluation of the vertical velocity perturbation given by

$$w(x,z,t) = \sum_{n=1}^{N} \int_{-\infty}^{\infty} A_n \hat{w}_n(\tilde{\alpha},z)\, e^{i(\tilde{\alpha}x - \omega t)} d\tilde{\alpha} \qquad (4.51)$$

is derived in Appendix B. The asymptotic form of the vertical velocity perturbation is given by eq. (B.12)

$$w(x,z,t) \sim \frac{\sqrt{2\pi}\ \hat{w}_n(\tilde{\alpha}^*,z)\ e^{it(\tilde{\alpha}^* x/t - \omega^*_n)}\ e^{i\theta}}{\left| t\,\frac{d^2\omega_n}{d\tilde{\alpha}^2}\,(\tilde{\alpha}^*)\right|^{1/2}} \tag{4.52}$$

where $\omega_n(\tilde{\alpha}^*)$ is the most unstable eigenmode.

Figure 39 shows the line of saddle points of the most unstable mode for an asymptotic expansion using Profile 1 with $\Delta\rho = 0.02$. Each point on the line, which is defined by $\partial\omega_i/\partial\alpha_r = 0$, represents a different value of x/t. The contours of $\frac{\partial\omega_i}{\partial\alpha_r}$ near the saddle point on the real axis are shown in Fig. 40. Figs. 41a and b show contours of ω_r and ω_i in the same region. The values of the wavenumber and frequency along the line of saddle points are given in Figs. 42 and 43, respectively. The argument of the exponential in the asymptotic expansion, $(\tilde{\alpha}_* x/t - \omega^*_n)$, is plotted as a function of x/t in Fig. 44. The region of growth of the exponential is clearly defined by the negative imaginary part of this function which extends approximately from -.15 to .95. Figs. 42a and 43a show that over this range the real part of the wavenumber and frequency is nearly constant.

The asymptotic expansion for a flat spectrum of wavenumbers is shown for t = 10 at different depths in Figs. 45, 46, 47 and 48. The same expansion evaluated at t = 100 is shown in Figs. 49, 50,

51 and 52. At this time the packet has become peaked around the most growing ray. For the same initial conditions the expansion of the second most growing mode is shown in Figs. 53 and 54 at $t = 10$ and in Figs. 55 and 56 at $t = 100$. At time $t = 10$, this mode has not fully developed into a wave packet, but the wave packet is obvious at $t = 100$. The amplitude factors indicate that this mode is two orders of magnitude smaller than the dominant mode at $t = 10$ and over 20 orders of magnitude smaller at $t = 100$.

Figs. 57 and 58 show the asymptotic expansion of the solution driven by a Gaussian distribution of standard deviation 0.1. The similarity of this profile and that for a flat spectrum is to be expected because of the nearly constant value of $\tilde{\alpha}$ along the line of saddle points.

The most difficult part of the asymptotic analysis is determination of the line of saddle points. The computation is straightforward but time consuming if $\omega(\tilde{\alpha})$ is a known analytic function. If ω is known only for real values of $\tilde{\alpha}$ and the first two derivatives of ω with respect to $\tilde{\alpha}$ are known or can be approximated, simple ray mathematics is often used to evaluate the asymptotic form. However, Gaster (1978) warns that in non-conservative systems this technique may lead to an incorrect result and should be used with care. To demonstrate the erroneous result which can occur an example is calculated to compare with the correct asymptotic expansion.

Following the description of the technique in Gaster (1978) the eigenvalue and its first derivative are expanded about a point on the real $\tilde{\alpha}$ axis. The wave number on the real axis and functions evaluated at that point are designated by the subscript o.

The Taylor series expansion for the eigenvalue ω about the point on the real axis $\tilde{\alpha}_o$ is given by

$$\omega = \omega_o + (\tilde{\alpha} - \tilde{\alpha}_o) \left.\frac{d\omega}{d\tilde{\alpha}}\right|_o + \frac{1}{2} (\tilde{\alpha} - \tilde{\alpha}_o) \frac{d^2\omega}{d\tilde{\alpha}^2} + \ldots \tag{4.53}$$

The expansion for the first derivative is

$$\frac{d\omega}{d\tilde{\alpha}} = \left.\frac{d\omega}{d\tilde{\alpha}}\right|_o + (\tilde{\alpha} - \tilde{\alpha}_o) \left.\frac{d^2\omega}{d\tilde{\alpha}^2}\right|_o + \ldots \tag{4.54}$$

The point $\tilde{\alpha}_o$ on the real axis is such that

$$x/t = \mathrm{Re}\left(\left.\frac{d\omega}{d\tilde{\alpha}}\right|_o\right)$$

Expanding eq. (4.54) into real and imaginary parts gives

$$\mathrm{Re}\left(\frac{d\omega}{d\tilde{\alpha}}\right) = \mathrm{Re}\left(\left.\frac{d\omega}{d\tilde{\alpha}}\right|_o\right) = x/t \tag{4.55}$$

$$\mathrm{Im}\left(\frac{d\omega}{d\tilde{\alpha}}\right) = \mathrm{Im}\left(\left.\frac{d\omega}{d\tilde{\alpha}}\right|_o\right) + (\tilde{\alpha} - \tilde{\alpha}_o) \left.\frac{d^2\omega}{d\tilde{\alpha}^2}\right|_o + \ldots \tag{4.56}$$

If $\tilde{\alpha}$ is to be a saddle point, $\mathrm{Im}\left(\frac{d\omega}{d\tilde{\alpha}}\right)$ must equal zero.

Equation (4.56) can be solved for the saddle point $\tilde{\alpha}_*$.

$$\tilde{\alpha}_* = \tilde{\alpha}_o - i \left.\frac{d\omega_i}{d\tilde{\alpha}_r}\right|_o \Big/ \left.\frac{d^2\omega}{d\tilde{\alpha}^2}\right|_o \tag{4.57}$$

It should be noted that this is valid only for small values of

$$\left| \left.\frac{d\omega_i}{d\alpha_r}\right|_o \Big/ \tilde{\alpha}_o \left.\frac{d^2\omega}{d\tilde{\alpha}^2}\right|_o \right|$$

which insures that the saddle point $\tilde{\alpha}_*$ lies close to the real axis. The value of the eigenvalue at the saddle point is evaluated by substituting eq. (4.57) into eq. (4.53).

$$\omega_* = \omega_o - i \left[\left.\frac{d\omega_i}{d\tilde{\alpha}_r}\right|_o \Big/ \left.\frac{d^2\omega}{d\tilde{\alpha}^2}\right|_o\right] \left.\frac{d\omega}{d\tilde{\alpha}}\right|_o + \frac{1}{2}\left[\left.\frac{d\omega_i}{d\tilde{\alpha}_r}\right|_o\right]^2 \Big/ \left.\frac{d^2\omega}{d\tilde{\alpha}^2}\right|_o + \ldots \tag{4.58}$$

The form of the asymptotic expansion as given by eq. (B.12) is

$$w(x,z,t) \sim \frac{\sqrt{2\pi}\ \hat{w}_n(\tilde{\alpha}_*, z)\ e^{it(\tilde{\alpha}_*\, x/t\, -\, \omega_*)}}{\left[\left| t \left.\frac{d^2\omega}{d\tilde{\alpha}^2}\right|_* \right|\right]^{1/2}} \tag{4.59}$$

Making the substitutions from eq. (4.55), (4.57) and (4.58), the exponent becomes

$$it(\tilde{\alpha}_*\, x/t - \omega_*) = it\left[\tilde{\alpha}_o\, x/t - \omega_o + \frac{1}{2}\left[\left.\frac{d\omega_i}{d\tilde{\alpha}_r}\right|_o\right]^2 \Big/ \left.\frac{d^2\omega}{d\tilde{\alpha}^2}\right|_o\right] \tag{4.60}$$

Substituting from eq. (4.60) into (4.59), the asymptotic form, assuming the validity of ray mathematics, is

$$w(x,z,t) \sim \frac{\sqrt{2\pi}\ \hat{w}_n(\tilde{\alpha}_*,z)\ e^{it\left[\tilde{\alpha}_o\ x/t - \omega_o + \frac{1}{2}\left(\frac{d\omega_i}{d\tilde{\alpha}_r}\Big|_o\right)^2 \Big/ \frac{d^2\omega}{d\tilde{\alpha}^2}\Big|_o\right]}}{\left|t\ \frac{d^2\omega}{d\tilde{\alpha}^2}\Big|_o\right|^{1/2}} \tag{4.61}$$

Figures 59-64 show the evaluation of the asymptotic form given by eq. (4.61) for an initial condition giving a flat spectrum and using eigenvalues from Profile 1. The form of the function indicates a caustic. The rays as defined above cross and the disturbance at two or more points map into the same region.

Comparing Figs. 59-64 with Figs. 45-52 which are the results of the asymptotic expansion for the same initial conditions and flow parameters clearly indicate the care which must be exercised in using simple ray mathematics as an approximation to the asymptotic limit.

5. Summary

The equations specifying the inviscid linear stability of stratified shear flows are derived and the solutions using normal modes and Fourier-Laplace transforms are discussed. It is shown that solution of the initial value problem by superposition of the normal modes can be accomplished only by including the continuous spectra of singular solutions because the normal modes do not form a complete set. Examination of the Fourier-Laplace transform solution indicates that it is equivalent to the normal mode solution including the singular solutions.

The infinite two layer system is used to demonstrate a power series technique for evaluating the short time distortion of an initial pulse. The three dimensional structure of the asymptotic development of the pulse is also shown.

The complicated interaction of boundaries, density interface, shear and curvature of the velocity profile in determining the stability of a system is demonstrated by the eigenvalues calculated for the finite two-layer piecewise-continuous velocity profile of Section 4. Varying the parameters of the system has led to generalizations which may be applicable to a salt-wedge estuary. Increasing shear in the velocity profile leads to more unstable modes. In the physical system this could occur during periods of increased river runoff. A downstream wind leads to a positive shear in the velocity profile at the surface and a decrease in the

curvature of the velocity profile which tends to stabilize the system. Conversely, an upstream wind increases the curvature and tends to destabilize the system. Over the range of density differences included in the calculations, it appears that increasing the stratification generally destabilizes the system.

For a conservative system which has only real eigenvalues the asymptotic expansion of the Fourier inversion integral is obtained by the technique of ray mathematics. However, in a non-conservative system the use of this technique combined with analytic continuation of the eigenvalues into the complex plane is shown to give incorrect results because the x/t mapping is not unique. The correct expansion using the saddle-point method demonstrates that solutions of the dispersion relation for real values of the wavenumber is not sufficient. The eigenvalues and derivatives in the complex α-plane are required for the correct asymptotic expansion of the initial-value problem for a non-conservative system.

References

Banks, W.H.H., P.G. Drazin and M.B. Zaturska (1976), "On the Normal Modes of Parallel Flow of Inviscid Fluid," Journal of Fluid Mechanics, Vol. 75, pp. 149-171.

Case, K.M. (1960), "Stability of Inviscid Plane Couette Flow," Physics of Fluids, Vol. 3, pp. 143-148.

Case, K.M. (1961), "Hydrodynamic Stability and the Inviscid Limit," Journal of Fluid Mechanics, Vol. 10, pp. 420-429.

Chimonas, G. (1979), "Algebraic Disturbances in Stratified Shear Flows," Journal of Fluid Mechanics, Vol. 90, pp. 1-19.

Criminale, William O., Jr. (1960), "Three-Dimensional Laminar Instability," Advisory Group for Aeronautical Research and Development. Report No. 266.

Davey, M.K. (1977), "Baroclinic Instability in a Fluid with Three Layers," Journal of the Atmospheric Sciences, Vol. 34, pp. 1224-1234.

Drazin, P.G. (1958), "The Stability of a Shear Layer in an Unbounded Heterogeneous Inviscid Fluid," Journal of Fluid Mechanics, Vol. 4, pp. 214-224.

Drazin, P.G. (1961), "Discontinuous Velocity Profiles for the Orr-Sommerfeld Equation," Journal of Fluid Mechanics, Vol. 10, pp. 571-583.

Gaster, M. (1968), "The Development of Three-Dimensional Wave Packets in a Boundary Layer," Journal of Fluid Mechanics, Vol. 32, pp. 173-184.

Gaster, M. (1977), "On the Application of Ray Mathematics to Non-Conservative Systems," Geofluiddynamical Wave Mathematics, Research Contributions. Conference Board of the Mathematical Sciences/National Science Foundation Regional Research Conference in the Mathematical Sciences, Applied Mathematics Group, University of Washington.

Hazel, Philip (1972), "Numerical Studies of the Stability of Inviscid Stratified Shear Flows," Journal of Fluid Mechanics, Vol. 51, pp. 39-61.

Jeffreys, H. and Bertha S. Jeffreys (1956), Methods of Mathematical Physics, Cambridge University Press.

Lalas, D.P., F. Einaudi and D. Fua (1976), "The Destabilizing Effect of the Ground on Kelvin-Helmholtz Waves in the Atmosphere," Journal of the Atmospheric Sciences, Vol. 33, pp. 59-69.

Lin, C.C. (1967), The Theory of Hydrodynamic Stability, Cambridge University Press.

Maslowe, S.A. and R.E. Kelly (1971), "Inviscid Instability of an Unbounded Heterogeneous Shear Layer," Journal of Fluid Mechanics, Vol. 48, pp. 405-415.

Pedlosky, Joseph (1964), "An Initial-Value Problem in the Theory of Baroclinic Instability," Tellus, Vol. 16, pp. 12-17.

Squire, H.B. (1933), "On the Stability for Three-Dimensional Disturbances of Viscous Fluid Flow Between Parallel Walls," Proceedings of the Royal Society. A, Vol. 142, pp. 621-628.

APPENDIX A

Fourier-Laplace transform solution of the initial value problem

In Section II Fourier-Laplace transforms are applied to the equations of motion to derive an ordinary differential equation in the vertical perturbation velocity, eq. 2.27, subject to the boundary conditions given by eq. 2.19 and 2.20. Applying the Squire transformation to these equations results in the following:

$$(s + i\tilde{\alpha}\tilde{U})\left(\frac{d^2}{dz^2} - \tilde{\alpha}^2\right)\hat{w} - (s + i\tilde{\alpha}\tilde{U})(i\tilde{\alpha}\tilde{U}'')\hat{w}$$

$$+ \tilde{J}(z)\hat{w} = (s + 2i\tilde{\alpha}\tilde{U})\left(\frac{d^2}{dz^2} - \tilde{\alpha}^2\right)\tilde{w}_o$$

$$- i\tilde{\alpha}\tilde{U}''\tilde{w}_o + \left(\frac{d^2}{dz^2} - \tilde{\alpha}^2\right)\frac{\partial \tilde{w}_o}{\partial t} \qquad (A.1)$$

$$= Q_o(\tilde{\alpha}, z; s)$$

$$\frac{d\hat{w}}{dz} + \left[\frac{g\tilde{\alpha}^2\Theta}{(s + i\tilde{\alpha}\tilde{U})^2} - \frac{i\tilde{\alpha}\tilde{U}_z}{(s + i\tilde{\alpha}\tilde{U})}\right]\hat{w} = 0 \qquad \text{at } z = 0$$

or

$$\frac{d\hat{w}}{dz} + \lambda(\tilde{\alpha}, s)\hat{w} = 0 \qquad (A.2)$$

and

$$\hat{w} = 0 \qquad \text{at } z = -h \qquad (A.3)$$

Dividing through the differential equation by the coefficient of the highest order term gives the form

$$\frac{d^2\hat{w}}{dz^2} + \left[\frac{\tilde{J}}{(s + i\tilde{\alpha}\tilde{U})^2} - \frac{i\tilde{\alpha}\tilde{U}''}{(s + i\tilde{\alpha}\tilde{U})} - \tilde{\alpha}^2 \right] \hat{w} = \frac{Q_o(\tilde{\alpha},z,s)}{(s + i\tilde{\alpha}\tilde{U})^2} \qquad (A.4)$$

or

$$\frac{d^2\hat{w}}{dz^2} + \Lambda(\tilde{J},\tilde{U},s,\tilde{\alpha})\ \hat{w} = \frac{Q_o(\tilde{\alpha},z,s)}{(s + i\tilde{\alpha}\tilde{U})^2}$$

Assume that $\phi_1(z;s)$ and $\phi_2(z;s)$ are two independent solutions of the homogeneous differential equation such that

$$\hat{w}(z,s) = A\phi_1(z,s) + B\phi_2(z,s) \qquad (A.5)$$

Making the substitution of the solution in the form A.5 into the boundary conditions A.2 and A.3 leads to the eigenvalue relation

$$F(\tilde{\alpha},s;\tilde{J},\tilde{U}) = 0 \qquad (A.7)$$

for a non-trivial solution of the form A.5.

The self-adjoint differential equation A.4 has the Green's function solution

$$\hat{w}(\tilde{\alpha},z;s) = \int_{-h}^{o} \frac{G(z,z_o)\ Q_o(\tilde{\alpha},z,s)}{(s + i\tilde{\alpha}\tilde{U})^2}\, dz_o \qquad (A.8)$$

where the Green's function, $G(z,z_o)$, is the solution of the differential equation

$$\frac{d^2G}{dz^2} + \Lambda G = \delta(z + z_o) \tag{A.9}$$

Let ψ_1 and ψ_2 be two independent solutions of equation A.9 subject to the following equations.

On ψ_1,

$$\frac{d\psi_1}{dz} + \lambda\psi_1 = 0 \qquad \text{at } z = 0 \tag{A.10}$$

On ψ_2,

$$\psi_2 = 0 \qquad \text{at } z = -h \tag{A.11}$$

At the point $z = -z_o$, the functions ψ_1 and ψ_2 are continuous and have a jump in the first derivative equal to unity, i.e.,

$$\psi_1(-z_o) = \psi_2(-z_o)$$

$$\left.\frac{d\psi_1}{dz}\right|_{z=-z_o} - \left.\frac{d\psi_2}{dz}\right|_{z=-z_o} = 1 \tag{A.12}$$

This implies that

$$\psi_1(-z_o)\left.\frac{d\psi_2}{dz}\right|_{z=-z_o} - \psi_2(-z_o)\left.\frac{d\psi_1}{dz}\right|_{z=-z_o} = W(\psi_1,\psi_2) \neq 0 \tag{A.13}$$

where $W(\psi_1,\psi_2)$ is the Wronskian of ψ_1 and ψ_2.

Applying the above conditions leads to the following form for the Green's function.

$$G(z,z_o) = \begin{cases} \dfrac{\psi_1(z)\psi_2(z_o)}{W(\psi_1,\psi_2)} & 0 \geq z \geq -z_o \\ \dfrac{\psi_2(z)\psi_1(z_o)}{W(\psi_1,\psi_2)} & z_o \geq z \geq -h \end{cases} \tag{A.14}$$

The functions, ψ_j can be rewritten in terms of the linearly independent solutions of the homogeneous differential equation, A.4, ϕ_1 and ϕ_2. The form of the solution is

$$\psi_1(z) = \phi_1(z)\phi_2(-h) - \phi_2(z)\phi_1(-h) \tag{A.15}$$

and

$$\psi_2(z) = \phi_1(z)\left[\frac{d\phi_2(o)}{dz} + \lambda\phi_2(o)\right] - \phi_2(z)\left[\frac{d\phi_1(o)}{dz} + \lambda\phi_1(o)\right] \tag{A.16}$$

From these definitions of the functions, ψ_j, it follows that the Wronskian can be written

$$W(\psi_1,\psi_2) = -\tilde{F(\alpha},s)W(\phi_1,\phi_2) \tag{A.17}$$

and the Green's function is of the form

$$G(z,z_o) = \frac{G'(z,z_o)}{F(\tilde{\alpha},s)W(\phi_1,\phi_2)} \tag{A.18}$$

Substituting the Green's function into equation A.8, gives the solution to the differential equation A.4 in the integral form:

$$\hat{\tilde{w}}(\tilde{\alpha},z,s) = \int_{-h}^{o} \frac{G'(z,z_o)Q_o(\tilde{\alpha},z,s)}{F(\tilde{\alpha},s)W(\phi_1,\phi_2)(s + i\tilde{\alpha}\tilde{U})^2}\, dz_o \tag{A.19}$$

The function $\hat{\tilde{w}}(\tilde{\alpha},z,s)$ is the Fourier-Laplace transform of the solution to the initial value problem which can be written as

$$w(x,z,t) = \frac{1}{2\pi i}\int_{-\infty}^{\infty}\int_{\varepsilon-i\infty}^{\varepsilon+i\infty}\cdot\int_{-h}^{o}\frac{G'(z,z_o)Q_o(\tilde{\alpha},z,s)\, e^{i\tilde{\alpha}x}e^{st}}{F(\tilde{\alpha},s)W(\phi_1,\phi_2)(s + i\tilde{\alpha}\tilde{U})^2} \cdot dz_o\, ds\, d\tilde{\alpha} \tag{A.20}$$

To understand the information contained in this equation, consider the problem of a linear shear in a homogeneous fluid, i.e., $\tilde{U}''(z) = 0$ and $\tilde{J}(z) = 0$. There are no singularities in the differential equation A.4 and the functions ϕ_1 and ϕ_2 are analytic. Evaluating the integral over s first in equation A.20 shows that contributions to the integral are from the poles of the integrand. These contributions are in the form of a sum of exponentials arising from the sum of the residues.

The poles of the integrand are at the zeros of $F(\tilde{\alpha},s)$ and of $[s + i\tilde{\alpha}\tilde{U}(z_o)]$. The function $F(\tilde{\alpha},s) = 0$ is the eigenvalue relation for the problem and the contribution to the integral from these poles is equivalent to the discrete normal modes solution. The

contributions from the zeros of $[s + i\tilde{\alpha}\tilde{\tilde{U}}(z_o)]$ form a continuous spectrum of modes, because the final solution is also integrated over z_o. As Case (1960) and Pedlosky (1964) pointed out, the singular solutions to the differential equation which arise from the continuous spectrum must be added to any normal modes solutions for the initial value problem in order to fit an arbitrary set of initial conditions.

If $\tilde{U}''(z)$ and $\tilde{J}(z)$ are not zero everywhere in the domain of the problem, the situation is more complicated because the differential equation is singular at z_* defined by

$$s - i\tilde{\alpha}\tilde{\tilde{U}}(z_*) = 0 \tag{A.21}$$

For simplicity assume that z_* is a regular singular point. One solution is then of the form

$$\phi_1(z) = (z - z_*)^r X_1(z) \tag{A.22}$$

where $X_1(z)$ is analytic.

The exponent r is one of the solutions to the indicial equation

$$r(r-1) + (s + i\tilde{\alpha}\tilde{\tilde{U}})^2 \left[\frac{\tilde{J}(z_*)}{(s + i\tilde{\alpha}\tilde{U})^2} - \frac{i\tilde{\alpha}\tilde{\tilde{U}}''(z_*)}{(s + i\tilde{\alpha}\tilde{U})} - \tilde{\alpha}^2\right] = 0 \tag{A.23}$$

If the difference between the two roots, $(r_1 - r_2)$, is not an integer, then the other independent solution to A.4 is of similar form:

$$\phi_2(z) = (z - z_*)^{r_2} X_2(z)$$

However, if $(r_1 - r_2)$ is an integer the form of the solution is

$$\phi_2(z) = (z - z_*)^{r_2} [X_1(z) ln(z - z_*) + X_2(z)] \qquad (A.25)$$

Evaluation of the inverse Fourier-Laplace transform in eq. A.20 now includes the possibility of branch points at the zeros of $(s + i\alpha\tilde{\tilde{U}})$ as well as poles.

This general problem is discussed in a paper by Chimonas (1979). He again establishes the necessity of including the continuous spectra of modes in the evaluation of an initial value problem. In addition, he establishes that these modes may indeed lead to instabilities of the system. They do not appear as instabilities of the vertical velocity perturbation, but as horizontal velocity or density perturbations which grow algebraically without limit. In addition, he establishes the instability of these solutions only if the Richardson number of the flow falls below 0.25 somewhere in the region of the flow.

APPENDIX B

Asymptotic Analysis

The solution to the initial-value problem can be evaluated as an integral of the form:

$$w(x,z,t) = \sum_{n=1}^{N} \int_{-\infty}^{\infty} A_n \hat{w}_n(\tilde{\alpha},z)\, e^{i(\tilde{\alpha}x - \omega_n t)} d\tilde{\alpha} \qquad (B.1)$$

The asymptotic evaluation of this integral can be accomplished using the method of steepest descents. The technique described below follows the discussion in Jeffreys and Jeffreys (1956).

Rewrite the integral in the form:

$$w(x,z,t) = \sum_{n=1}^{N} \int_{-\infty}^{\infty} A_n \hat{w}_n(\tilde{\alpha},z)\, e^{tq_n(\tilde{\alpha})} d\tilde{\alpha} \qquad (B.2)$$

where $q_n(\tilde{\alpha}) = i(\tilde{\alpha}\, x/t - \omega_n)$ is a complex function of the complex variable $\tilde{\alpha}$. The saddle point of the function $q_n(\tilde{\alpha})$ is at a point $\tilde{\alpha}_*$ defined by

$$\left.\frac{dq_n}{d\tilde{\alpha}}\right|_{\tilde{\alpha}=\tilde{\alpha}_*} = 0 \qquad \text{or} \qquad x/t - \left.\frac{d\omega_n}{d\tilde{\alpha}}\right|_{\tilde{\alpha}=\tilde{\alpha}_*} = 0 \qquad (B.3)$$

If the second derivative of $q_n(\tilde{\alpha})$ is not zero at $\tilde{\alpha}_*$, expand $q_n(\tilde{\alpha})$ in a Taylors series about the saddle point.

$$q_n(\tilde{\alpha}) = q_n(\tilde{\alpha}_*) + \frac{1}{2}(\tilde{\alpha} - \tilde{\alpha}_*) \left.\frac{d^2 q_n}{d\tilde{\alpha}^2}\right|_{\tilde{\alpha}=\tilde{\alpha}_*} + \ldots \tag{B.4}$$

The direction of the path of integration is chosen such that

$(\tilde{\alpha} - \tilde{\alpha}_*) \left.\frac{d^2 q_n}{d\tilde{\alpha}^2}\right|_{\tilde{\alpha}_*}$ is real and negative.

Define a new variable ζ such that

$$\frac{1}{2}\zeta^2 = q_n(\tilde{\alpha}) - q_n(\tilde{\alpha}_*) \tag{B.5}$$

Change the variable in the integral to ζ and the integral becomes

$$\begin{aligned} w(x,z,t) &= \sum_{n=1}^{N} \int_{-\infty}^{\infty} \hat{w}_n(\tilde{\alpha},z)\, e^{q_n(\tilde{\alpha}_*)t}\, e^{-\frac{1}{2}\zeta^2 t} \frac{d\tilde{\alpha}}{d\zeta}\, d\zeta \\ &= \sum_{n=1}^{N} e^{q_n(\tilde{\alpha}_*)t} \int_{-\infty}^{\infty} \hat{w}_n(\tilde{\alpha},z)\, e^{-\frac{1}{2}\zeta^2 t} \frac{d\tilde{\alpha}}{d\zeta}\, d\zeta \end{aligned} \tag{B.6}$$

Along the path of integration let

$$\tilde{\alpha} - \tilde{\alpha}_* = r\, e^{i\theta} \tag{B.7}$$

where r is real. Then ζ becomes

$$\zeta^2 = -\left.\frac{d^2 q_n}{d\tilde{\alpha}^2}\right|_{\tilde{\alpha}_*} r^2\, e^{2i\theta} \tag{B.8}$$

real and negative, or

$$\zeta = \pm\, r \left|\left.\frac{d^2 q}{d\tilde{\alpha}^2}\right|_{\alpha_*}\right|^{1/2}$$

and

$$\frac{d\zeta}{d\tilde{\alpha}} = \pm e^{i\theta} \left| \frac{d^2 q_n}{d\tilde{\alpha}^2} \Big|_{\tilde{\alpha}_*} \right|^{1/2}$$

because the path is chosen such that $(\tilde{\alpha} - \tilde{\alpha}_*) \frac{d^2 q_n}{d\tilde{\alpha}^2}\Big|_{\tilde{\alpha}_*}$ is real and negative. There are two possible choices for the value of θ. The correct value is determined by the specific problem to insure that the path of integration goes through the saddle point in the correct sense.

The integral in B.6 can now be written

$$w(x,z,t) = \sum_{n=1}^{N} \int_{-\infty}^{\infty} \frac{\hat{w}_n(\tilde{\alpha},z)\, e^{-\frac{1}{2}t\zeta^2}\, e^{i\theta}}{\left| \frac{d^2 q_n}{d\tilde{\alpha}^2} \Big|_{\alpha_*} \right|^{1/2}} \, d\zeta \qquad \text{(B.9)}$$

Watson's lemma states that an integral of the form

$$I = \int_A^B e^{-\frac{1}{2}b^2 z^2} f(z)\, dz \qquad \text{(B.10)}$$

is asymptotic to

$$\sim \sqrt{2\pi} \left(\frac{a_o}{b} + \frac{a_2}{b^3} + \ldots + 1.3 \ldots (2n+1) \frac{a_{2n}}{b^{2n+1}} \right) \qquad \text{(B.11)}$$

where

$$f(z) = a_o + a_1 z + \ldots + a_n z^n + \ldots$$

The integral in eq. B.9 is of the form of Watson's lemma. The first term of the asymptotic expansion of eq. B.9 using Watson's lemma is

$$w(x,z,t) \sim \frac{\sqrt{2\pi}\,\hat{w}_m(\tilde{\alpha}_*,z)\; e^{it(\tilde{\alpha}_* x/t - \omega^*_m)}\; e^{i\theta}}{\left\| t\,\dfrac{d^2\omega_m}{d\tilde{\alpha}^2}\Big|_{\tilde{\alpha}_*} \right\|^{1/2}} \tag{B.12}$$

The expansion of the asymptotic analysis from the two-dimensional case described above to the three-dimensional problem is accomplished following the derivation by Gaster (1968).

The integral to be evaluated is given by

$$w\,(x,y,z,t) = \sum_{m=1}^{N} \int_{-\infty}^{\infty}\int_{-\infty}^{\infty} A_m \hat{w}_m(\alpha,\gamma,z)\; e^{i(\alpha x + \gamma y - \omega_m t)} \tag{B.13}$$

$$\cdot\, d\alpha d\gamma$$

Again in the asymptotic limit only the most growing mode will contribute to the leading terms of the expansion. The integral to be evaluated is of the form

$$I_k = \int_{-\infty}^{\infty} A_k \hat{w}_k(\alpha,\gamma,z)\; e^{i(\alpha x + \gamma y - \omega_k t)}\, d\alpha d\gamma \tag{B.14}$$

In Gaster's analysis the asymptotic form of the integral over α is evaluated first. For this integration, γ is treated as a parameter. This integration is of the same form as described in the

two-dimensional case and can be evaluated using eq. B.12. The integral becomes

$$I_k = \int_{-\infty}^{\infty} \frac{A_k \hat{w}(\alpha_*, \gamma, z)}{\left[t \frac{d^2\omega}{d\alpha^2} (\alpha_*, \gamma) \right]^{1/2}} e^{i[\alpha_* x/t + \gamma y/t - \omega(\alpha_*, \gamma)]t} d\gamma \tag{B.15}$$

where α_* is defined by eq. B.3.

$$x/t - \frac{\partial \omega}{\partial \alpha} (\alpha_*, \gamma) = 0 \tag{B.16}$$

The next step is to expand the exponent in the integral in eq. B. 15 about the point γ_*. The exponent takes the form

$$i[\alpha_* x/t + \gamma_* y/t - \omega(\alpha_*, \gamma_*)]\, t + i[y/t - \frac{\partial \omega}{\partial \gamma} (\alpha_*, \gamma_*)]\, t(\gamma - \gamma_*)$$

$$- i\left[\frac{\partial^2 \omega}{\partial \gamma^2} + 2 \frac{\partial^2 \omega}{\partial \alpha \partial \gamma} \frac{d\alpha_*}{d\gamma} + \frac{\partial^2 \omega}{\partial \alpha^2} \left(\frac{d\alpha_*}{d\gamma} \right)^2 \right] t \frac{(\gamma - \gamma_*)^2}{2} + \ldots \tag{B.17}$$

The choice of γ_* to be the saddle point defined by

$$y/t - \frac{\partial \omega}{\partial \gamma} (\alpha_*, \gamma_*) = 0 \tag{B.18}$$

eliminates the linear terms in the expansion. Evaluating the integral as before and making substitutions from above, the asymptotic form becomes

$$; I_k \sim \frac{A_k \hat{w}_k(\alpha_*, \gamma_*, z)\, e^{i(\alpha_* x + \gamma_* y - \omega_* t)}}{t\left[\left.\frac{\partial^2 \omega}{\partial \alpha^2}\right|_{\alpha_*, \gamma_*} \cdot \left.\frac{\partial^2 \omega}{\partial \gamma^2}\right|_{\alpha_*, \gamma_*} - \left(\left.\frac{\partial^2 \omega}{\partial \alpha \partial \gamma}\right|_{\alpha_*, \gamma_*} \right)^2 \right]^{1/2}} \qquad \text{(B.19)}$$

The phase factor and constant have not been carried along in the three-dimensional analysis because it is the shape of the function that is of primary interest and they alter only the amplitude, not the shape.

AD-A079 525 WASHINGTON UNIV SEATTLE DEPT OF OCEANOGRAPHY F/G 20/4
INITIAL-VALUE PROBLEMS IN STRATIFIED SHEAR FLOWS.(U)
1979 J E BRADT AFOSR-78-3655
UNCLASSIFIED AFOSR-TR-79-1358 NL

2 OF 2
AD
A079525

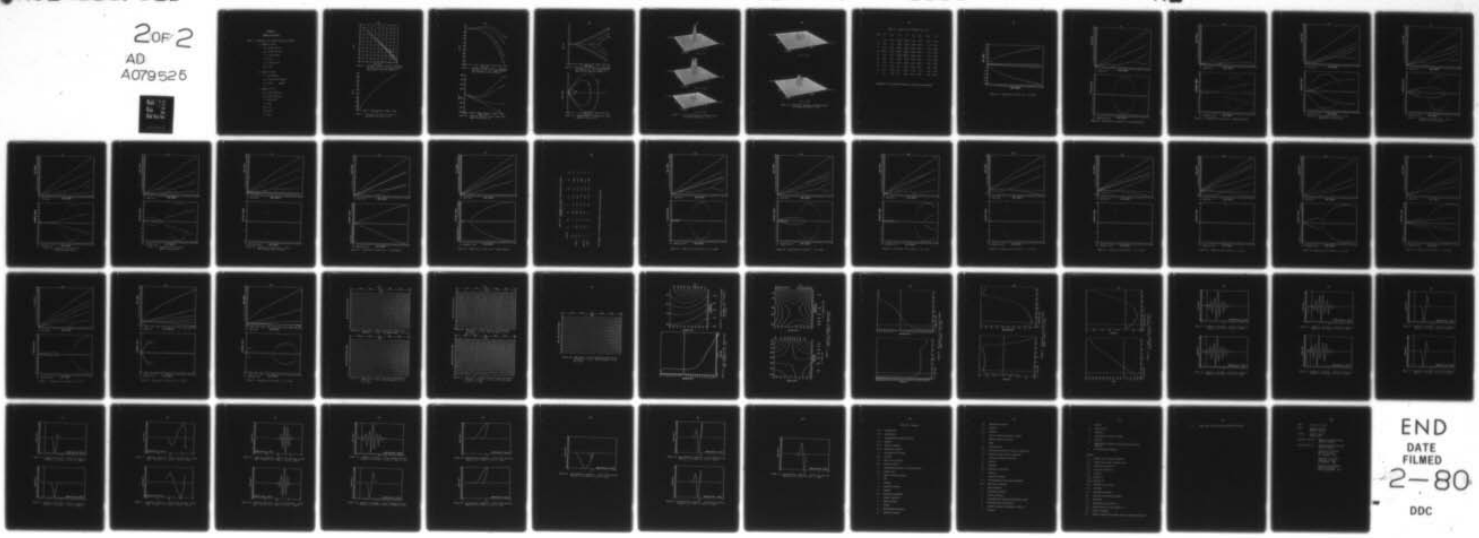

END
DATE FILMED
2-80
DDC

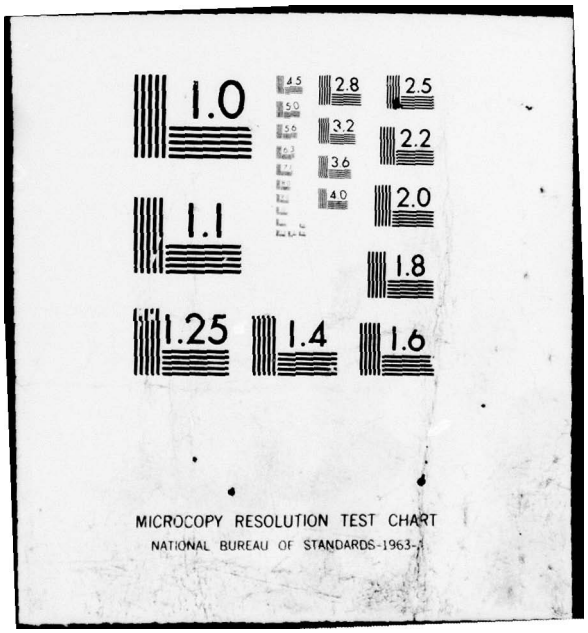
1.0
1.1
1.25
1.4
1.6
1.8
2.0
2.2
2.5
2.8
3.2
3.6
4.0
4.5
5.0
5.6
6.3
MICROCOPY RESOLUTION TEST CHART
NATIONAL BUREAU OF STANDARDS-1963-A

APPENDIX C

Tables and Figures

Table I. Parameters for Infinite Two-Layer Example.

a. Figures 5 and 6

$h_o = 1.02 \times 10^{1}$ cm

$t_o = 1.02 \times 10^{-1}$ sec

$\tau = 7.227 \times 10^{-4}$

$u = 1.0$

$\Theta_1 = 1.293 \times 10^{-3}$

$\Theta_2 = 1.02$

b. Figures 7 and 8

$\underline{\tau} = 74$ cm^3/sec^2

$\rho_1 = 1.293 \times 10^{-3}$ gm/cm^3

$\rho_2 = 1.02$ gm/cm^3

c. Figures 9 to 12

$h_o = 1.02 \times 10^{-1}$ cm

$t_o = 1.02 \times 10^{-2}$ sec

$\tau = 9.8 \times 10^{-2}$

$u = 1.0$

$\Theta_1 = 1.0$

$\Theta_2 = 1.02$

$\lambda = 0.1$

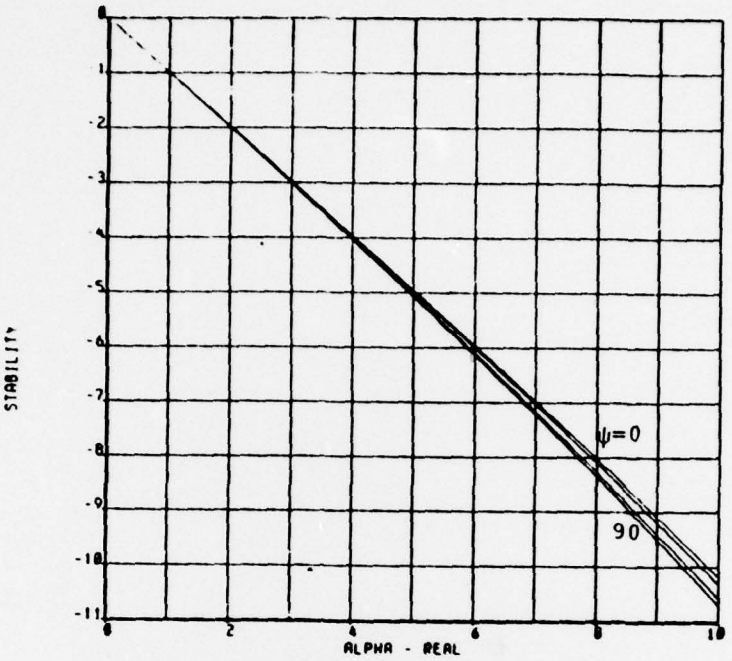

Figure 5. Stability function (-Q) vs. wavenumber for data set Ia. (ψ = angle between mean velocity and wave normal.)

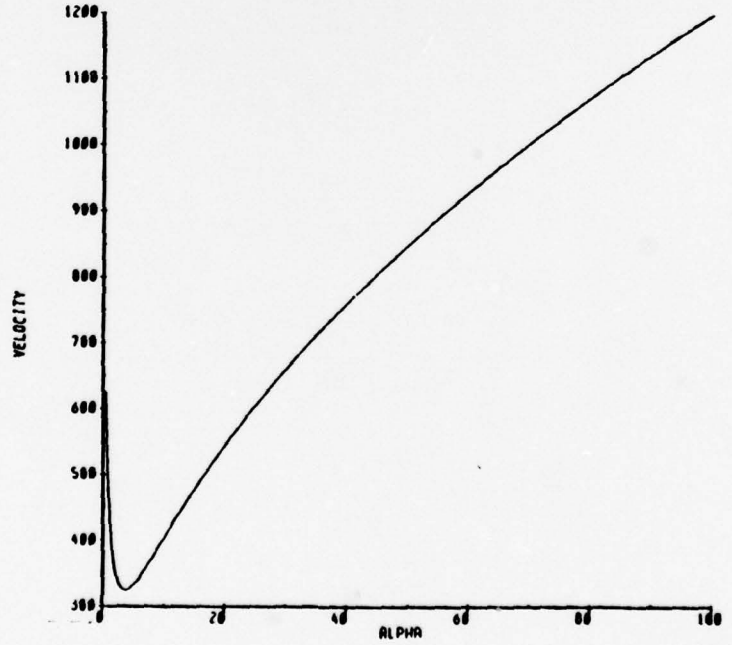

Figure 6. Velocity of stability boundary vs. wavenumber for data set Ia.

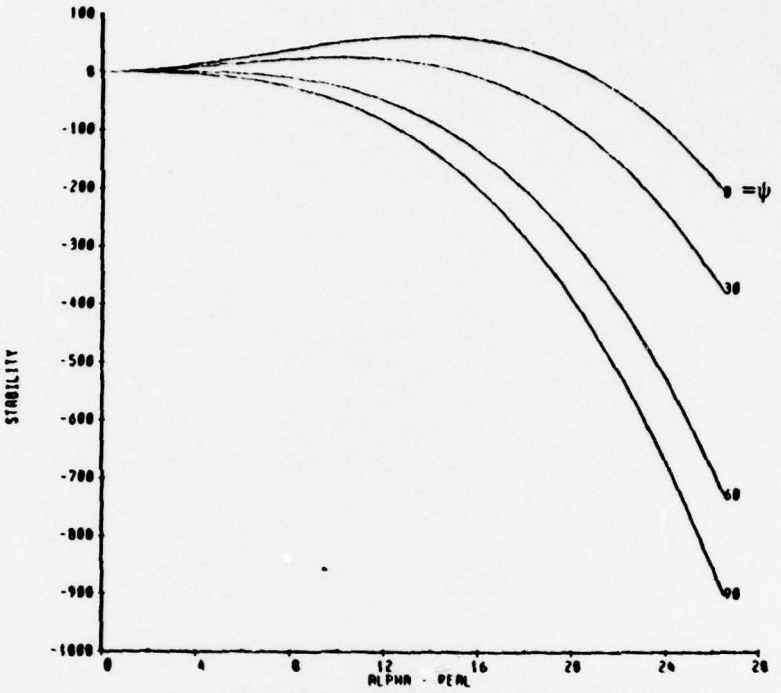

Figure 7. Stability function (-Q) vs. wavenumber for data set Ib. (ψ = angle between mean velocity and wave normal.)

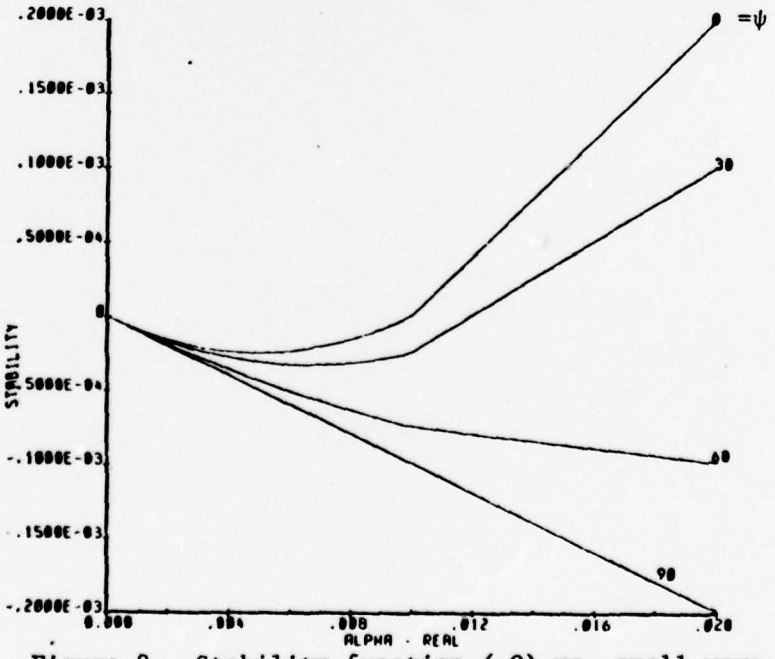

Figure 8. Stability function (-Q) vs. small wavenumber for data set Ib.

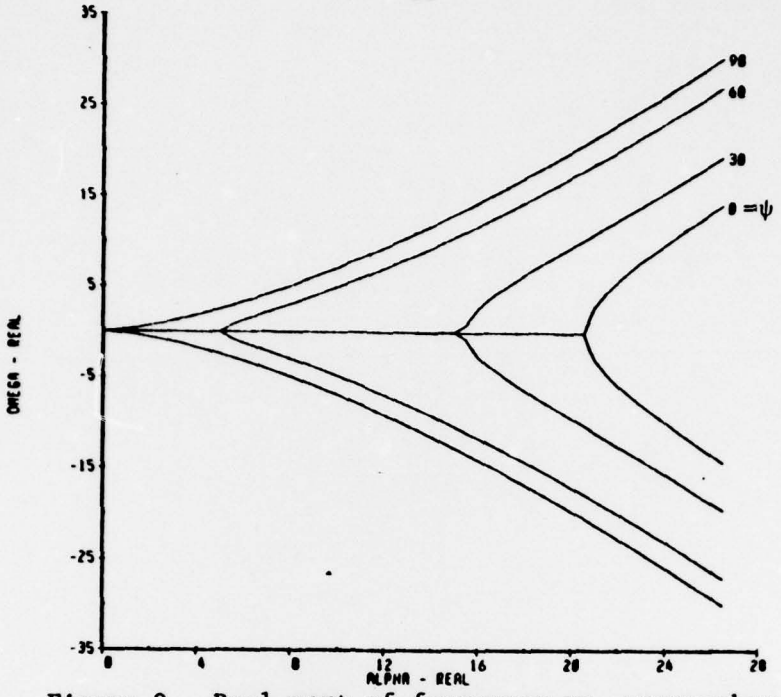

Figure 9. Real part of frequency vs. wavenumber for data set Ic. (ψ = angle between mean velocity and wave normal.)

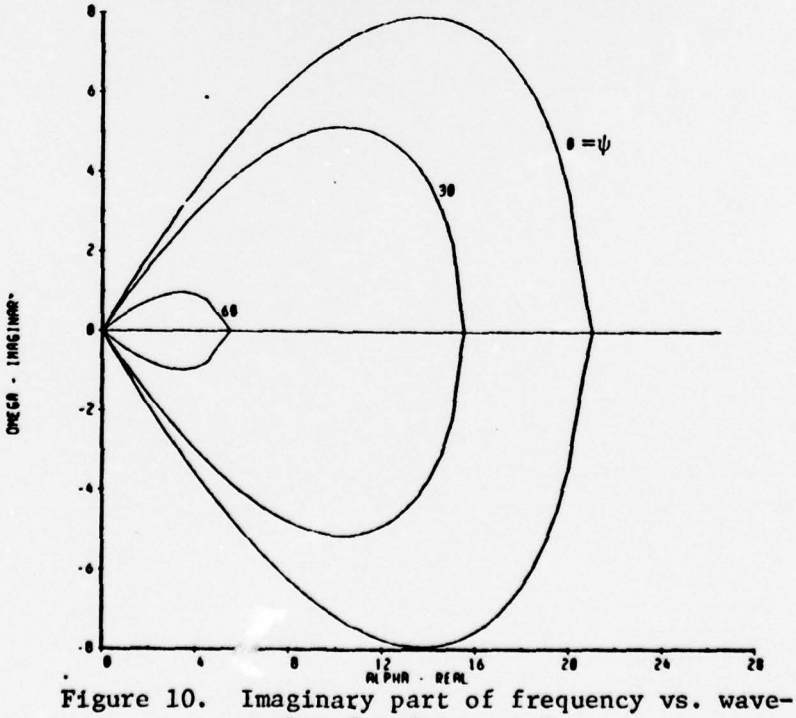

Figure 10. Imaginary part of frequency vs. wavenumber for data set Ic.

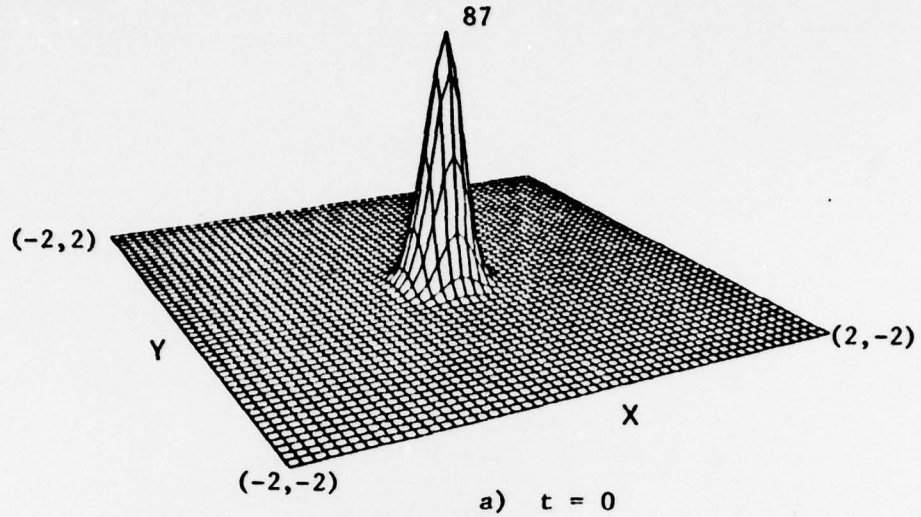

a) t = 0

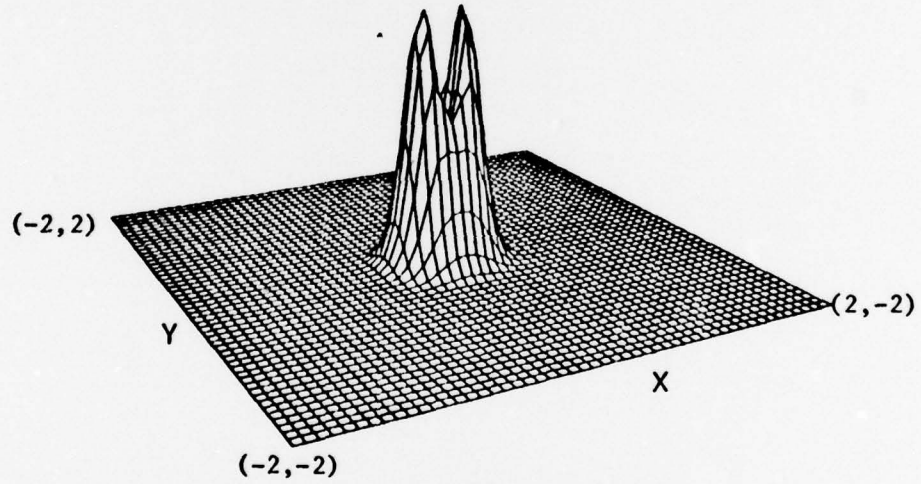

b) t = 0.05

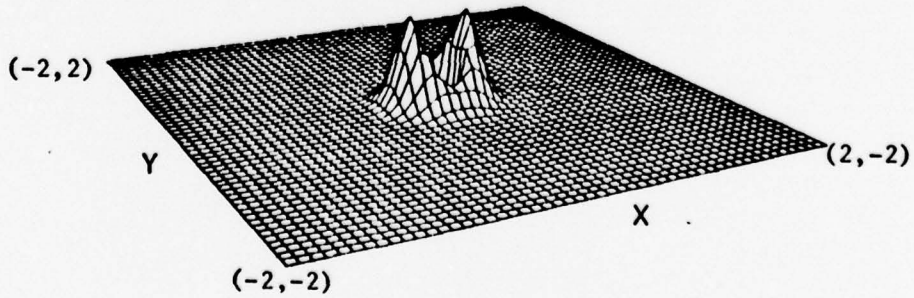

c) t = 0.75

Figure 11. Initial distortion of Gaussian pulse of standard deviation $\lambda = 0.1$.

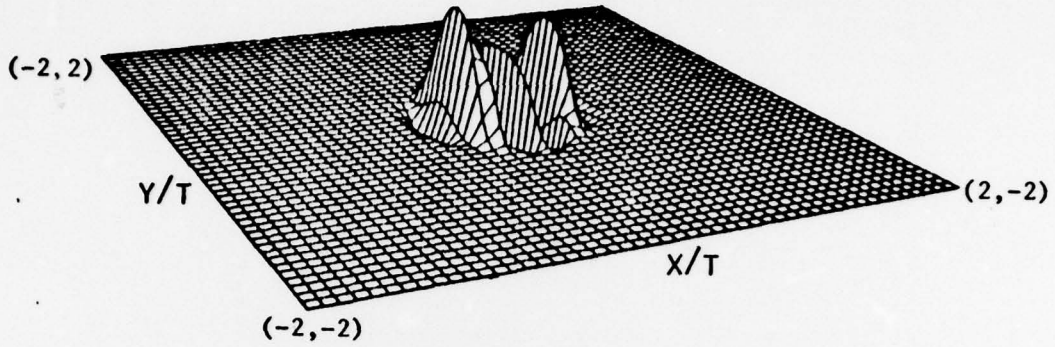

a) t = 20

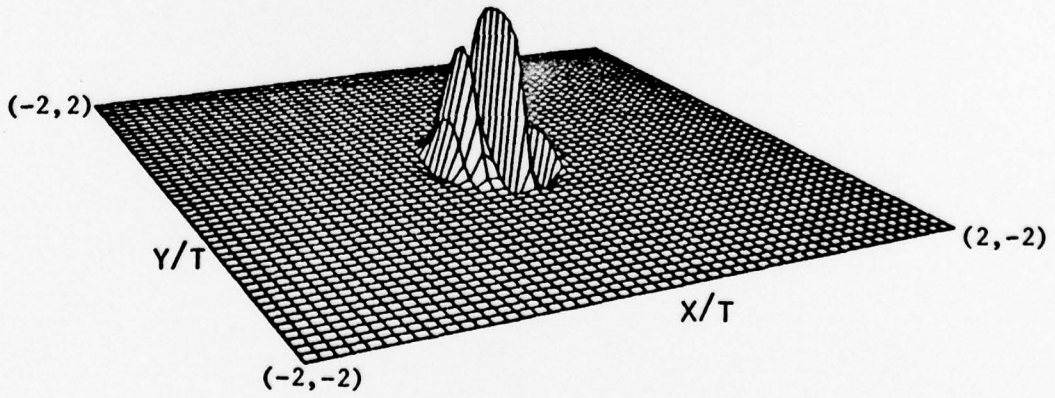

b) t = 60

Figure 12. Asymptotic expansion of Gaussian pulse of standard deviation $\lambda = 0.1$.

Table II. Parameters for Figures 13 to 22.

Set	d_1	d_2	d_3	h	U_s	U_m	U_b	$\Delta\Theta$
A	1.0	2.0	3.85	10.0	0.0	0.0	0.0	0.02
B	1.0	2.0	3.85	10.0	10.0	10.0	-.14	0.0
C	1.0	2.0	3.85	10.0	10.0	10.0	-.14	0.02
D	91.0	92.0	93.85	100.0	10.0	10.0	-.14	0.02
E	1.0	2.0	3.85	100.0	10.0	10.0	-.14	0.02
F	1.0	2.0	3.85	10.0	11.0	10.0	-.14	0.02
G	1.0	2.0	3.85	10.0	9.0	10.0	-.14	0.02
H	1.0	7.45	8.0	10.0	10.0	10.0	-.14	0.02
I	2.5	2.53	3.5	10.0	7.11	7.11	-.89	0.02
J	2.5	2.53	3.5	10.0	16.0	16.0	-.20	0.02

See Figure 4 for schematic diagram of profiles and parameters.

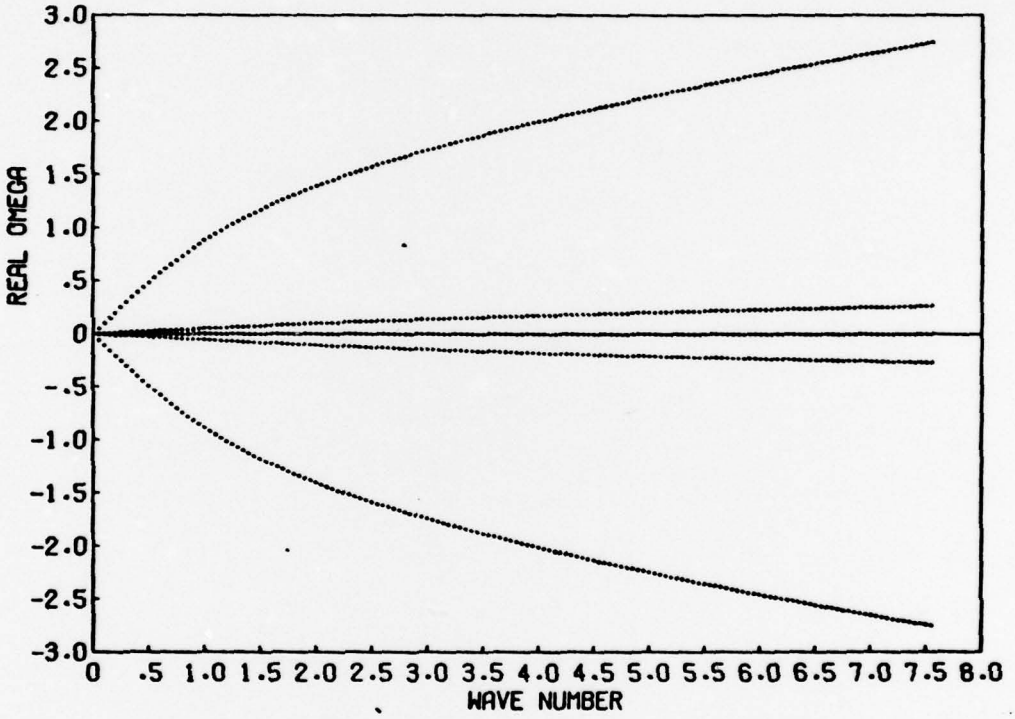

Figure 13. Eigenvalues for data set A. No shear.

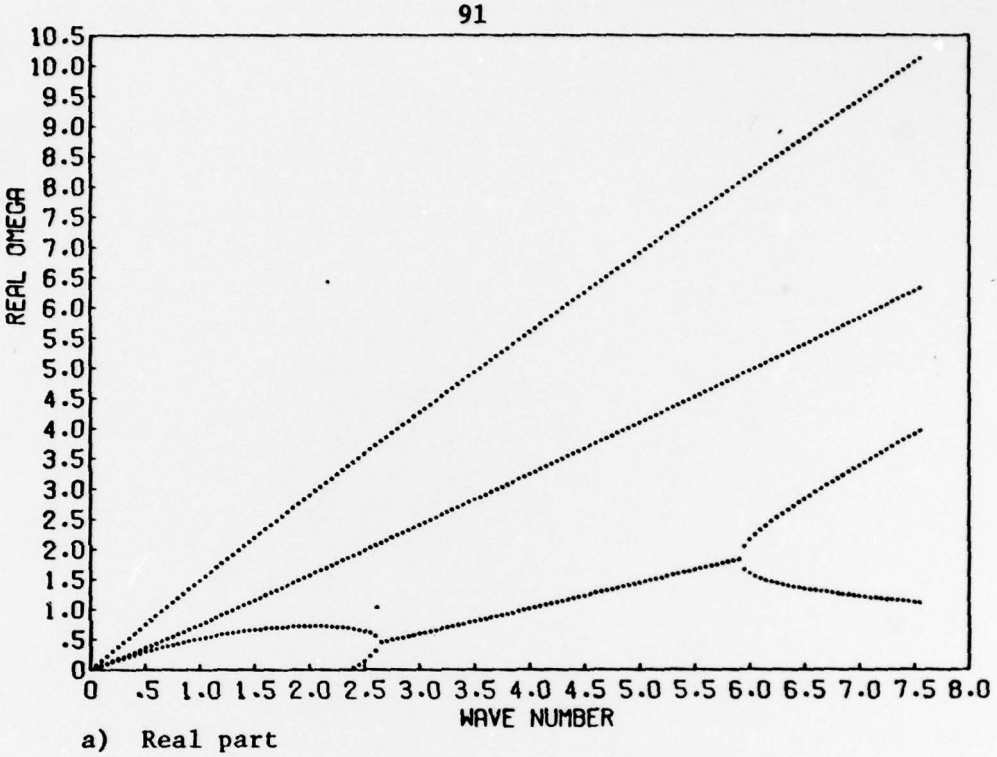

a) Real part

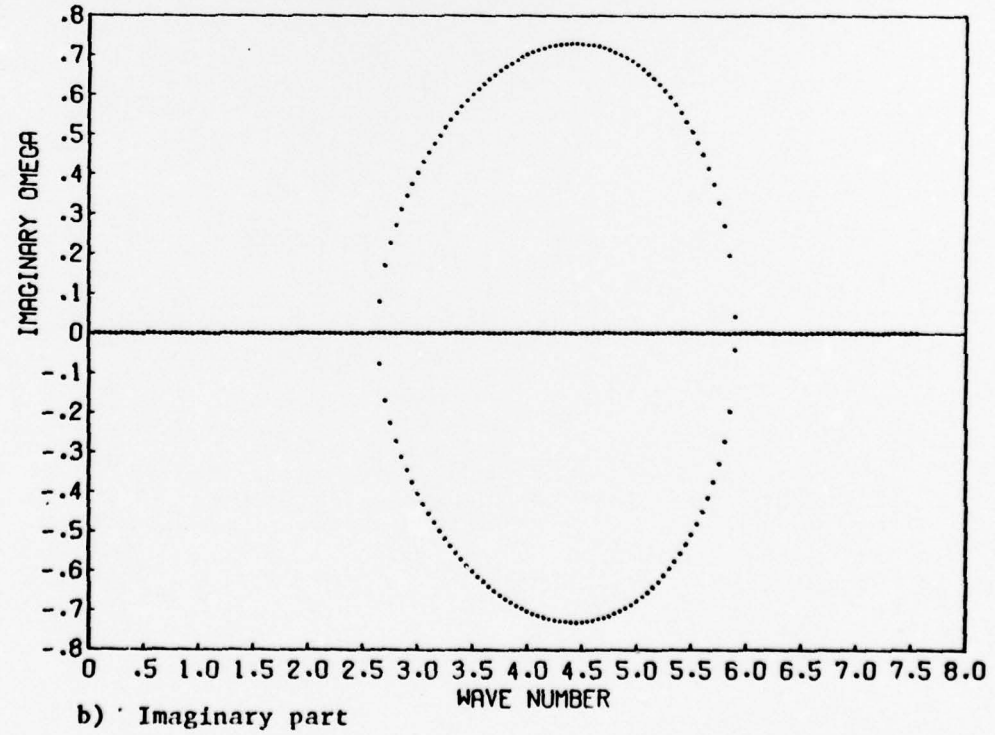

b) Imaginary part

Figure 14. Eigenvalues for data set B. No stratification.

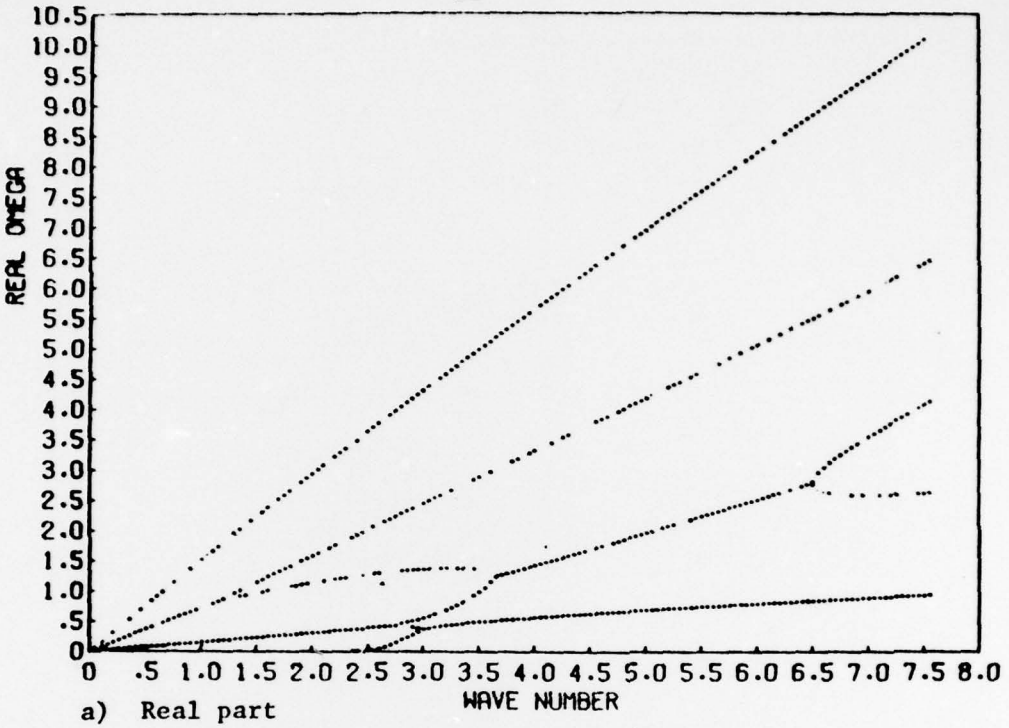

a) Real part

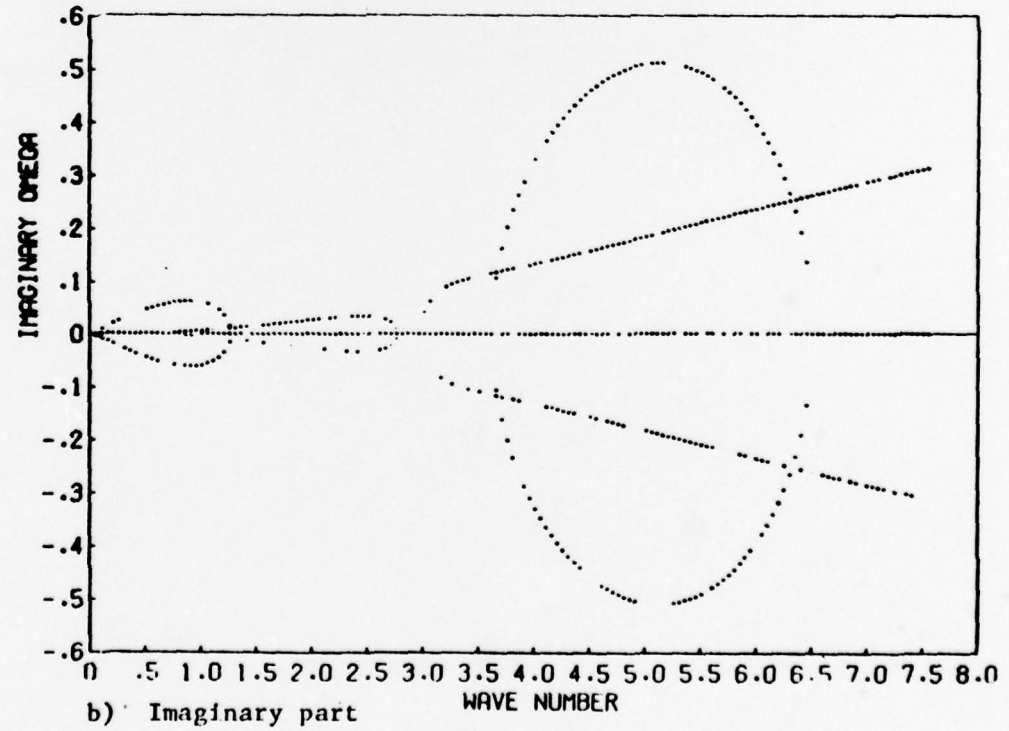

b) Imaginary part

Figure 15. Eigenvalues for data set C. Combined profiles.

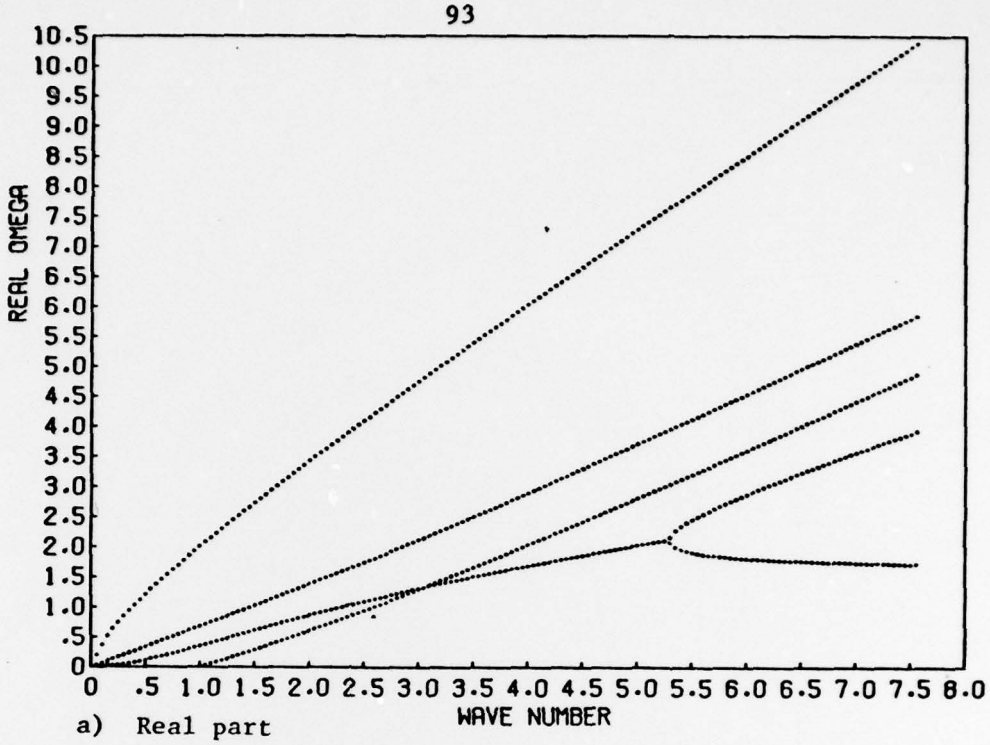

a) Real part

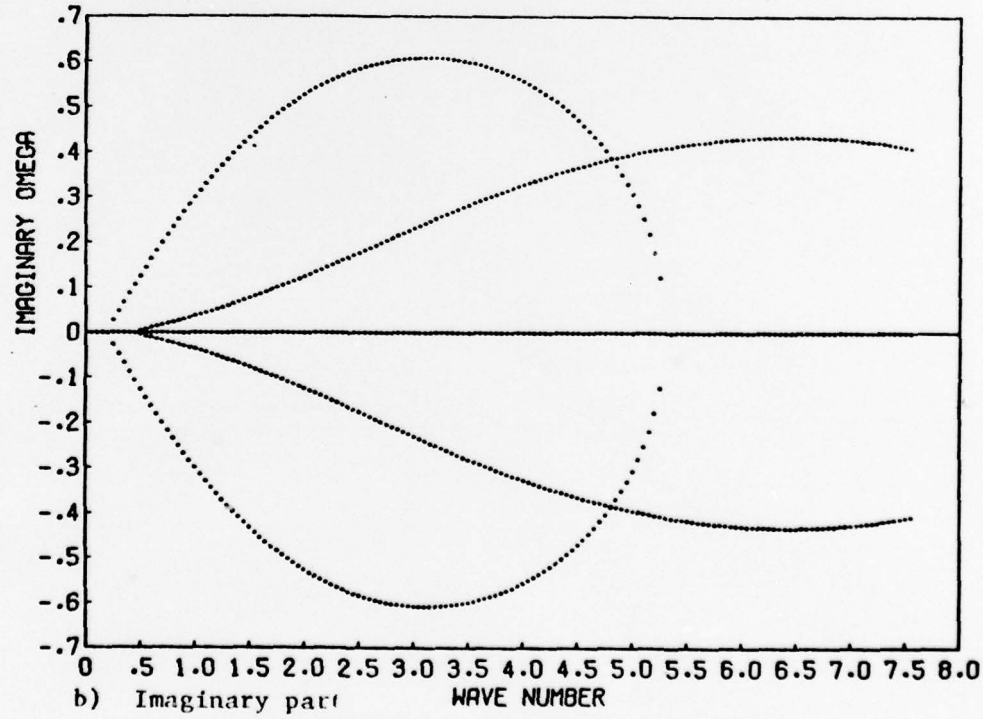

b) Imaginary part

Figure 16. Eigenvalues for data set D. Top boundary far from interface.

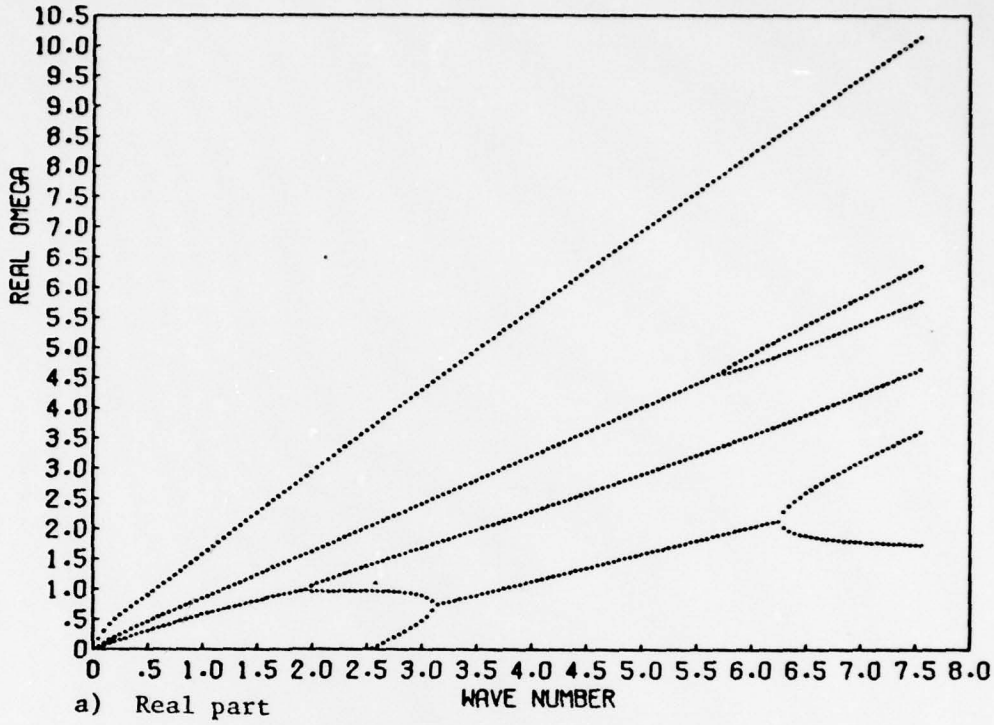

a) Real part

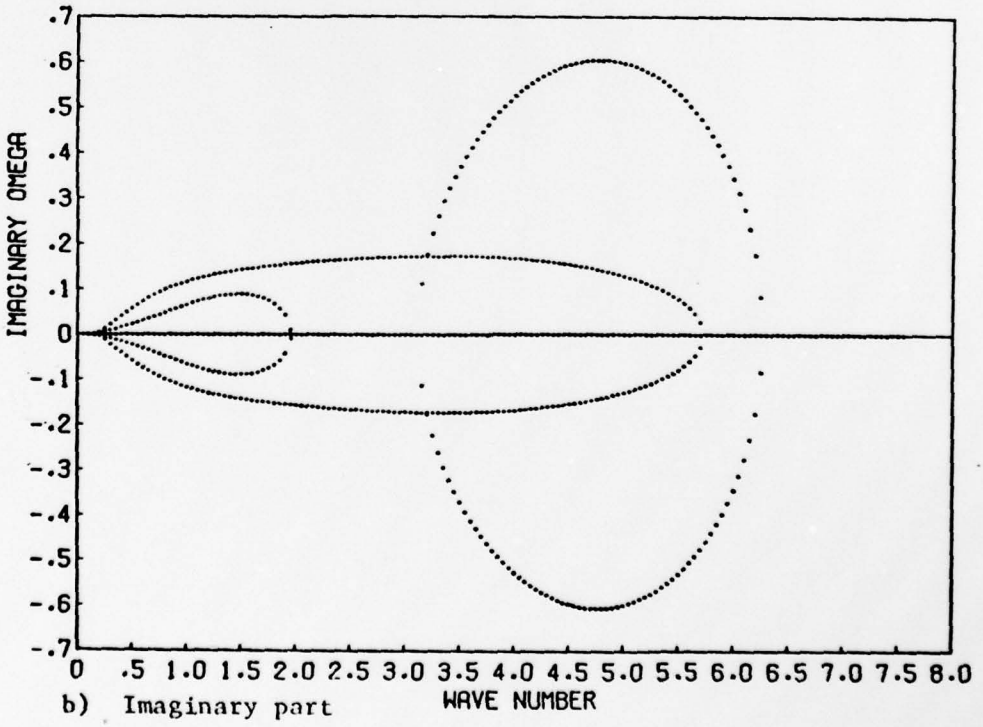

b) Imaginary part

Figure 17. Eigenvalues for data set E. Bottom boundary far from interface.

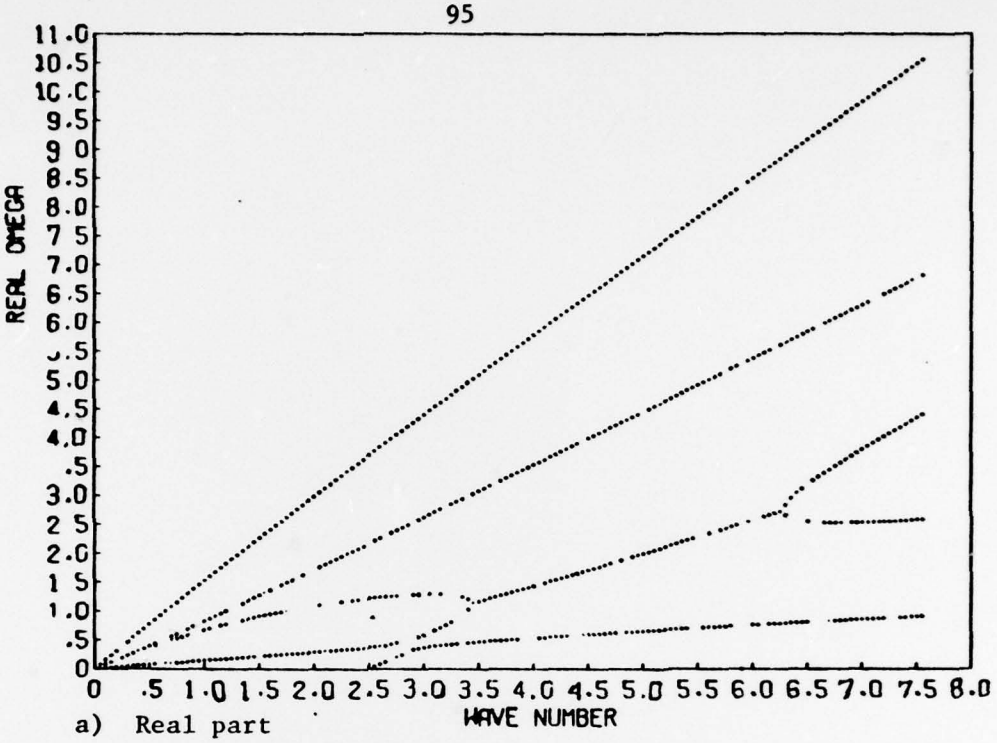

a) Real part

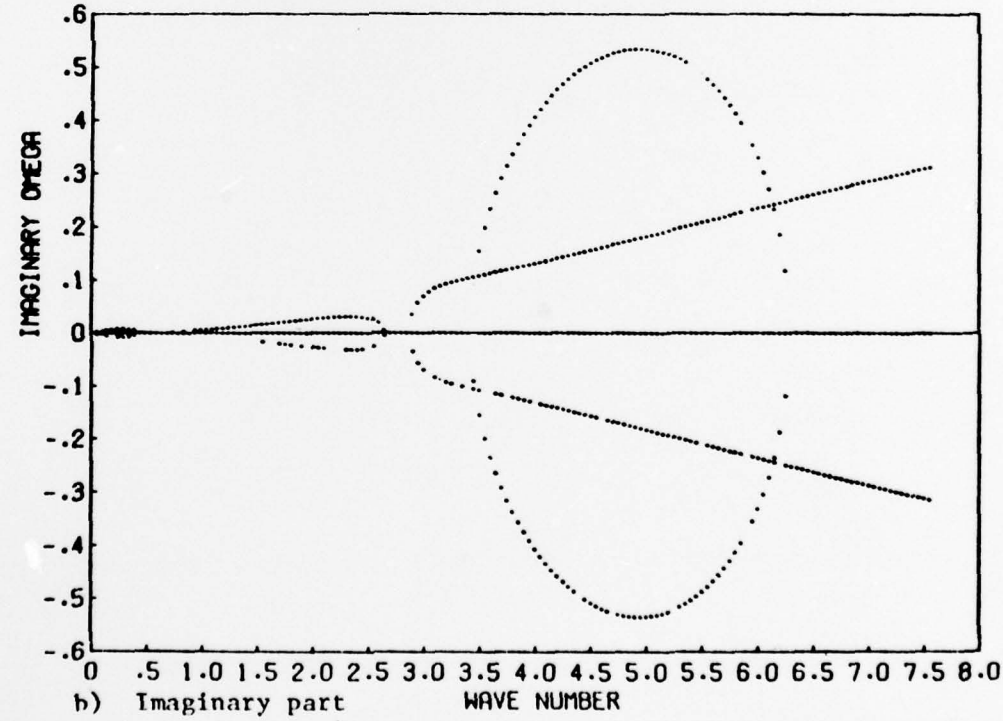

b) Imaginary part

Figure 18. Eigenvalues for data set F. Positive surface shear.

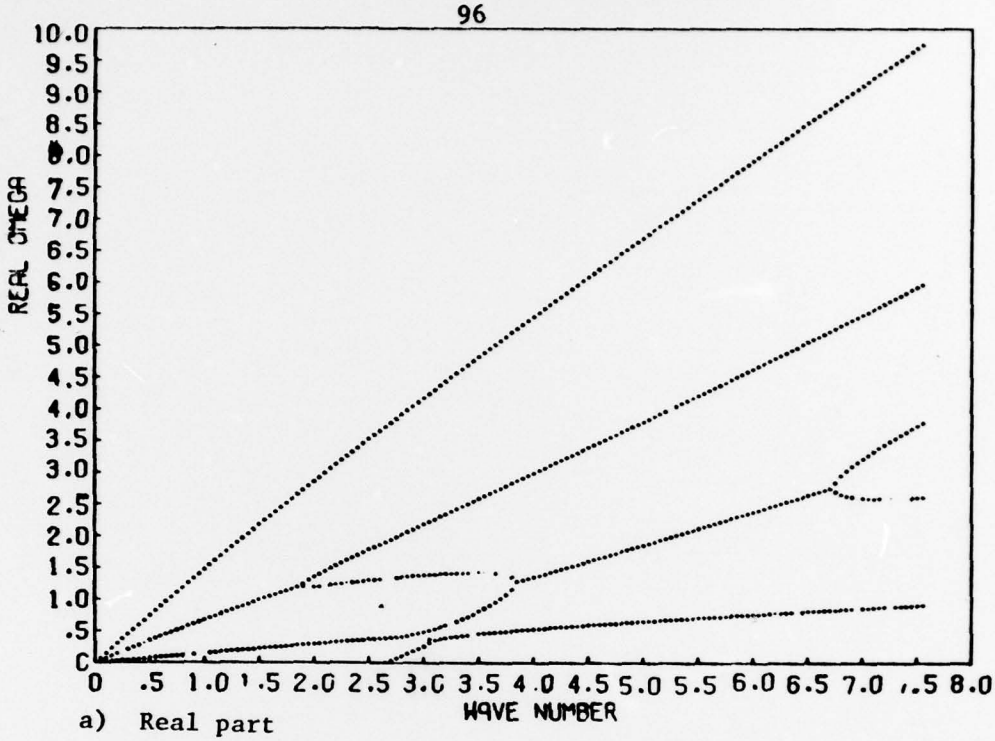

a) Real part

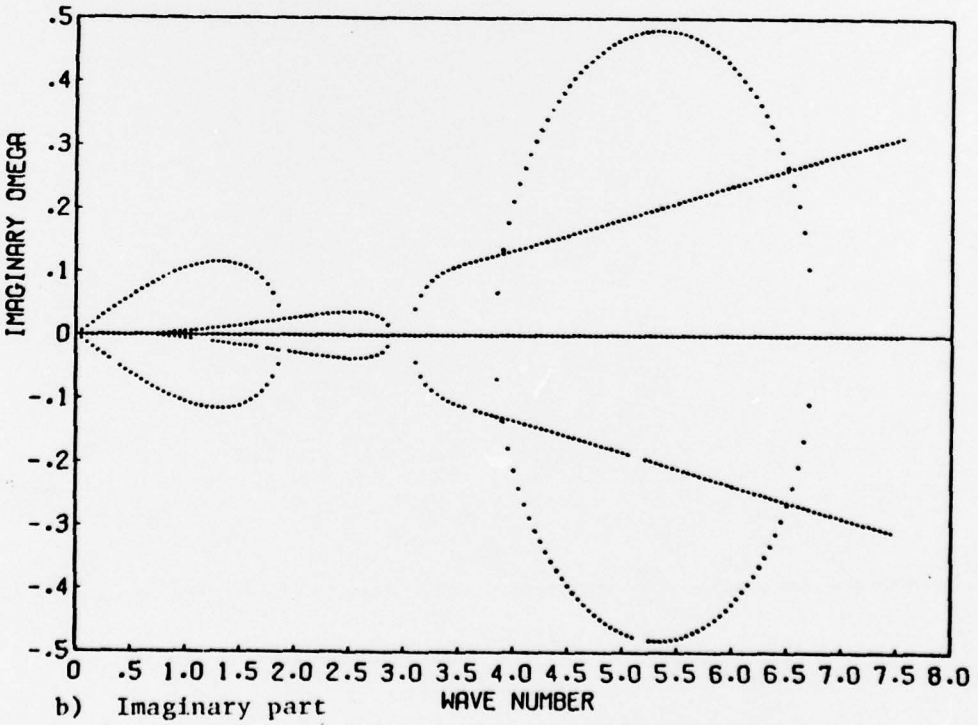

b) Imaginary part

Figure 19. Eigenvalues for data set G. Negative surface shear.

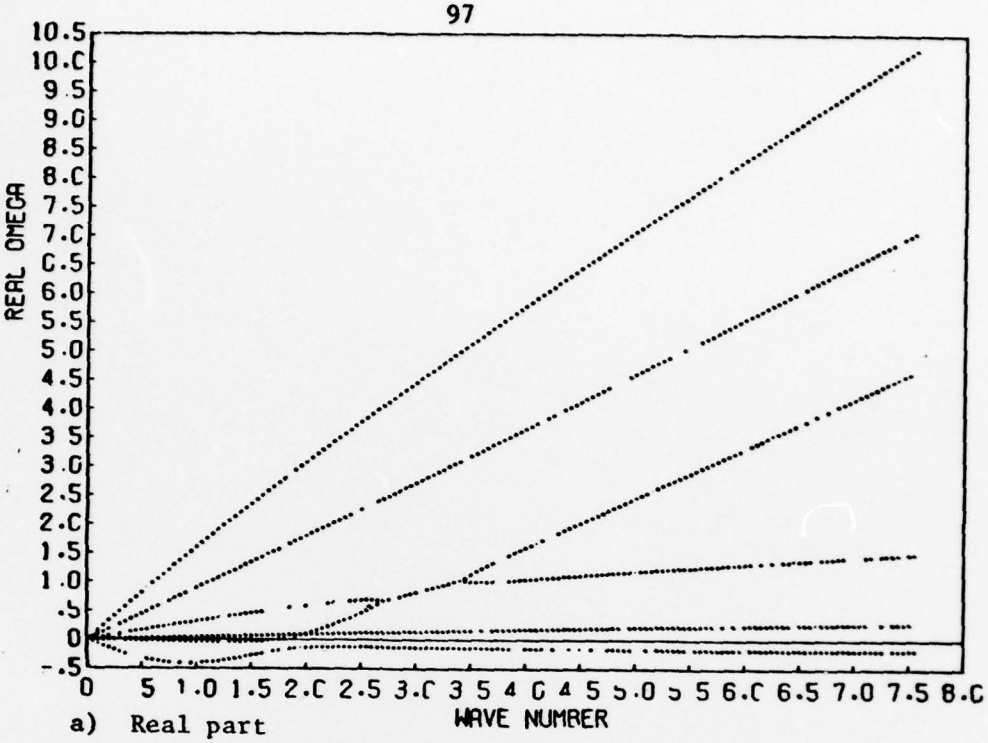

a) Real part

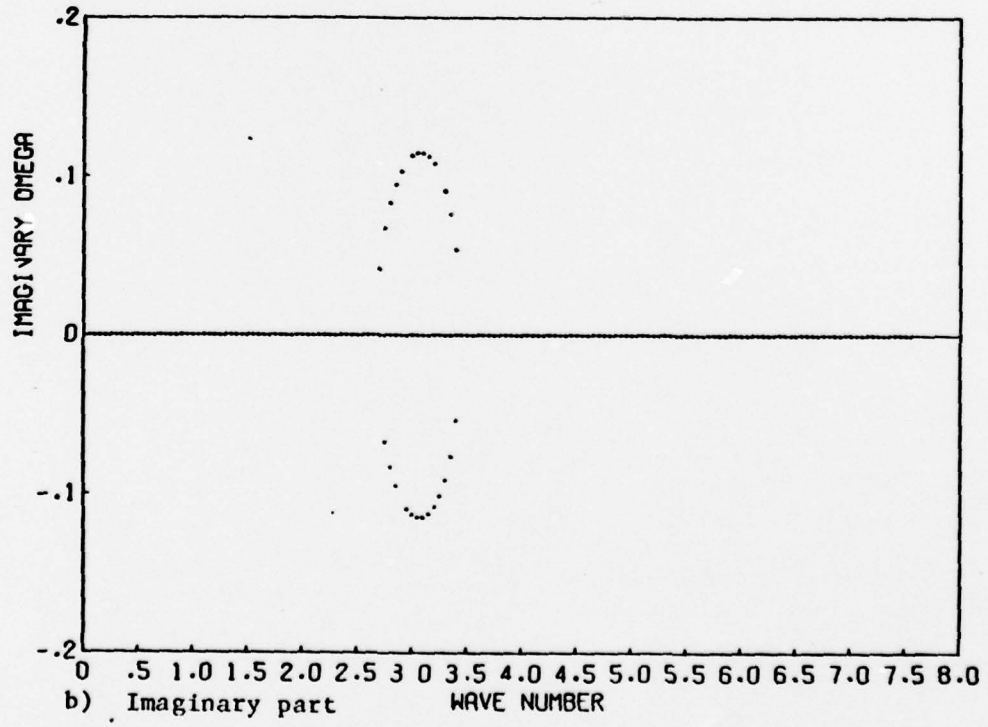

b) Imaginary part

Figure 20. Eigenvalues for data set H. Interface in lower half of profile.

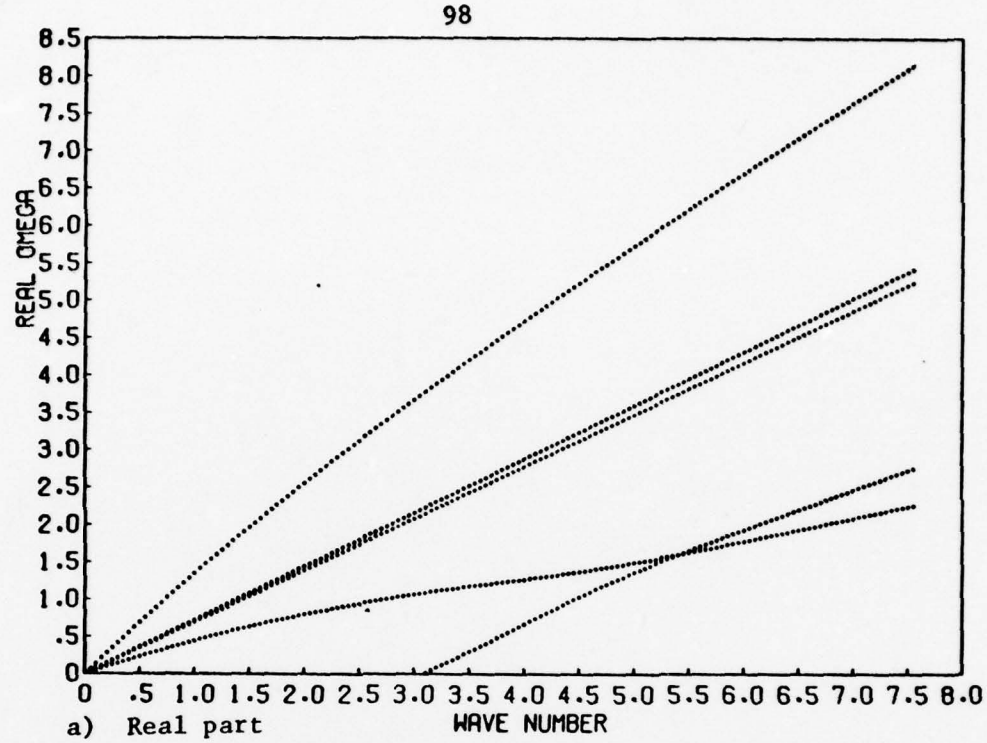

a) Real part

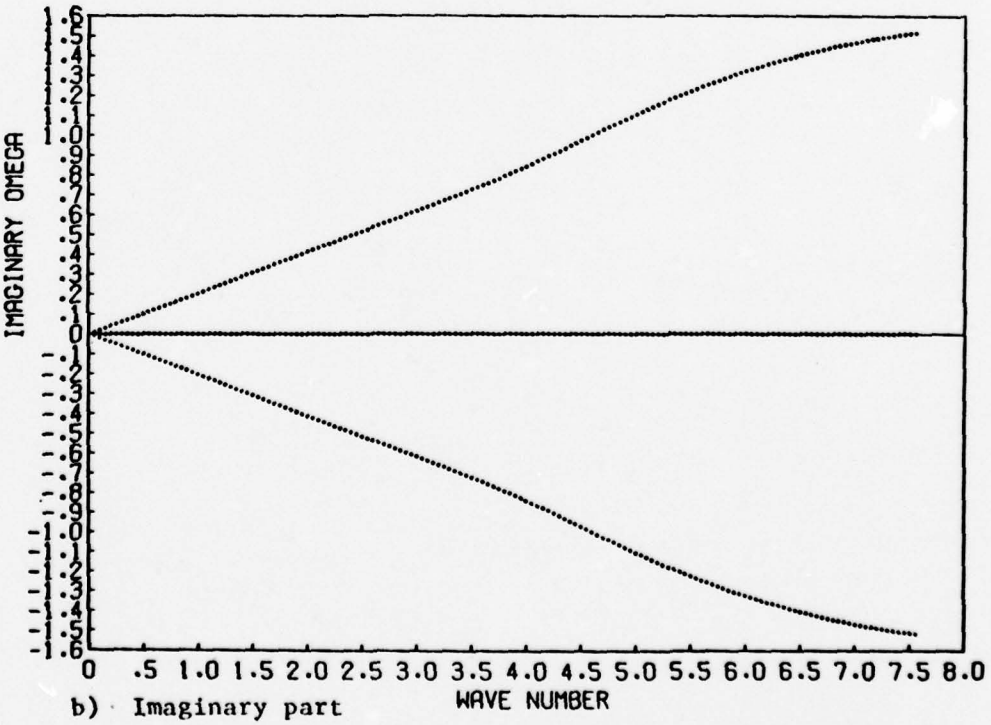

b) Imaginary part

Figure 21. Eigenvalues for data set I. Low discharge.

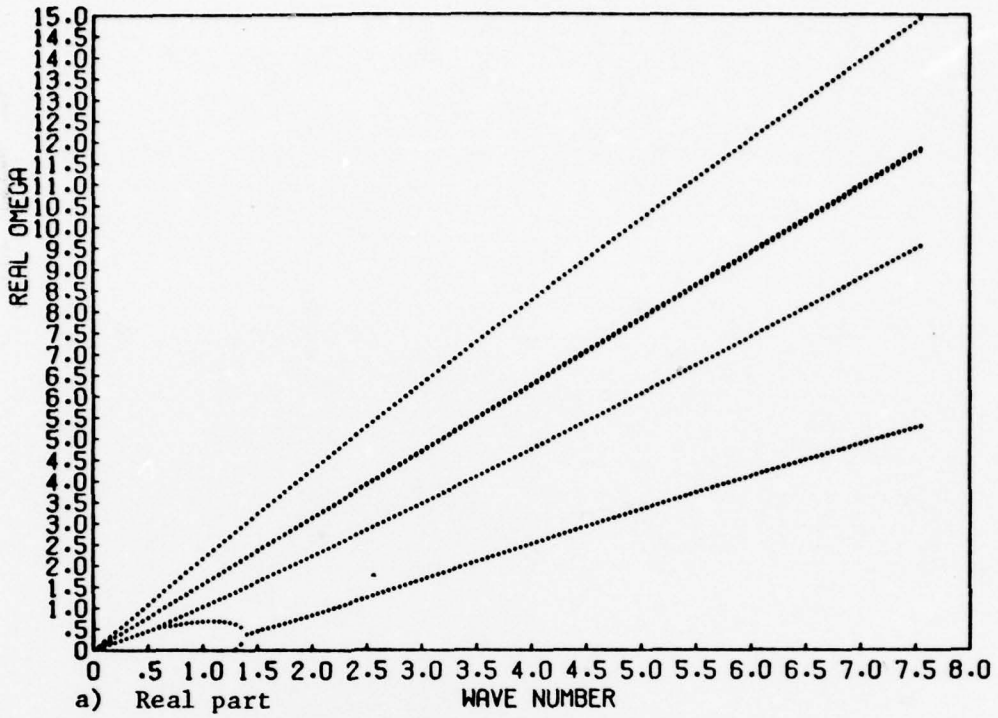

a) Real part

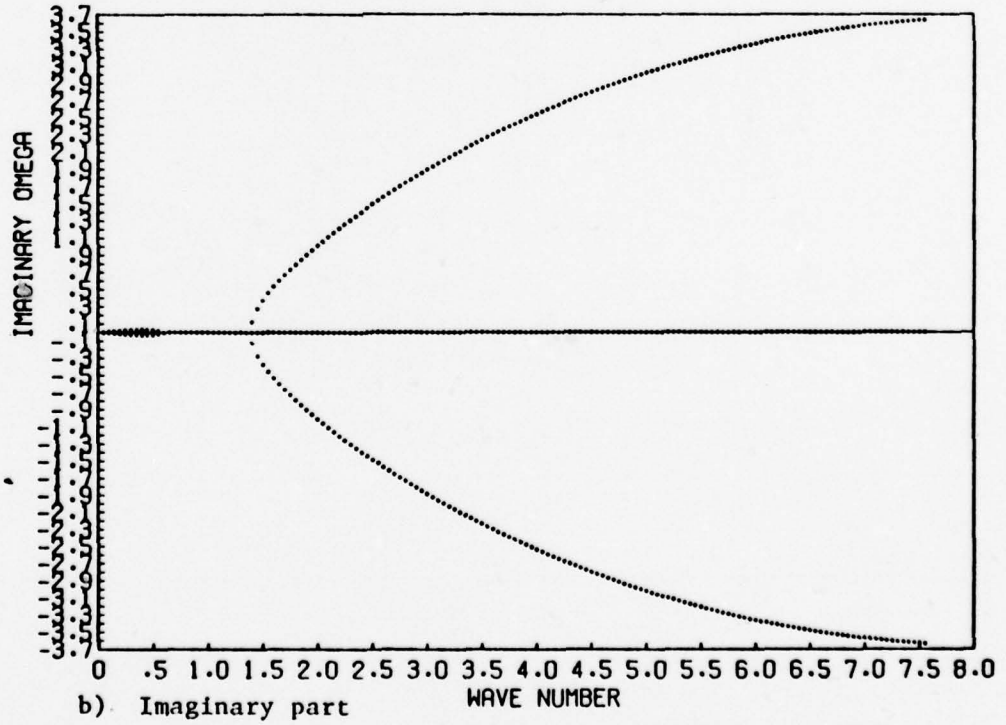

b) Imaginary part

Figure 22. Eigenvalues for data set J. High discharge.

Table III. Parameters for Salt Wedge Estuary Profiles. Figures 23 to 33.

	Profile	d_1	d_2	d_3	h	U_s	U_m	U_b	U_s'
Outer	1	.1	.2	.385	1.0	1.0	1.0	-.138	0
	2	.05	.2	.922	1.0	1.05	1.0	-.647	+1
	3	.15	.2	.305	1.0	.85	1.0	-.085	-1
Central	4	.25	.5	.75	1.0	1.47	1.47	-.41	0
Inner	5	.4	.8	.9	1.0	1.42	1.42	-.158	0

See Figure 4 for schematic diagram of profiles and parameters.

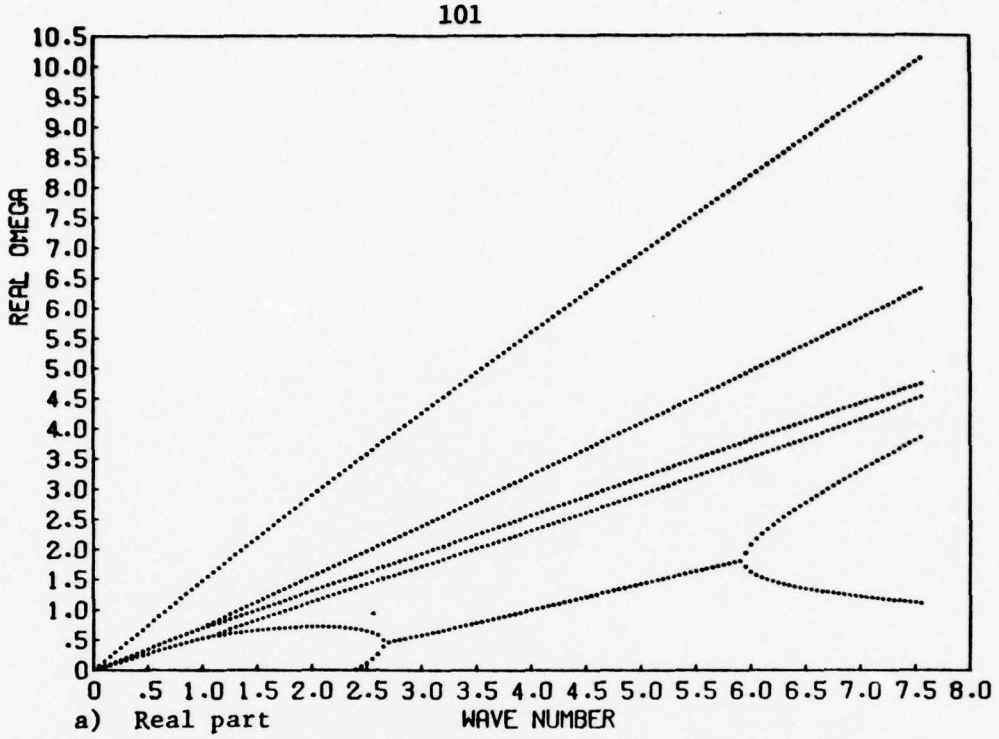

a) Real part

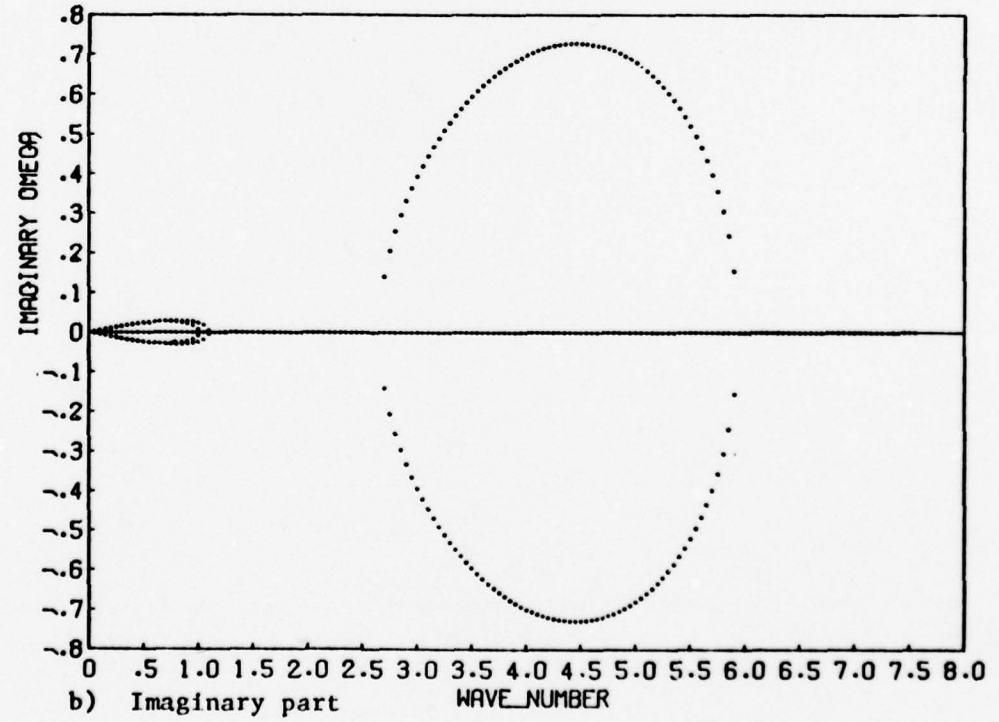

b) Imaginary part

Figure 23. Eigenvalues for Profile 1. $\Delta\rho = 0.002$.

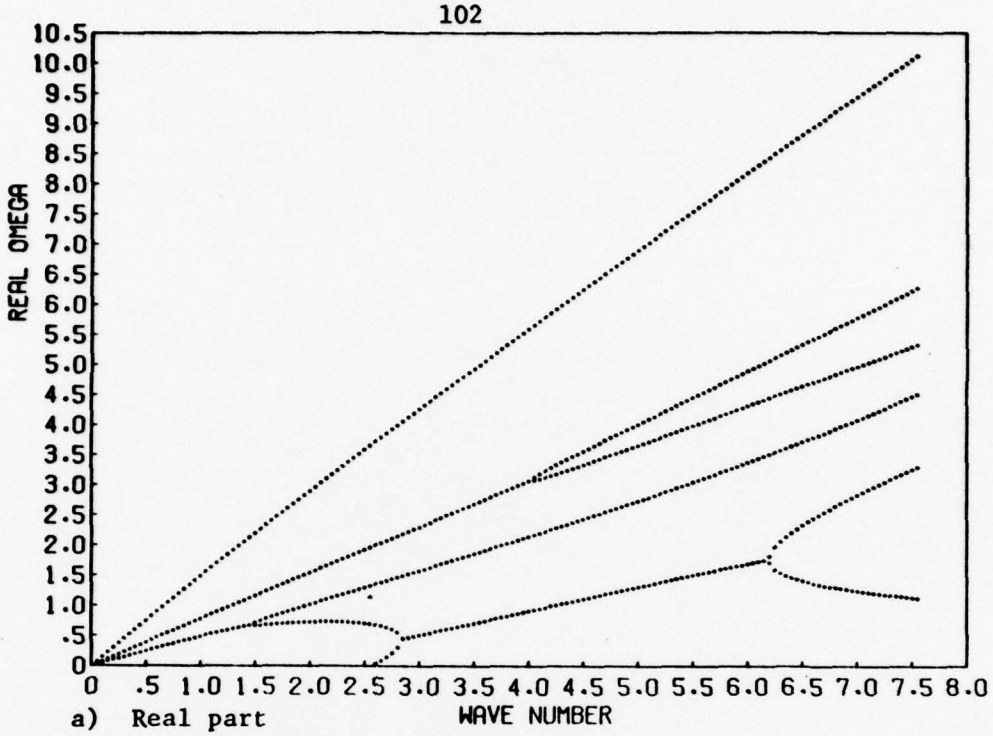

a) Real part

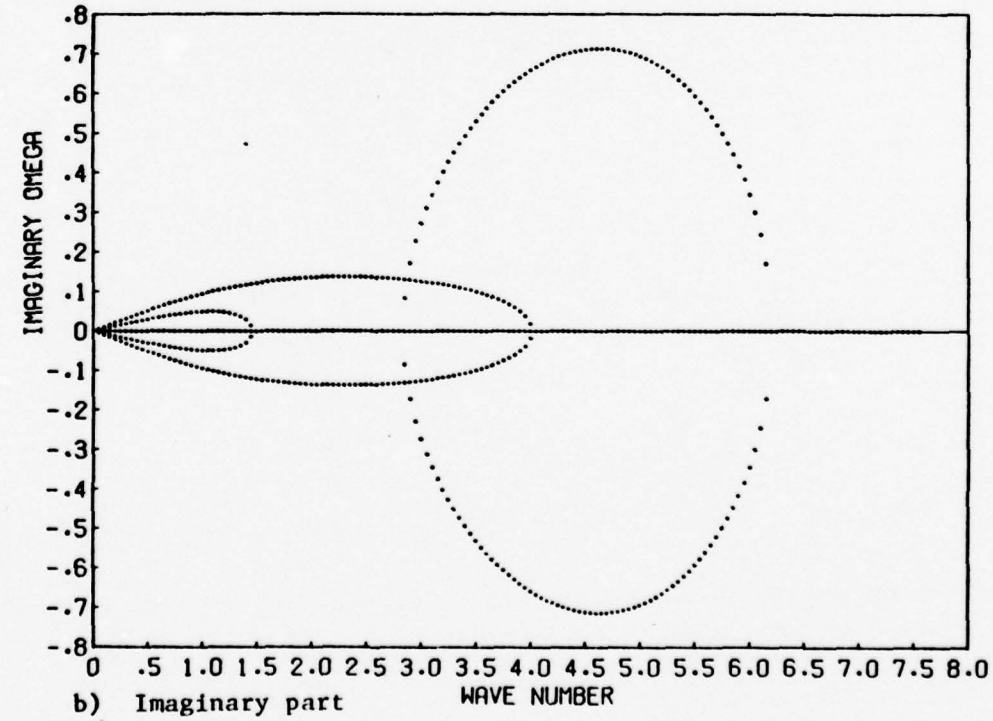

b) Imaginary part

Figure 24. Eigenvalues for Profile 1. $\Delta\rho = 0.02$.

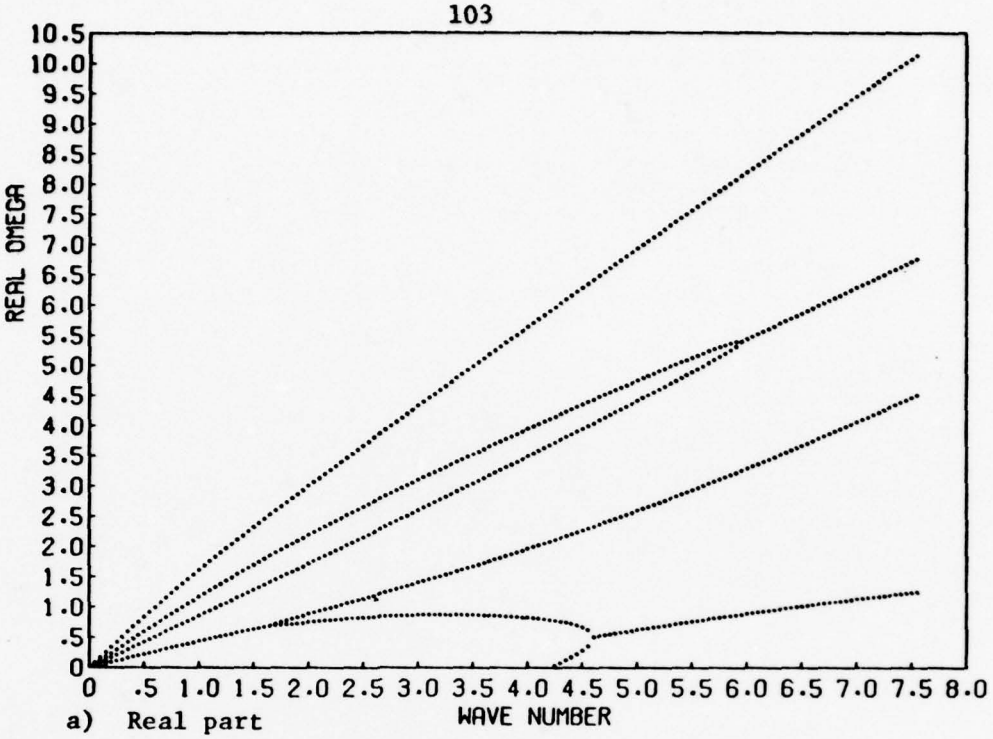

a) Real part

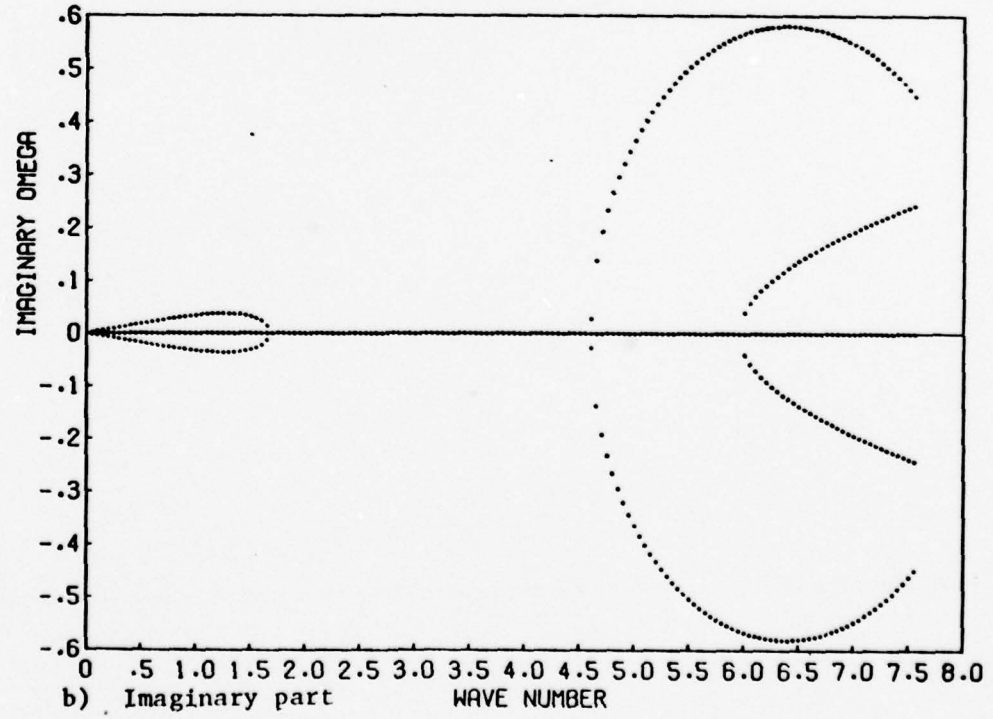

b) Imaginary part

Figure 25. Eigenvalues for Profile 1. $\Delta\rho = 0.2$.

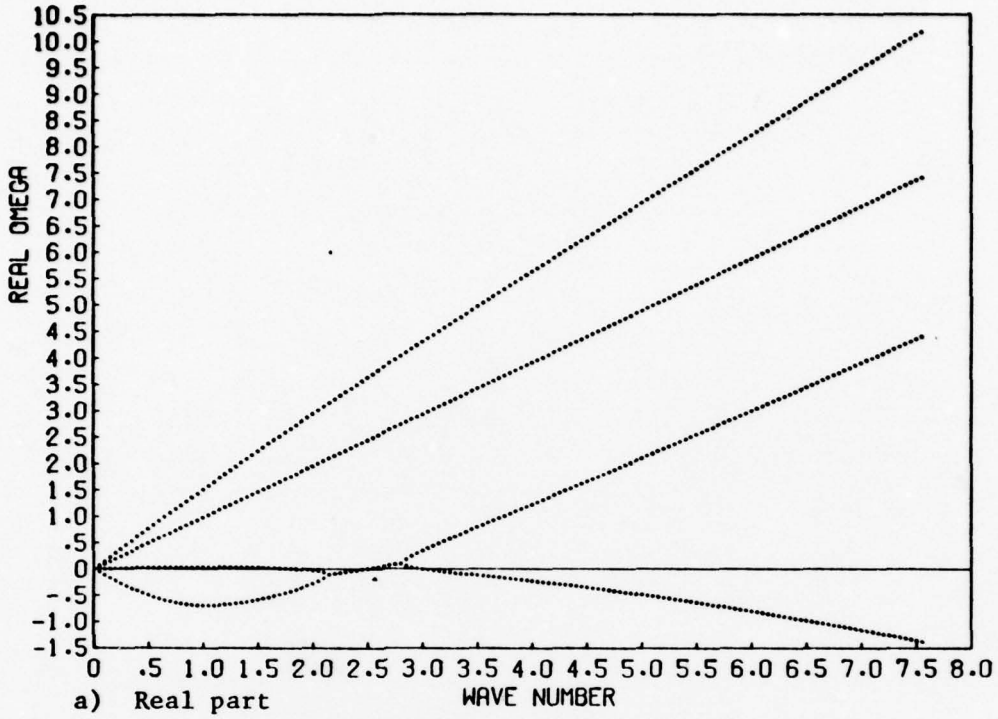

a) Real part

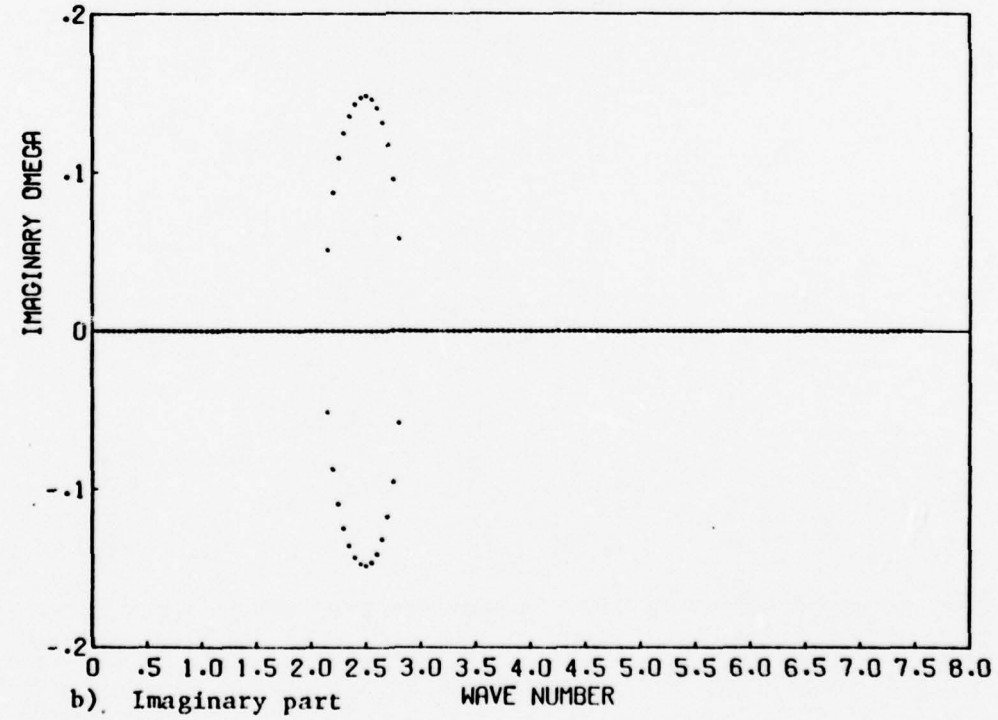

b) Imaginary part

Figure 26. Eigenvalues for Profile 2. $\Delta\rho$ = 0.0.

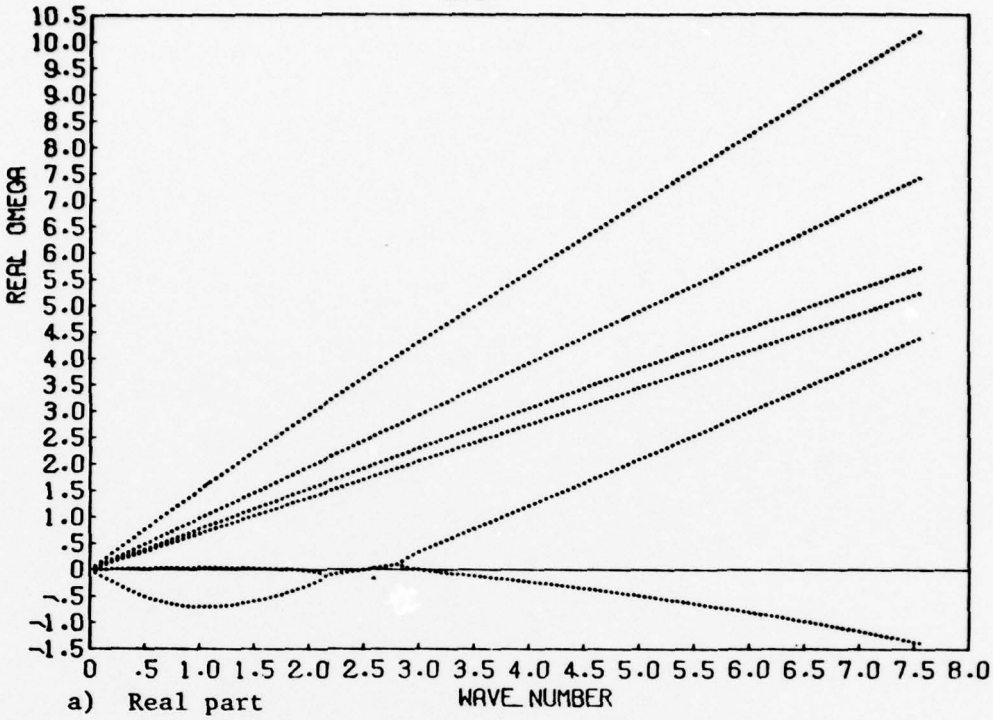

a) Real part

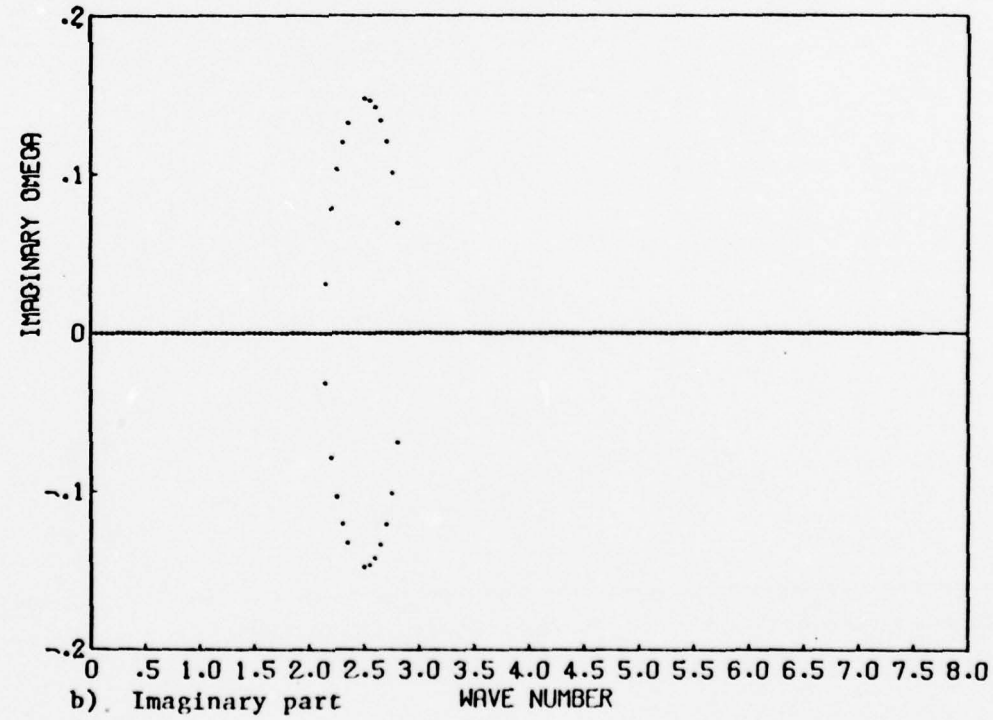

b) Imaginary part

Figure 27. Eigenvalues for Profile 2. $\Delta\rho$ = 0.02.

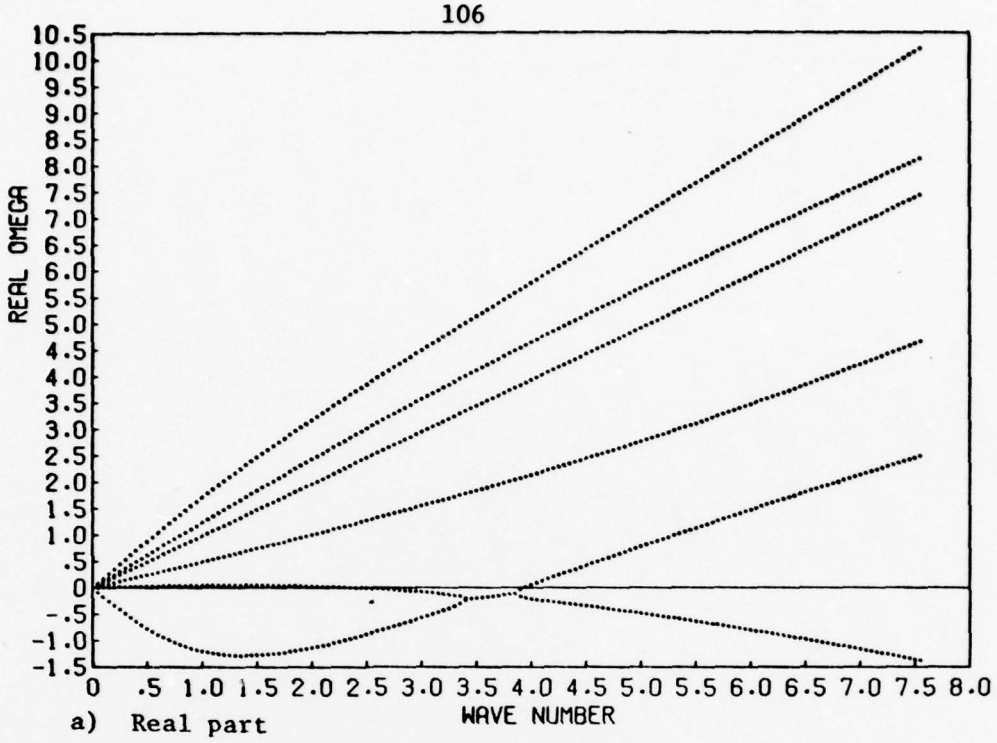

a) Real part

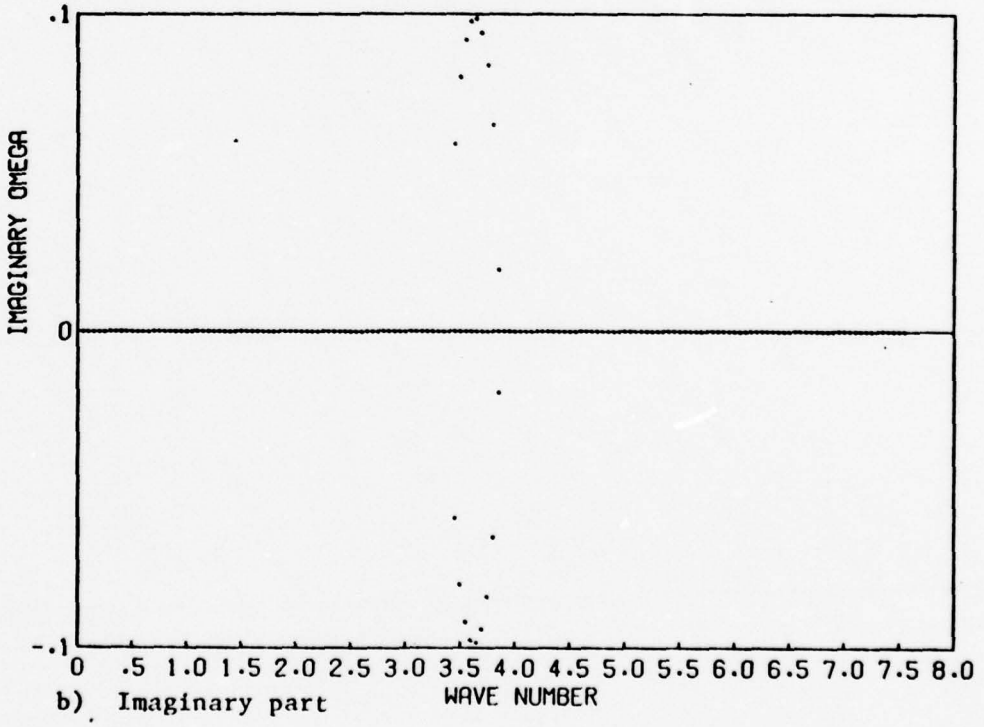

b) Imaginary part

Figure 28. Eigenvalues for Profile 2. $\Delta\rho = 0.2$.

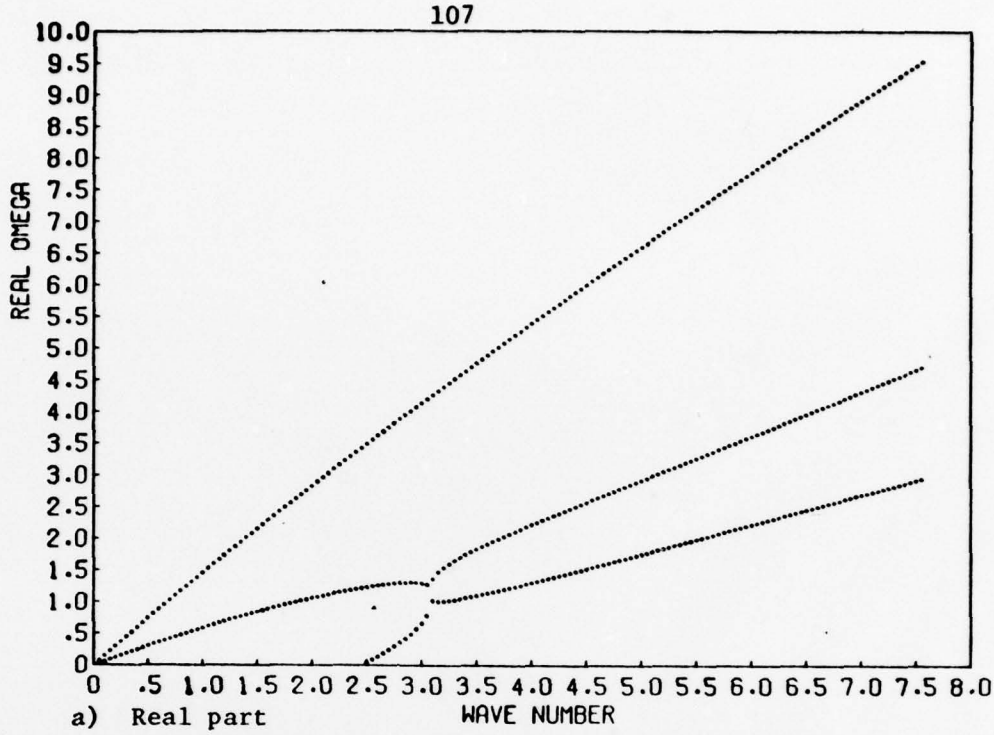

a) Real part

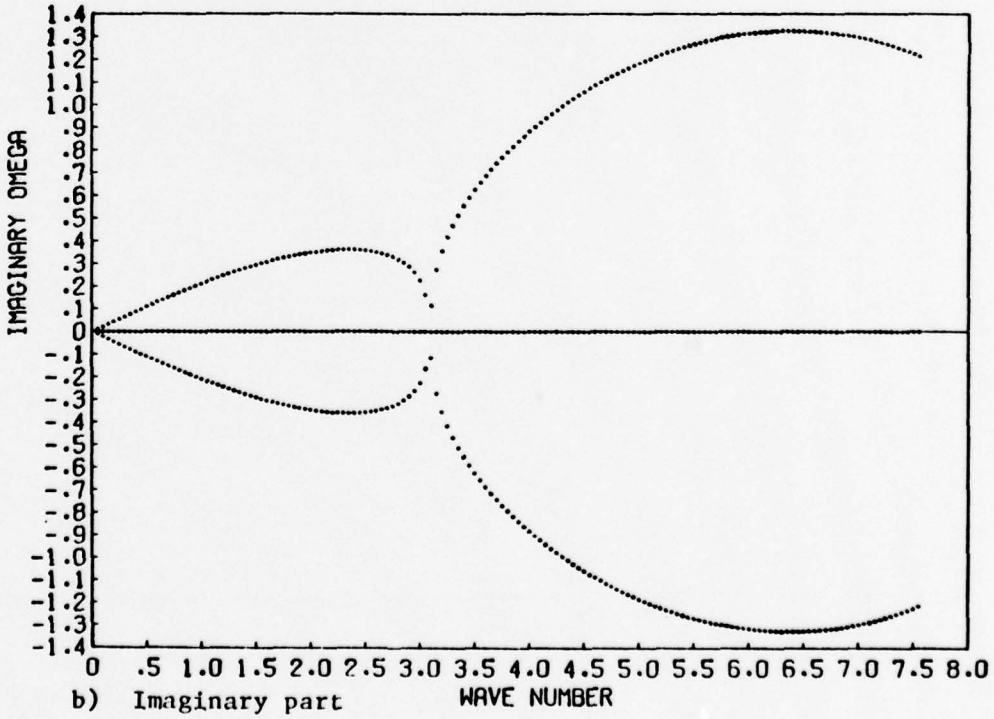

b) Imaginary part

Figure 29. Eigenvalues for Profile 3. $\Delta\rho$ = 0.0.

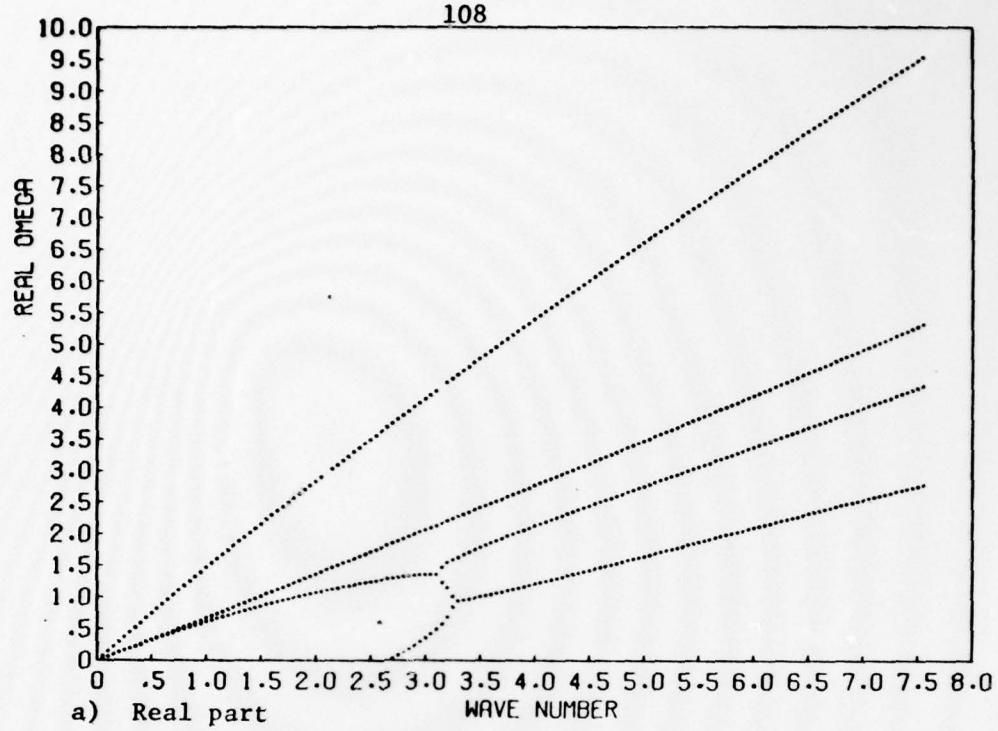

a) Real part

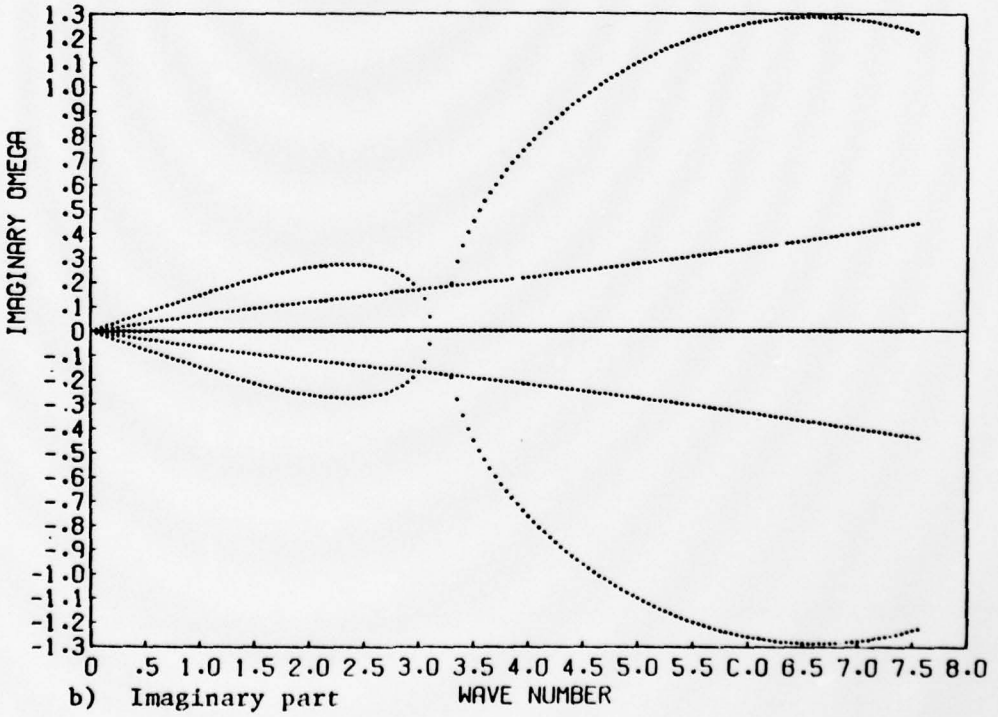

b) Imaginary part

Figure 30. Eigenvalues for Profile 3. $\Delta\rho = 0.02$.

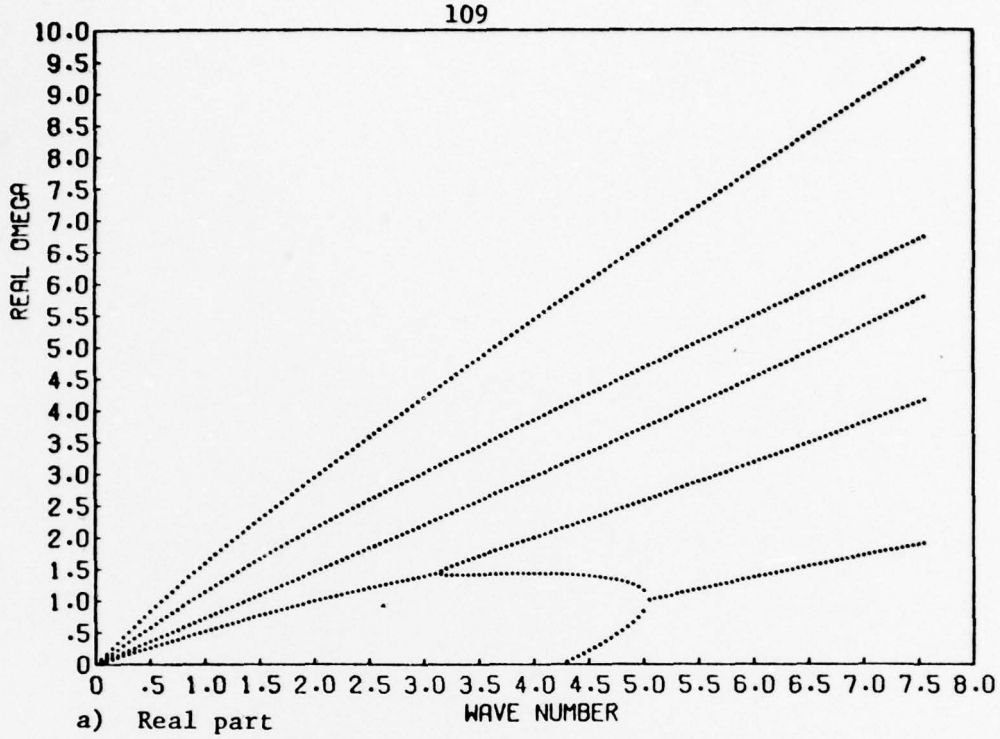

a) Real part

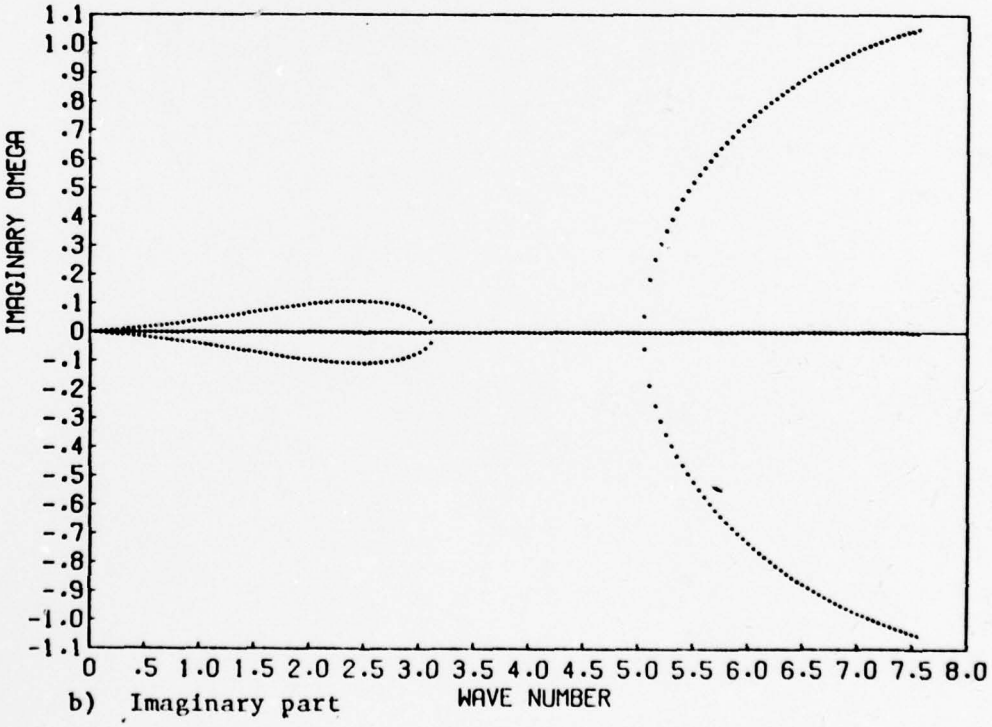

b) Imaginary part

Figure 31. Eigenvalues for Profile 3. $\Delta\rho = 0.2$.

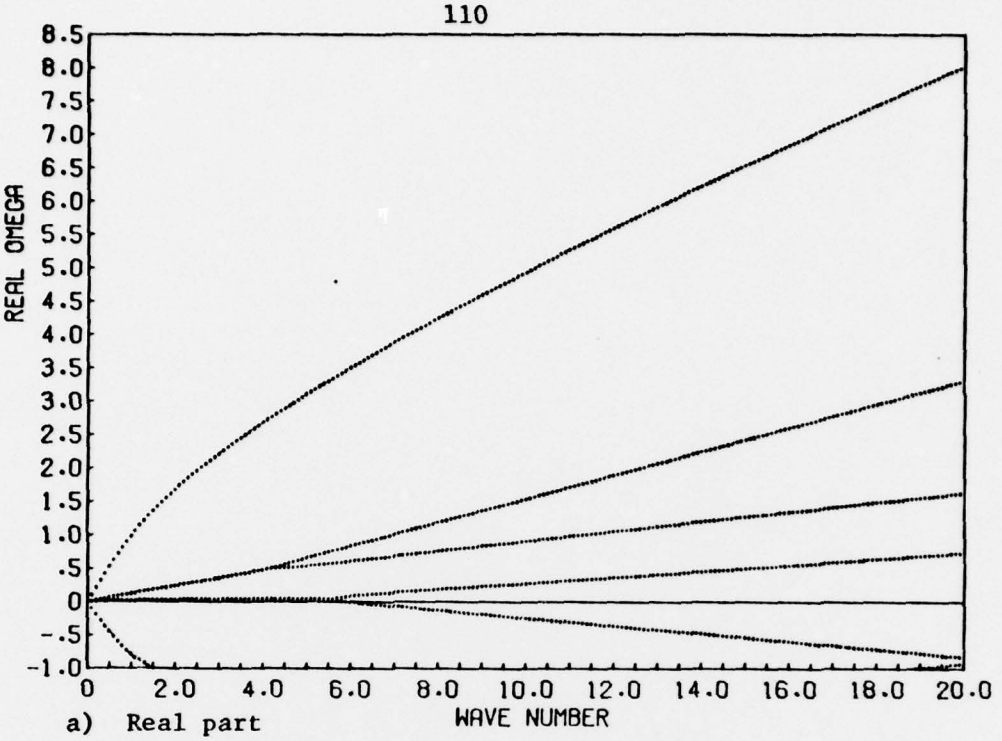

a) Real part

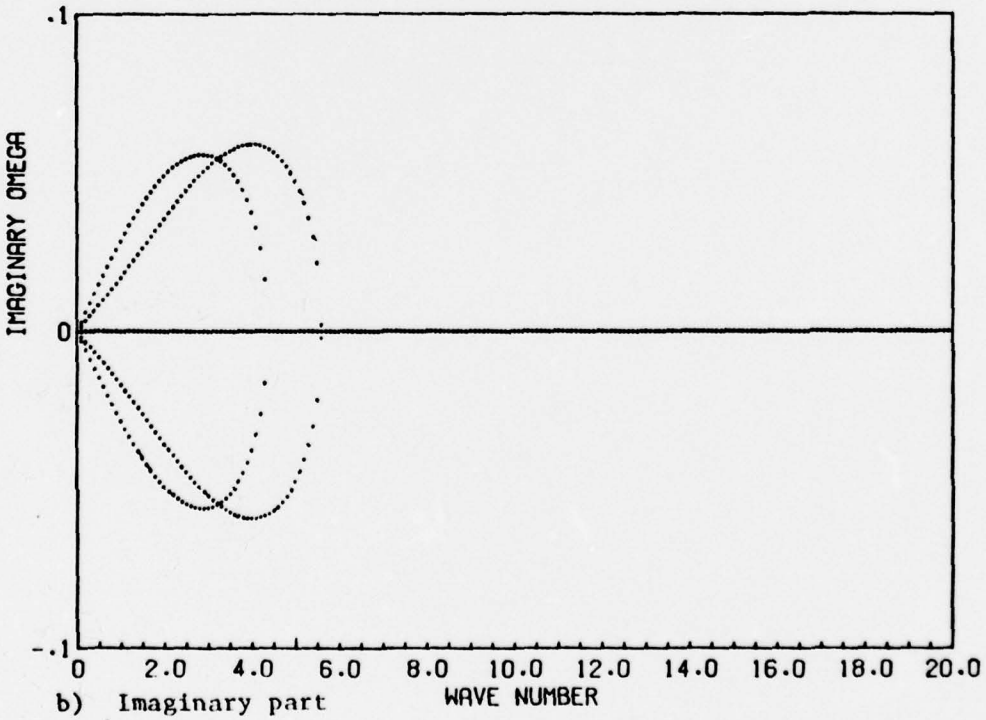

b) Imaginary part

Figure 32. Eigenvalues for Profile 4. $\Delta\rho = 0.02$.

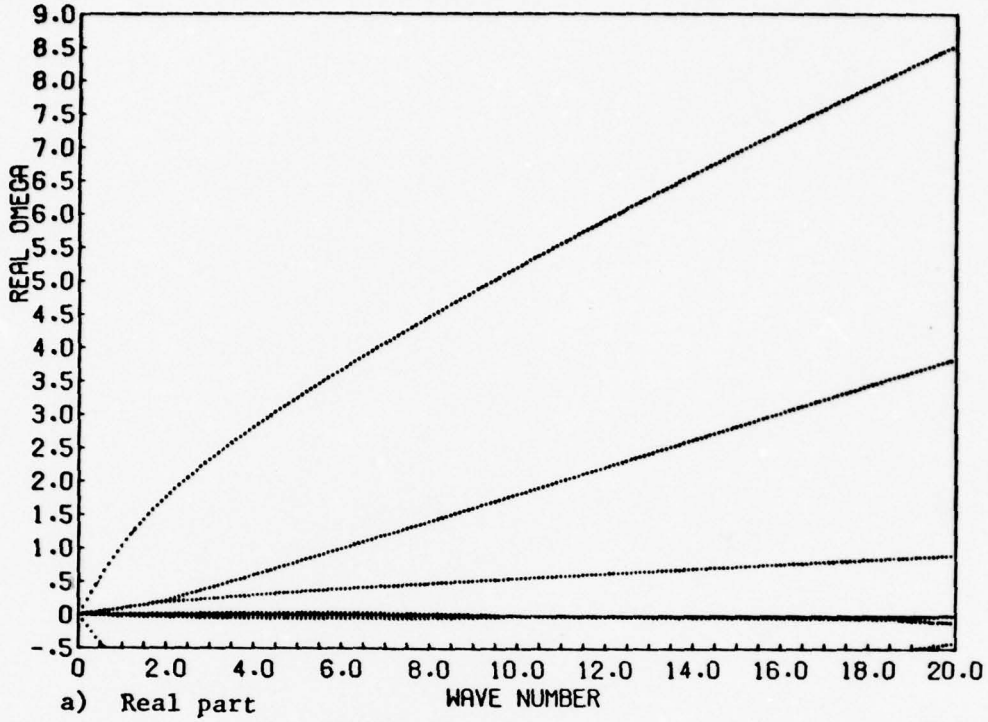

a) Real part

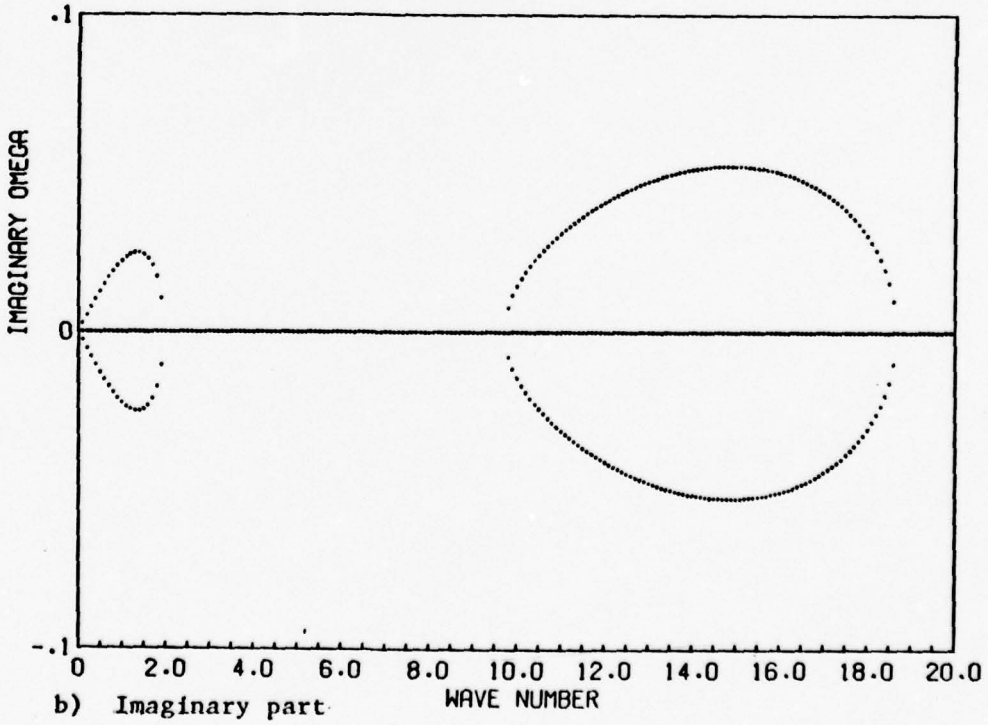

b) Imaginary part

Figure 33. Eigenvalues for Profile 5. $\Delta\rho = 0.02$.

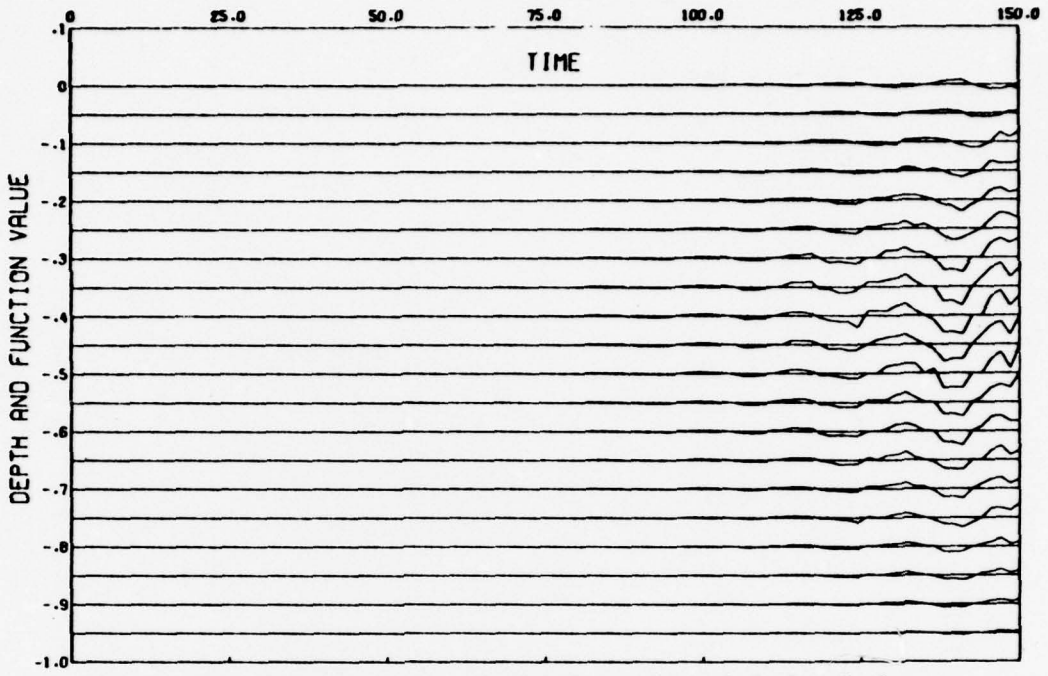

Figure 34. Time series. Initial exponential depth decay. Profile 1. $\tilde{\alpha} = 0.5$. Six normal modes. $\Delta\rho = 0.02$.

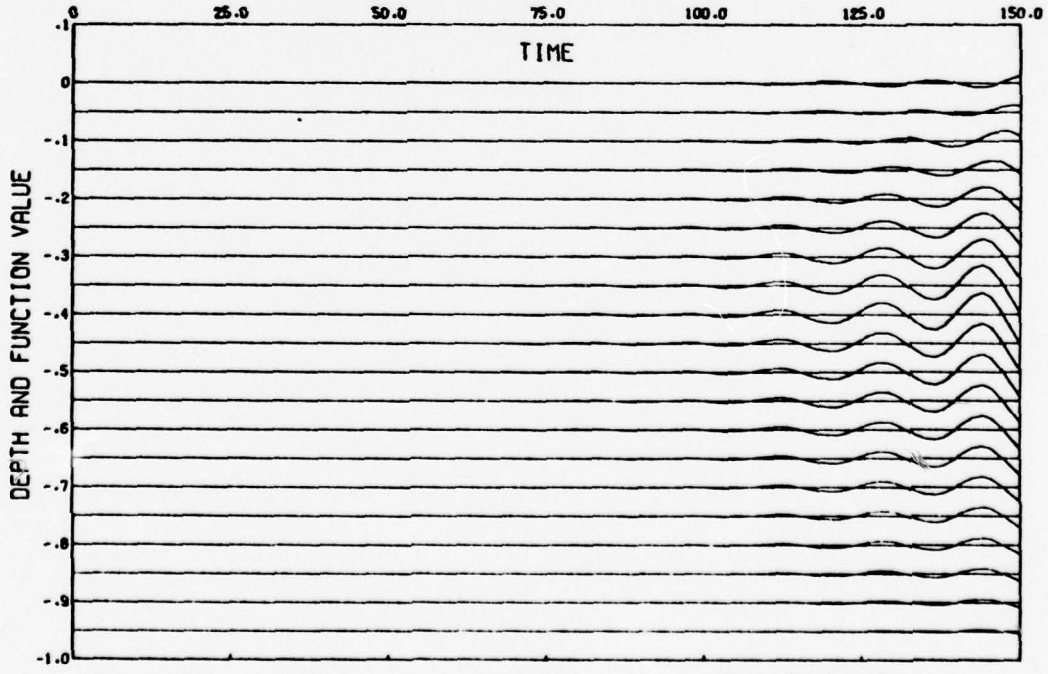

Figure 35. Time series. Initial exponential depth decay. Profile 1. $\tilde{\alpha} = 0.5$. $(2N + 6)$ modes. $N = 21$. $\Delta\rho = 0.02$.

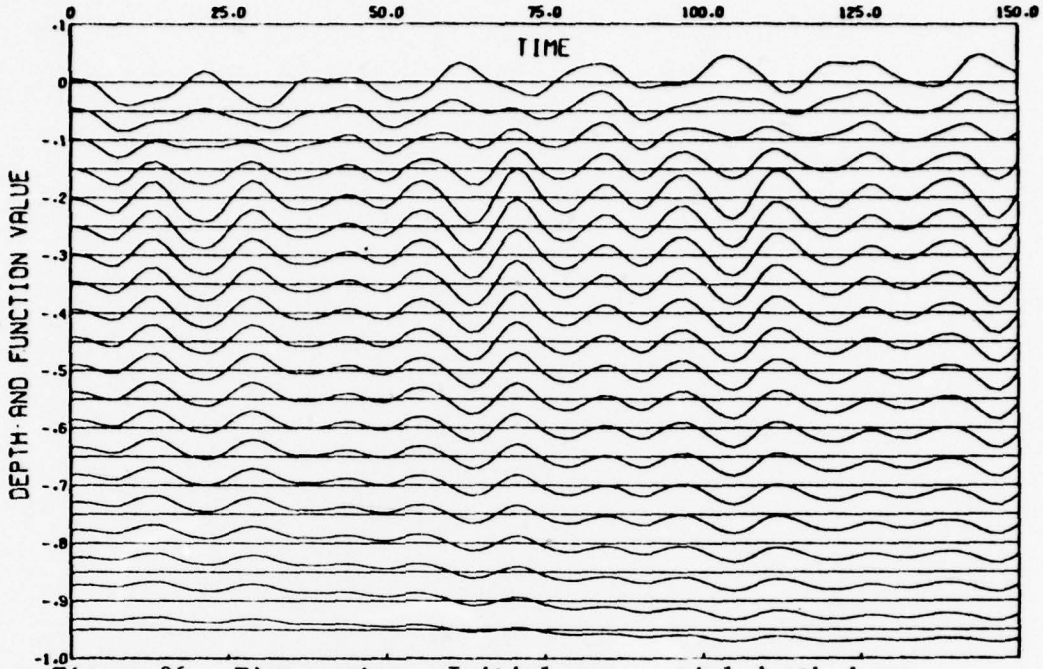

Figure 36. Time series. Initial exponential depth decay. Profile 2. $\tilde{\alpha} = 0.5$. (2N + 6) modes. N = 21. $\Delta\rho = 0.02$.

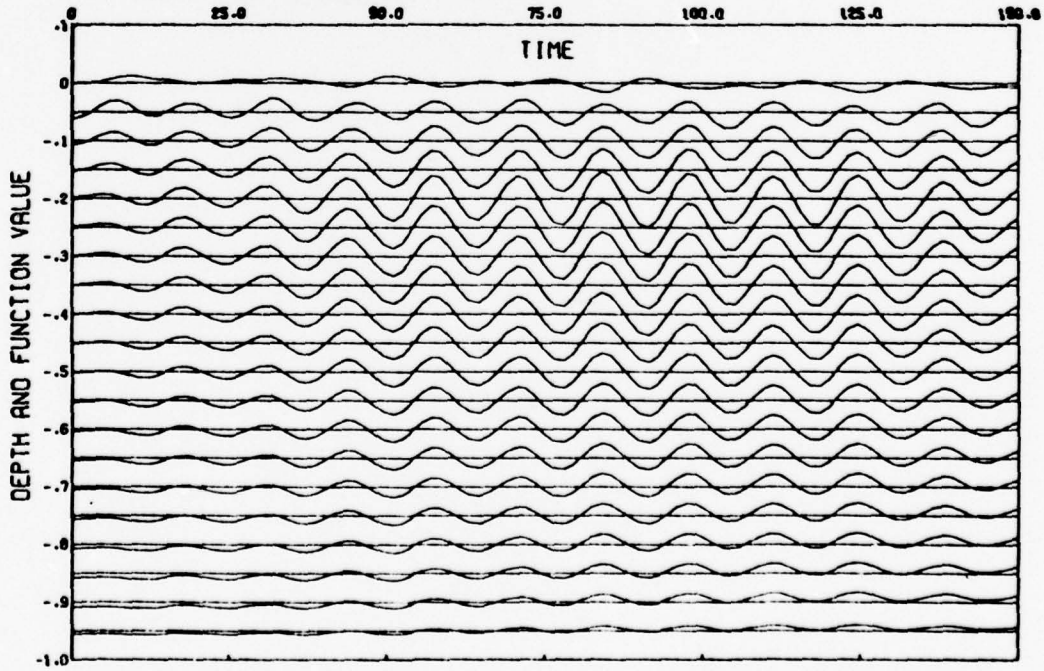

Figure 37. Time series. Initial Gaussian centered at density interface. Profile 2. $\tilde{\alpha} = 0.5$. (2N + 6) modes. N = 21. $\Delta\rho = 0.02$.

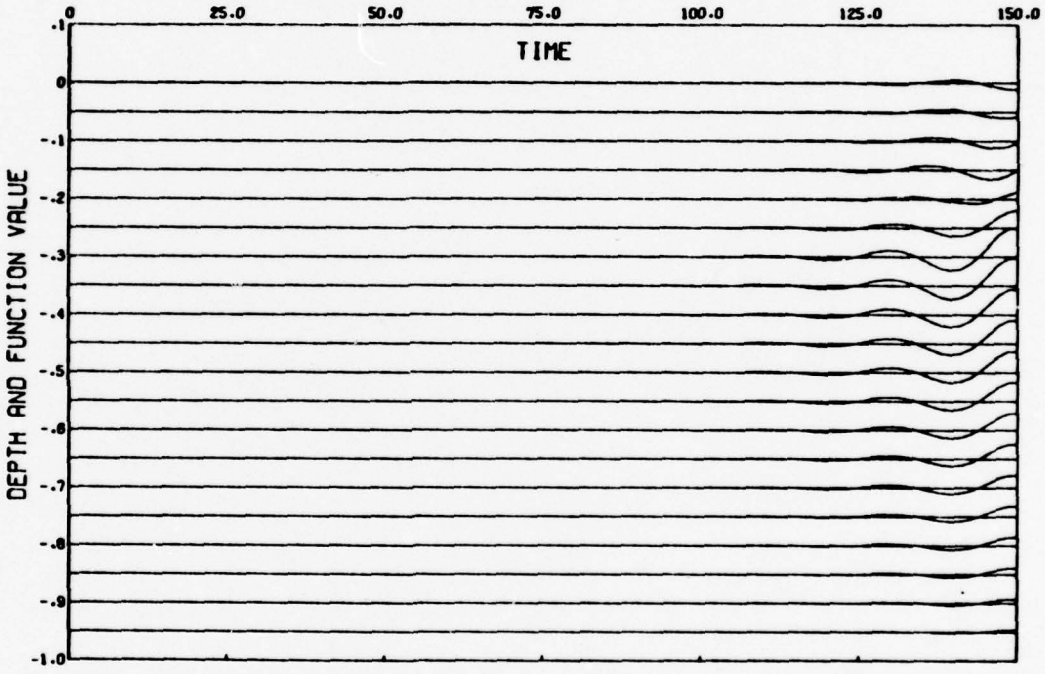

Figure 38. Time series. Initial exponential depth decay. Profile 3. $\tilde{\alpha} = 0.5$. (2N + 6) modes. N = 21. $\Delta\rho = 0.02$.

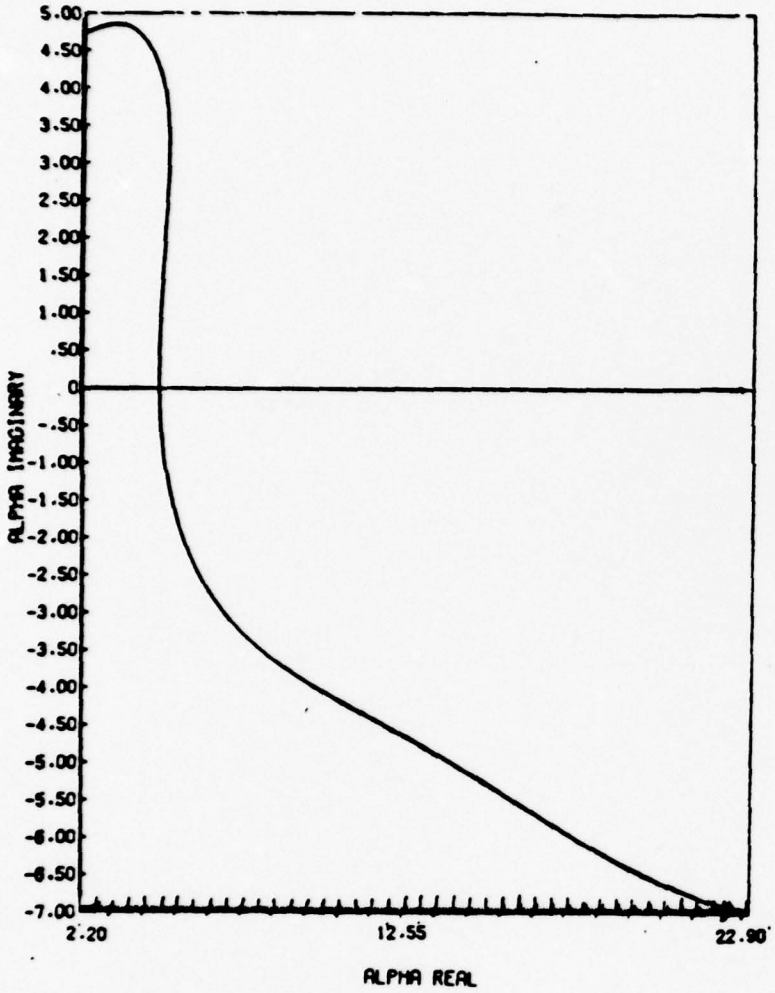

Figure 39. Line of saddle points. Most growing mode. Profile 1. $\Delta\rho = 0.02$

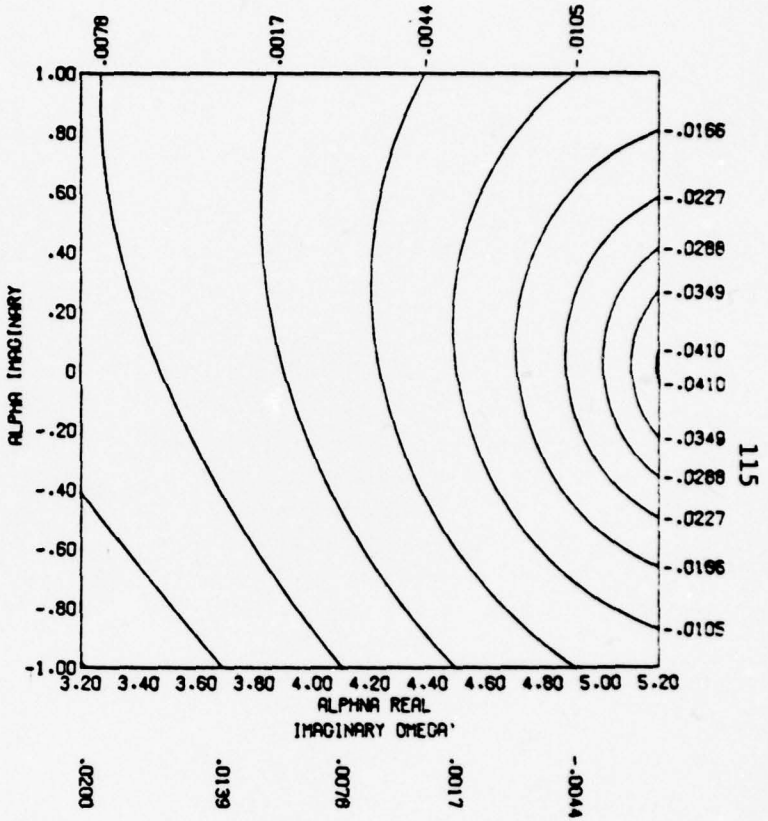

Figure 40. Contours of $\partial\omega_i/\partial\omega_r$ in complex wavenumber plane. Profile 1. $\Delta\rho = 0.02$.

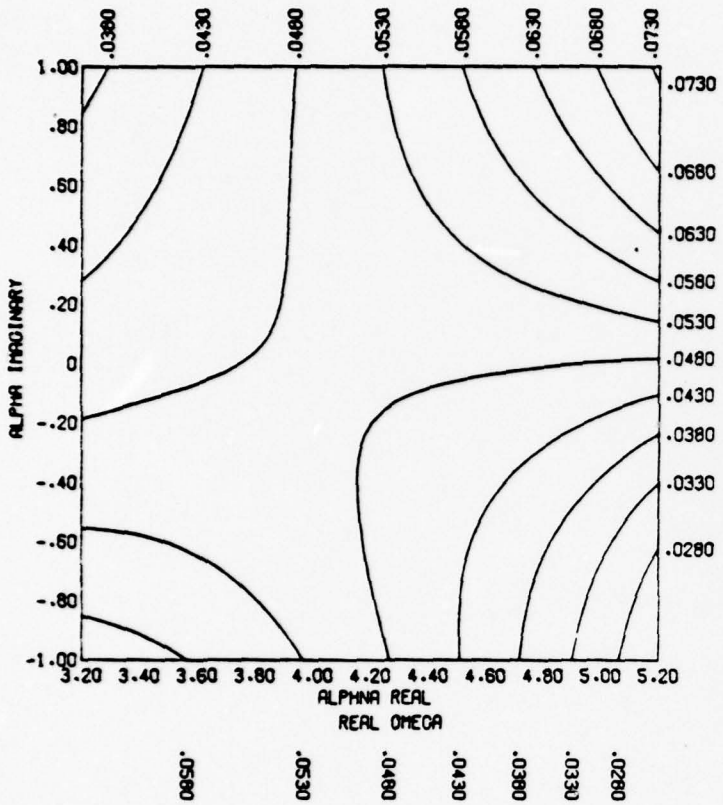

a) Real part

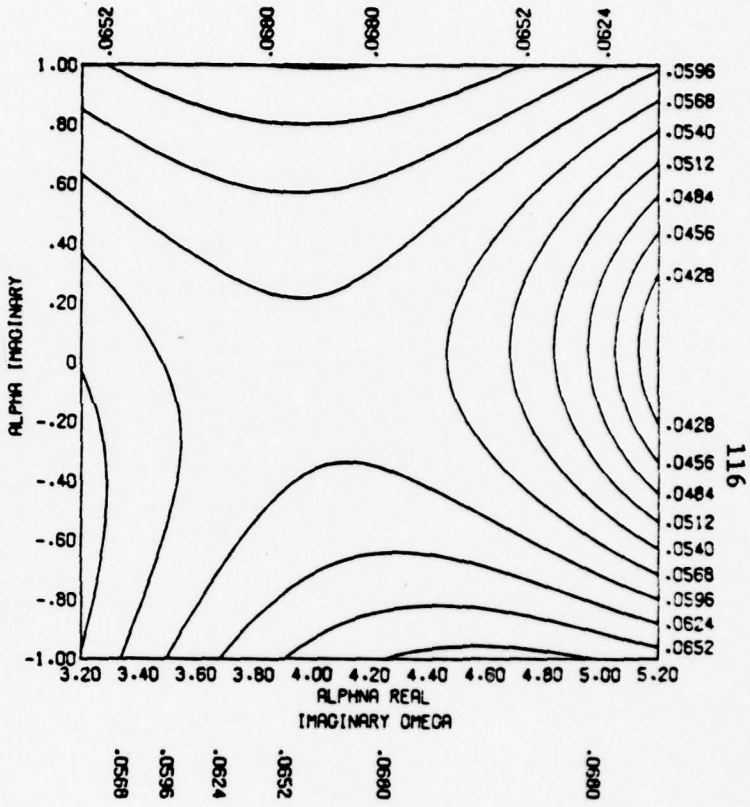

b) Imaginary part

Figure 41. Contours of frequency in complex wavenumber plane. Profile 1. $\Delta\rho = 0.02$.

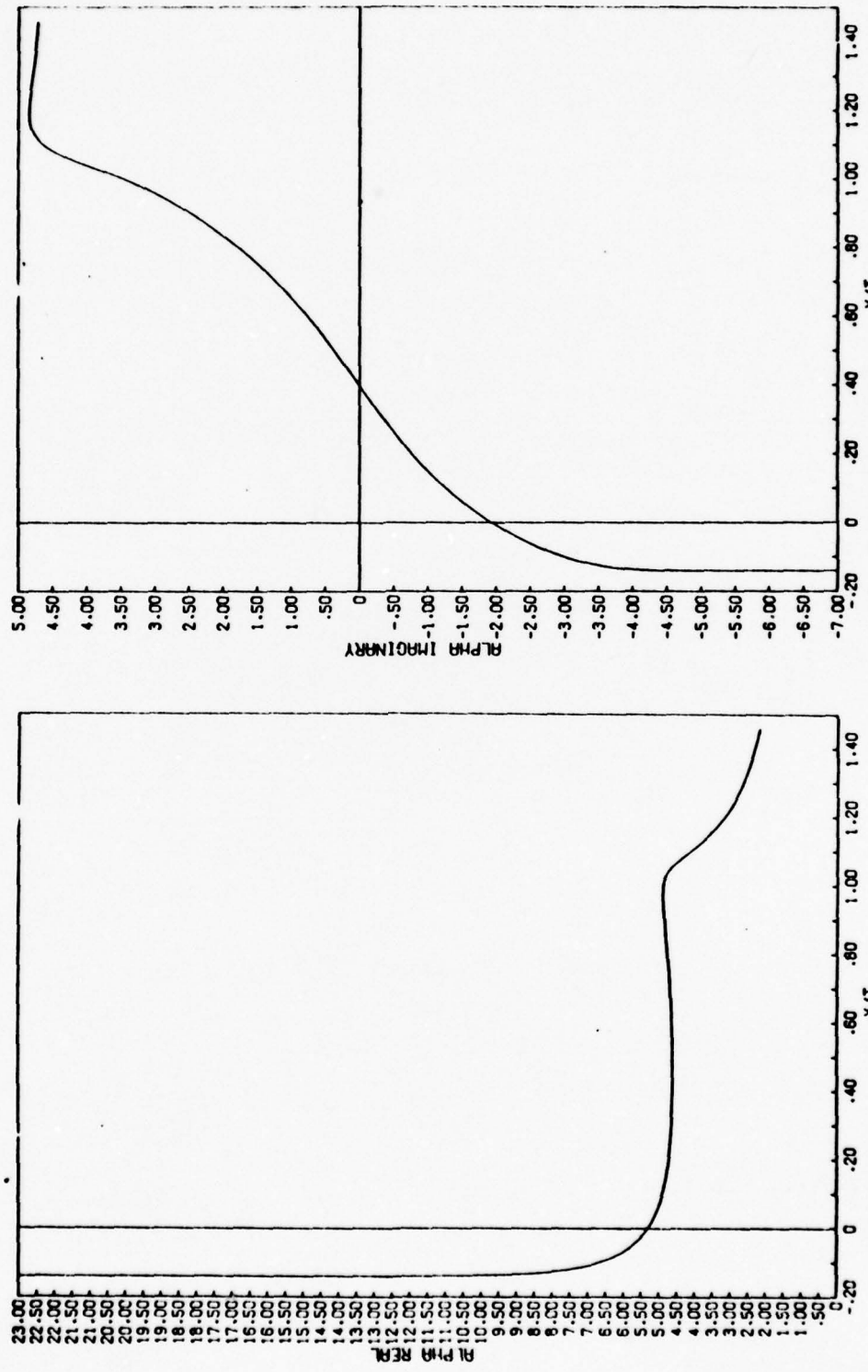

a) Real part

b) Imaginary part

Figure 42. Wavenumber vs. x/t along line of saddle points. Profile 1. $\Delta\rho = 0.02$.

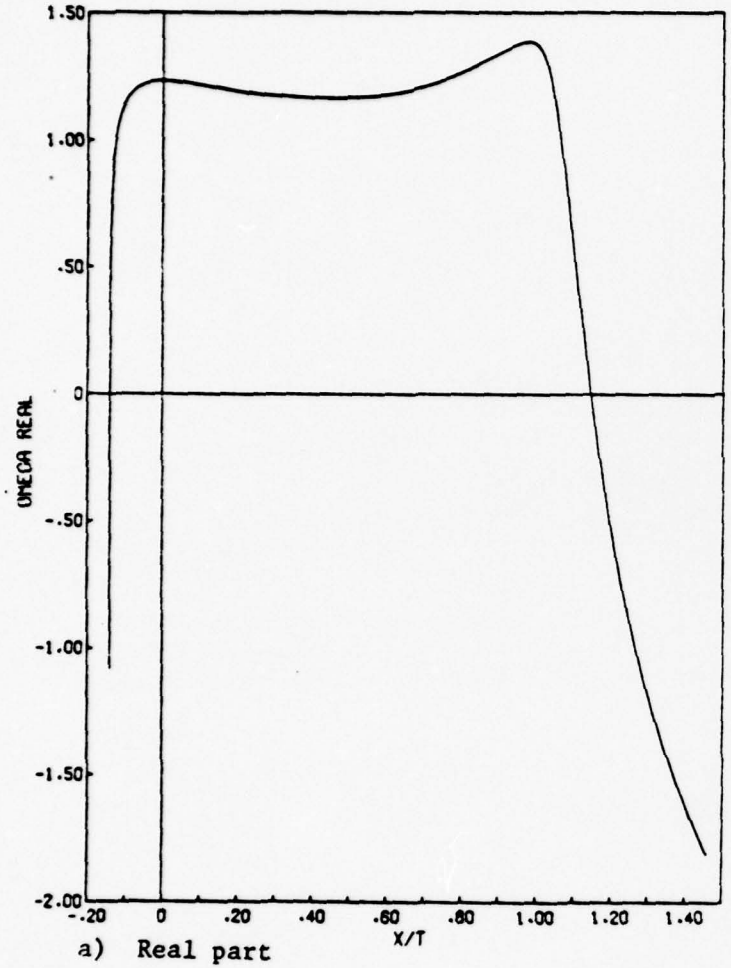

a) Real part

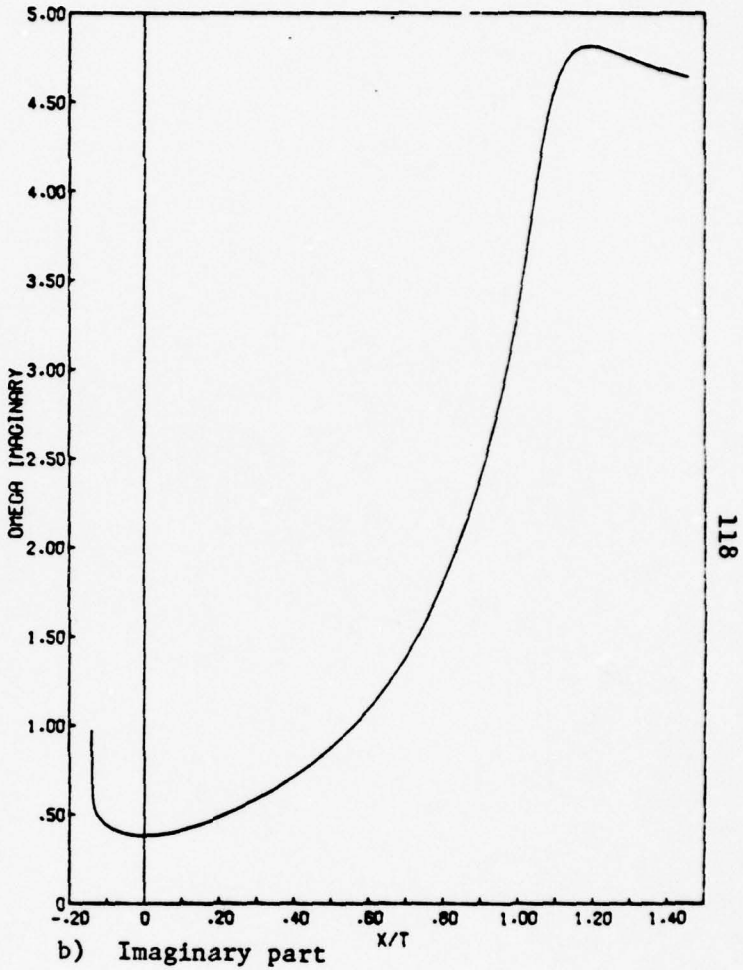

b) Imaginary part

Figure 43. Frequency vs. x/t along line of saddle points. Profile 1. $\Delta\rho = 0.02$.

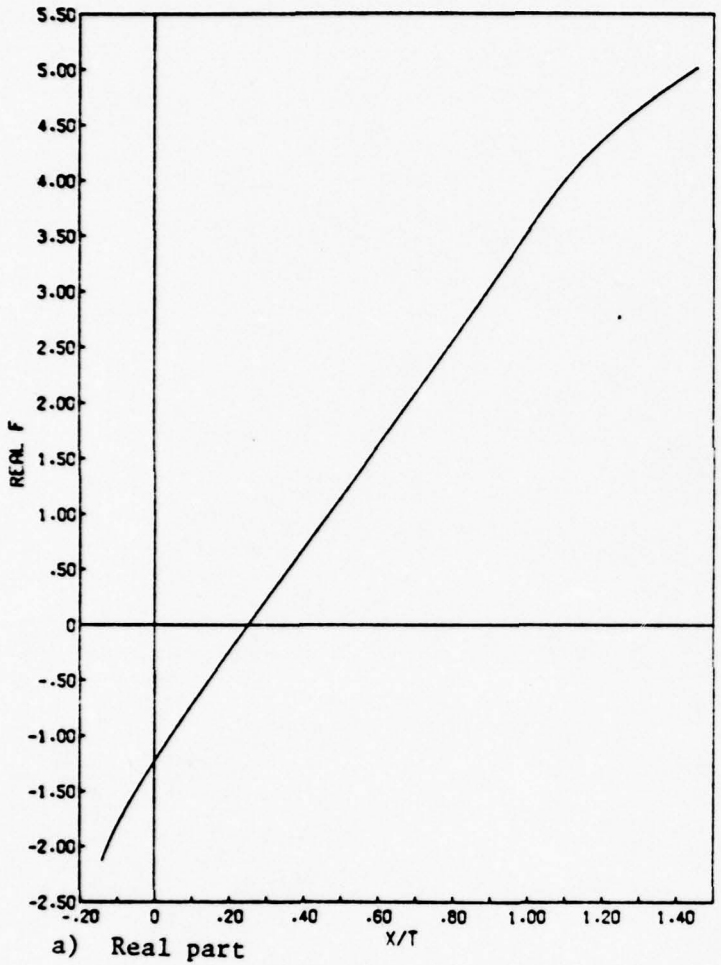

a) Real part

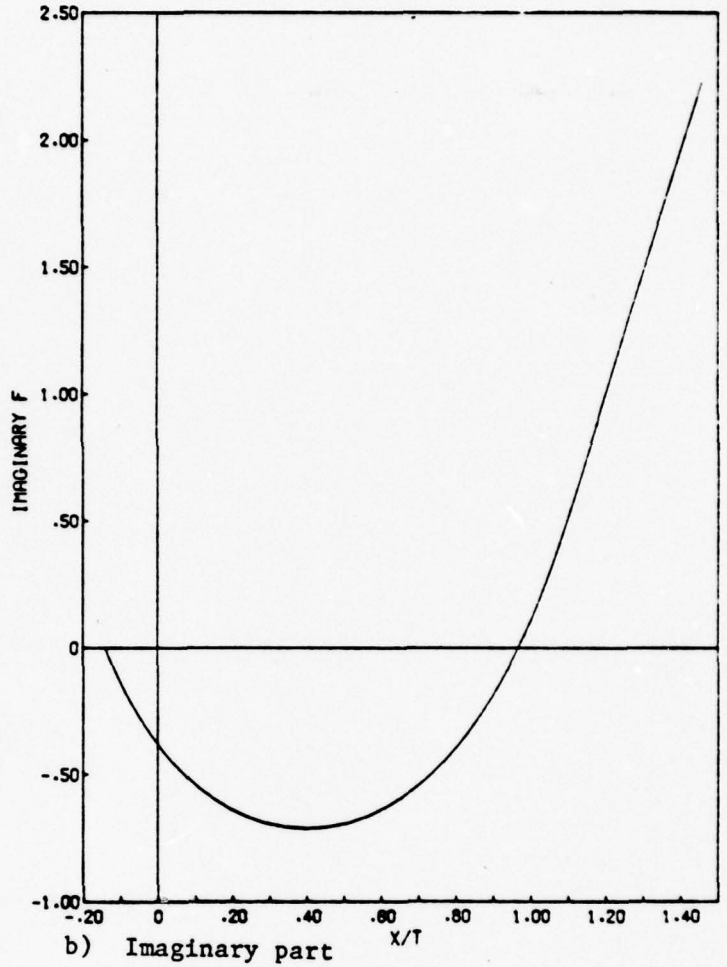

b) Imaginary part

Figure 44. $F = (\tilde{\alpha}_* x/t - \omega_*)$ vs. x/t along line of saddle points. Profile 1. $\Delta\rho = 0.02$.

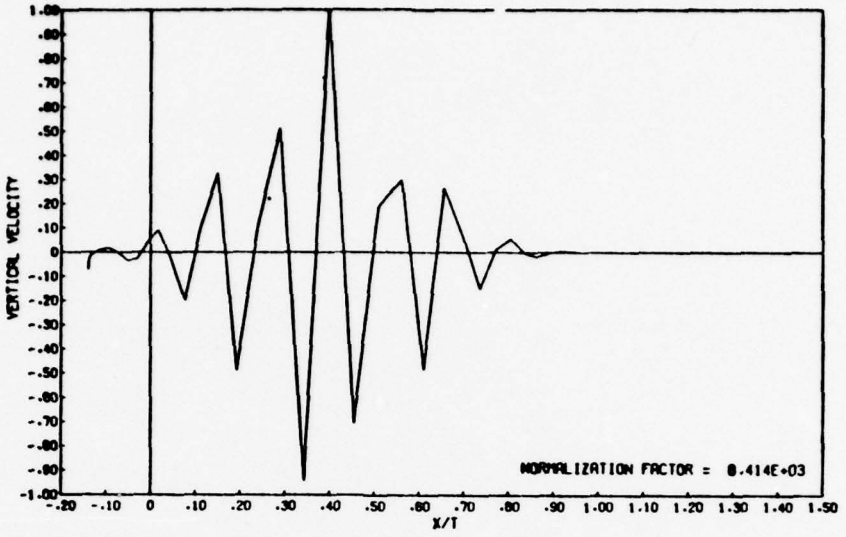

Figure 45. Asymptotic expansion. Initial flat spectrum. Profile 1, $\Delta\rho = 0.02$, $z = 0.0$, $t = 10.0$.

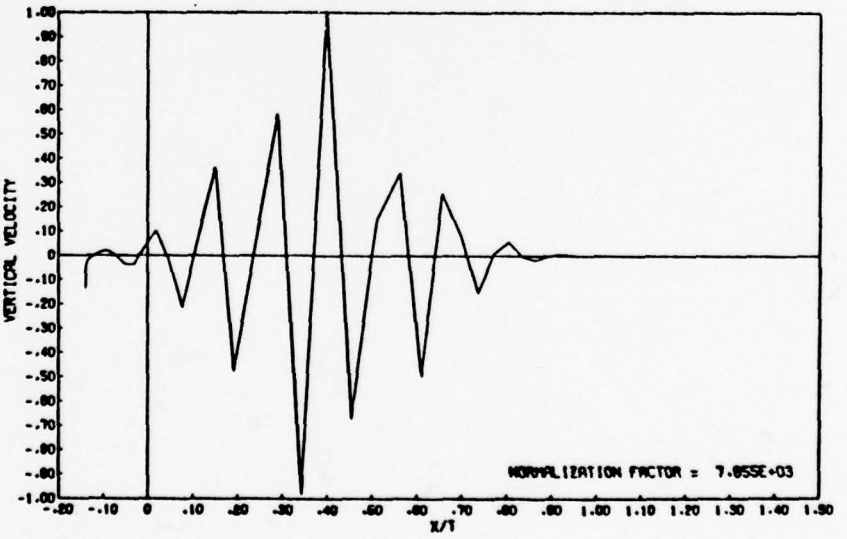

Figure 46. Asymptotic expansion. Initial flat spectrum. Profile 1, $\Delta\rho = 0.02$, $z = -0.1$, $t = 10.0$.

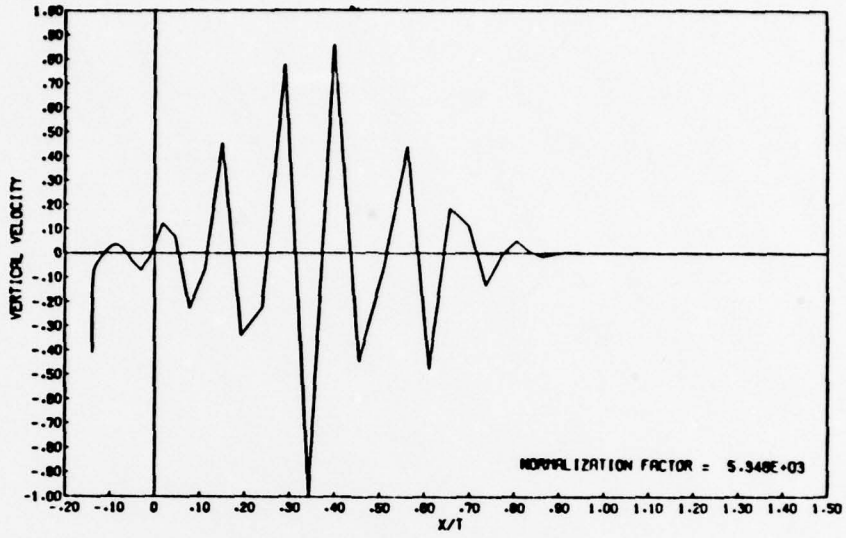

Figure 47. Asymptotic expansion. Initial flat spectrum. Profile 1, $\Delta\rho = 0.02$, $z = -0.2$, $t = 10.0$.

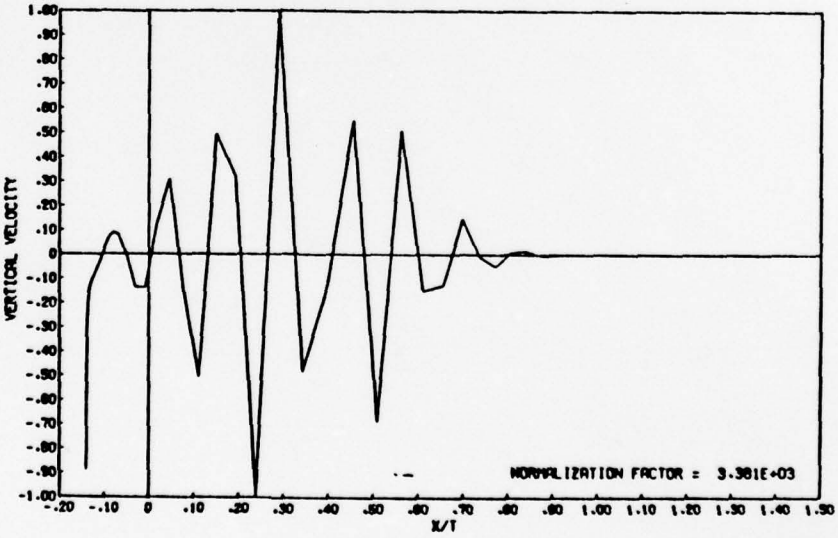

Figure 48. Asymptotic expansion. Initial flat spectrum. Profile 1, $\Delta\rho = 0.02$, $z = -0.5$, $t = 10.0$.

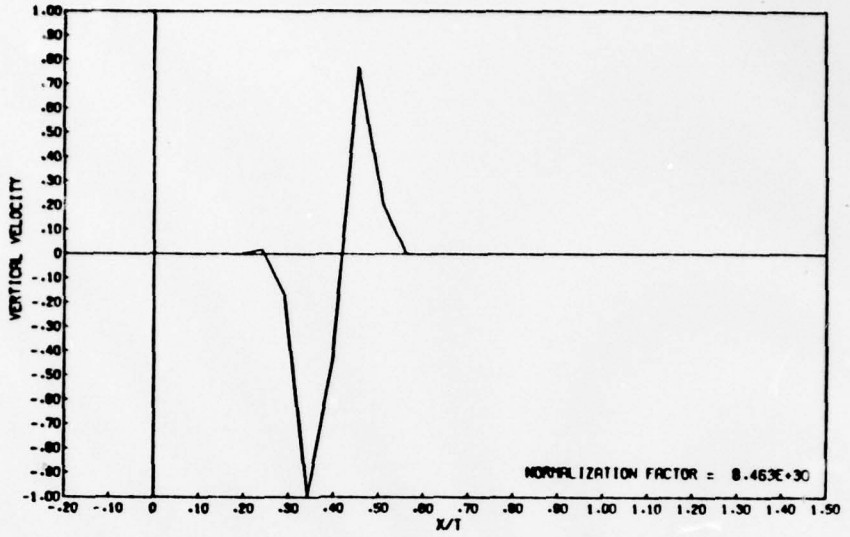

Figure 49. Asymptotic expansion. Initial flat spectrum. Profile 1, $\Delta\rho$ = 0.02, z = 0.0, t = 100.0.

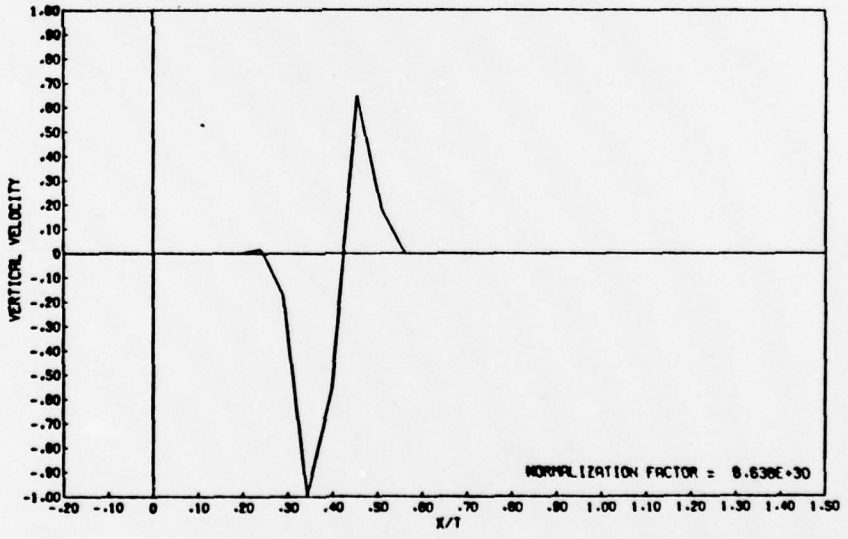

Figure 50. Asymptotic expansion. Initial flat spectrum. Profile 1, $\Delta\rho$ = 0.02, z = -0.1, t = 100.0.

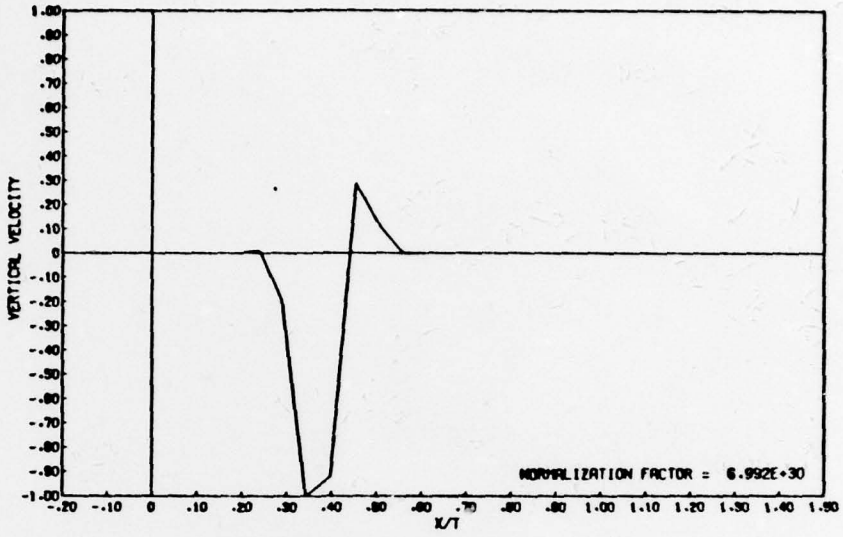

Figure 51. Asymptotic expansion. Initial flat spectrum. Profile 1, $\Delta\rho = 0.02$, $z = -0.2$, $t = 100.0$.

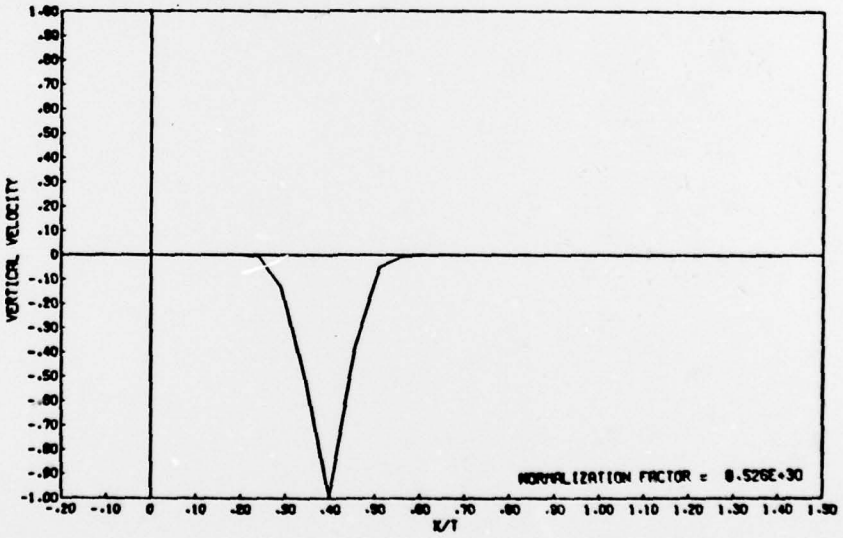

Figure 52. Asymptotic expansion. Initial flat spectrum. Profile 1, $\Delta\rho = 0.02$, $z = -0.5$, $t = 100.0$.

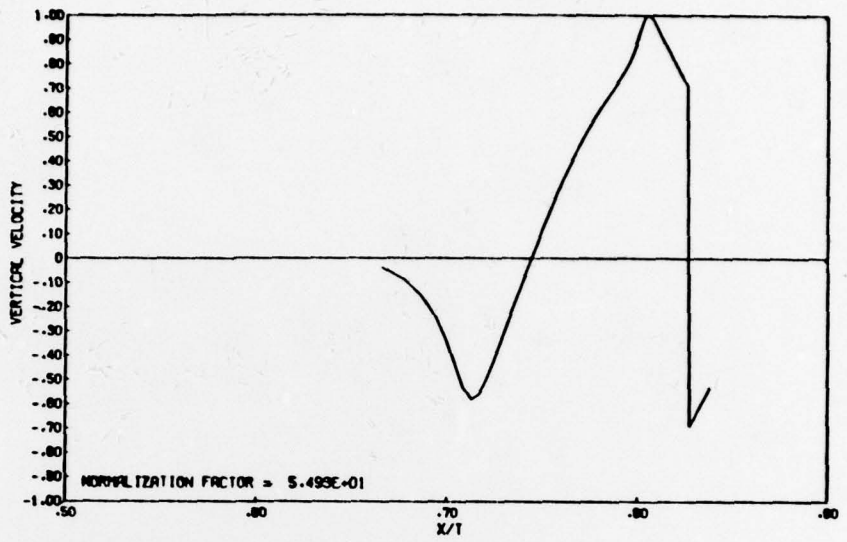

Figure 53. Asymptotic expansion. Initial flat spectrum. Second mode. Profile 1, $\Delta\rho = 0.02$, $z = 0.0$, $t = 10.0$.

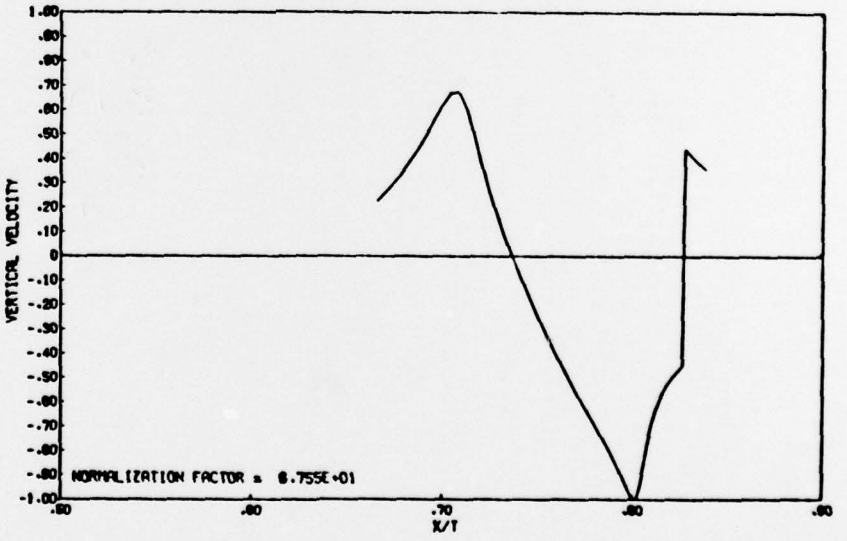

Figure 54. Asymptotic expansion. Initial flat spectrum. Second mode. Profile 1, $\Delta\rho = 0.02$, $z = -0.5$, $t = 10.0$.

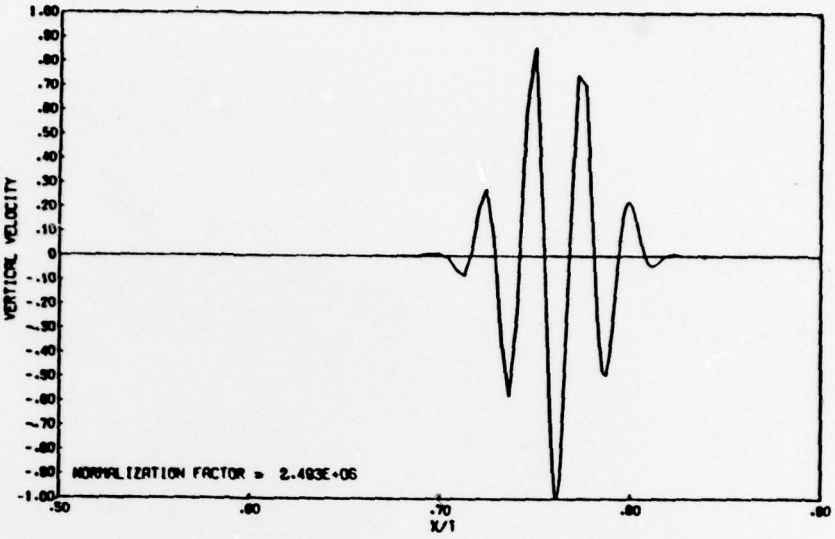

Figure 55. Asymptotic expansion. Initial flat spectrum. Second mode. Profile 1, $\Delta\rho = 0.02$, $z = 0.0$, $t = 100.0$.

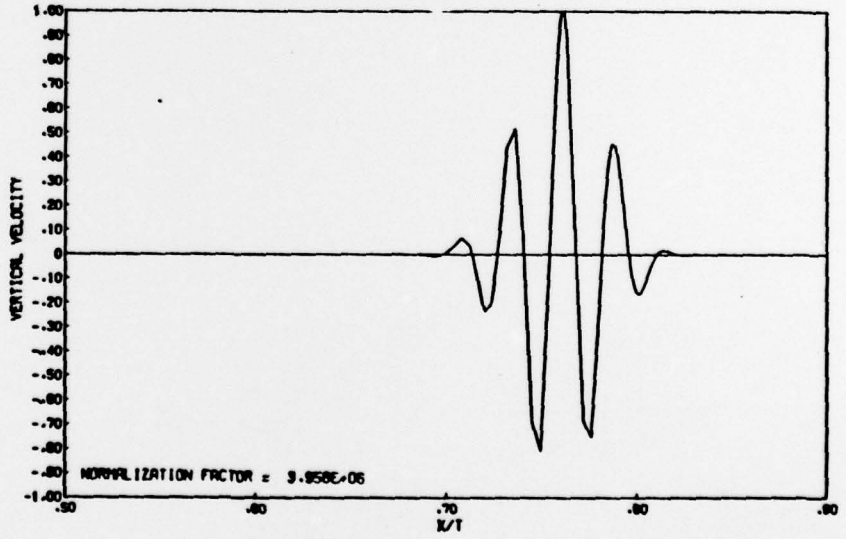

Figure 56. Asymptotic expansion. Initial flat spectrum. Second mode. Profile 1, $\Delta\rho = 0.02$, $z = -0.5$, $t = 100.0$.

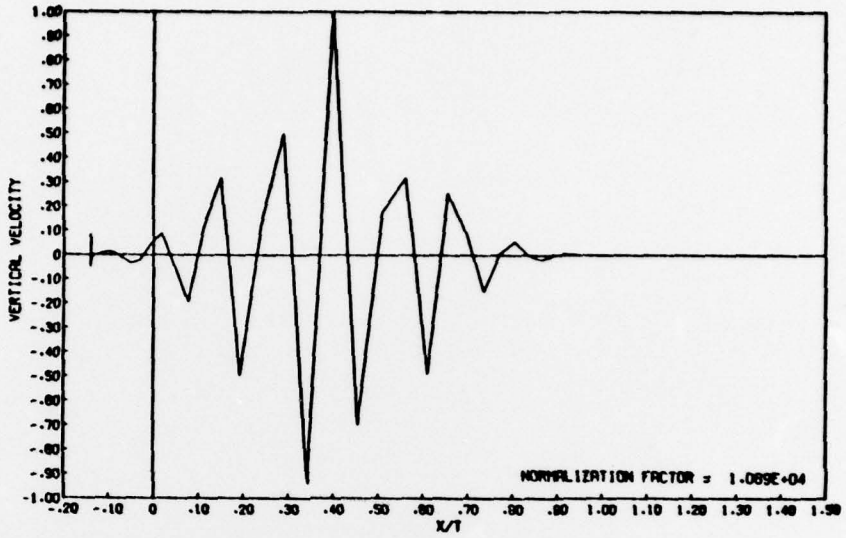

Figure 57. Asymptotic expansion. Initial Gaussian spectrum. Profile 1, $\Delta\rho = 0.02$, $z = 0.0$, $t = 10.0$, $\lambda = 0.1$.

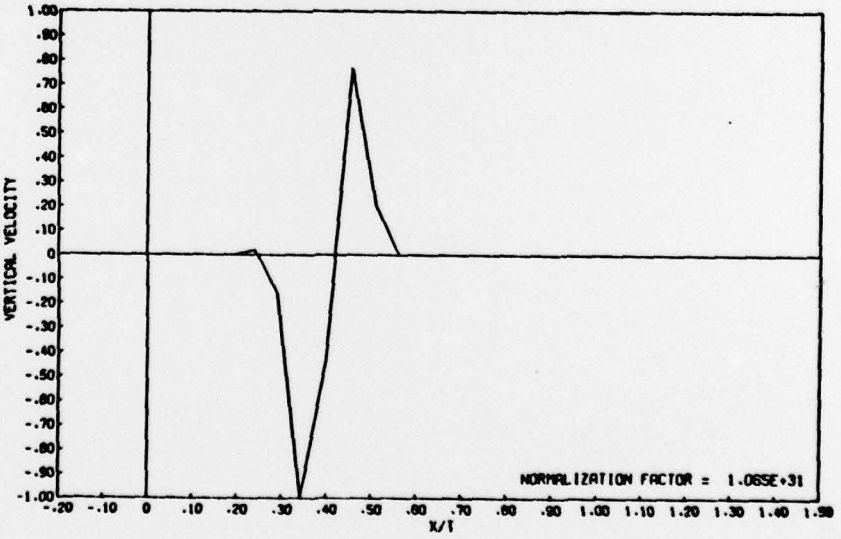

Figure 58. Asymptotic expansion. Initial Gaussian spectrum. Profile 1, $\Delta\rho = 0.02$, $z = 0.0$, $t = 100.0$, $\lambda = 0.1$.

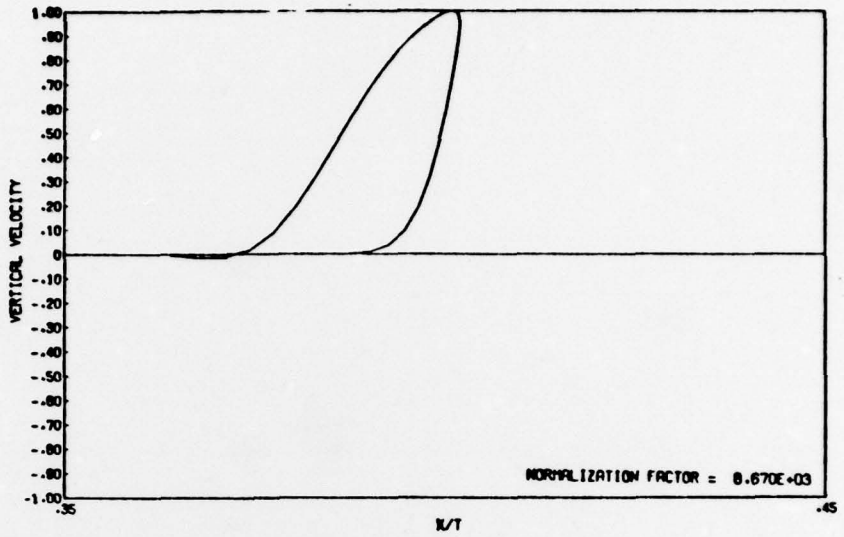

Figure 59. Ray mathematics expansion. Initial flat spectrum. Profile 1, $\Delta\rho = 0.02$, $z = -0.1$, $t = 10.0$.

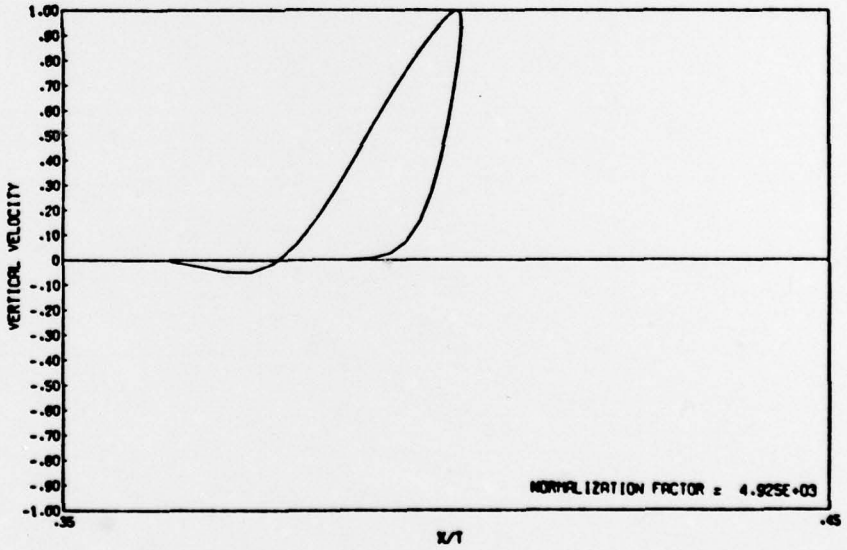

Figure 60. Ray mathematics expansion. Initial flat spectrum. Profile 1, $\Delta\rho = 0.02$, $z = -0.2$, $t = 10.0$.

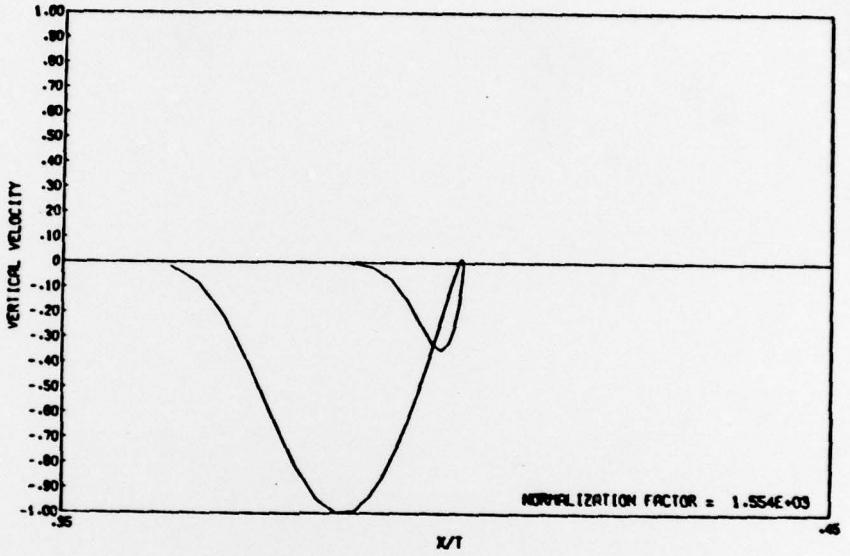

Figure 61. Ray mathematics expansion. Initial flat spectrum. Profile 1, $\Delta\rho = 0.02$, $z = -0.5$, $t = 10.0$.

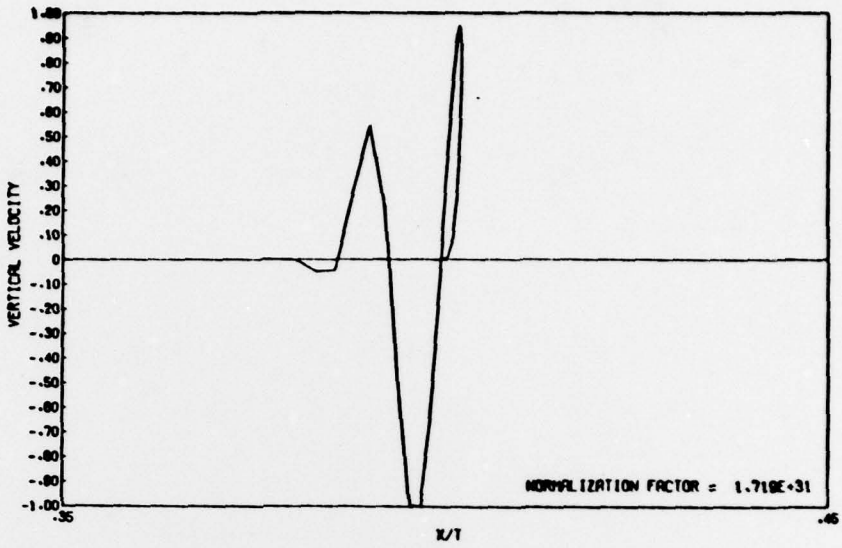

Figure 62. Ray mathematics expansion. Initial flat spectrum. Profile 1, $\Delta\rho = 0.02$, $z = -0.1$, $t = 100.0$.

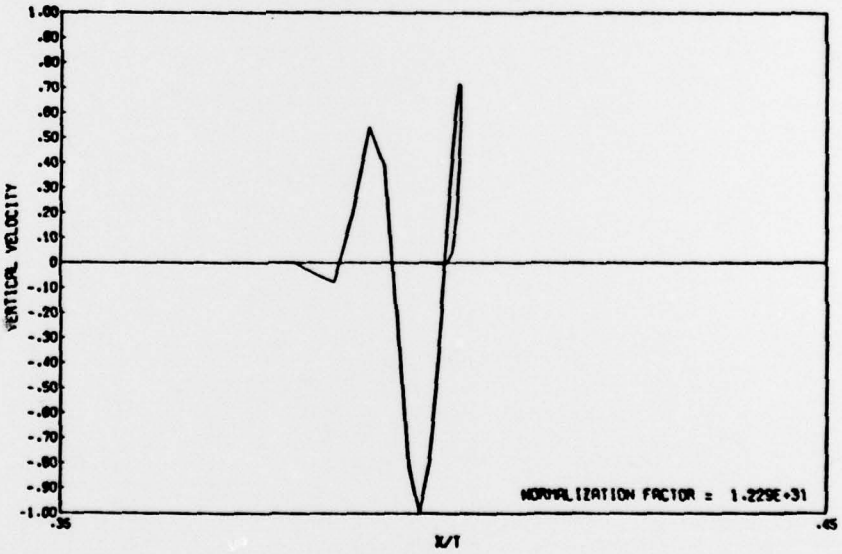

Figure 63. Ray mathematics expansion. Initial flat spectrum. Profile 1, $\Delta\rho = 0.02$, $z = -0.2$, $t = 100.0$.

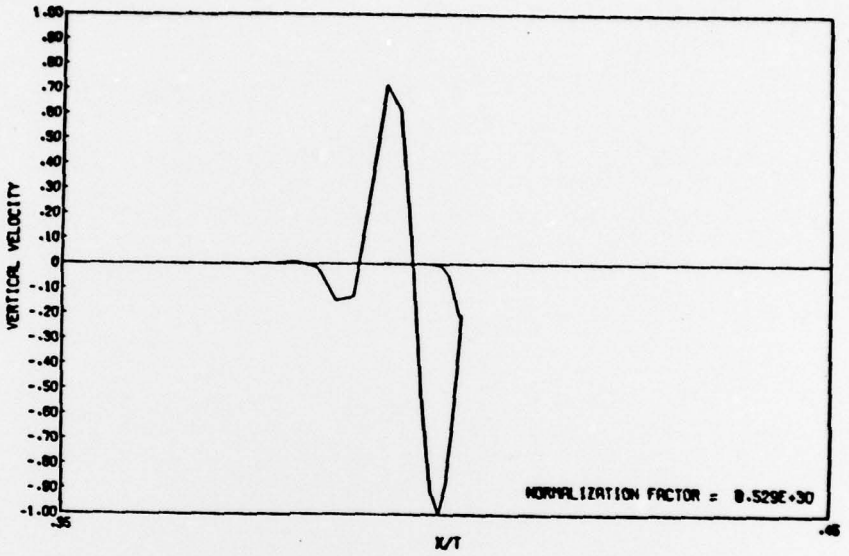

Figure 64. Ray mathematics expansion. Initial flat spectrum. Profile 1, $\Delta\rho = 0.02$, $z = -0.5$, $t = 100.0$.

Table IV. Notation

a, b	coefficients
A, B	coefficients
d	non-dimensional depth parameter
f( )	function
F( )	Fourier transform
F( )	dispersion relation
g	acceleration of gravity
g( )	function
$\underline{G}$	body force potential
G( )	Green's function
h	non-dimensional depth of bottom boundary
h_o	length scale
H	depth of bottom boundary
i	$\sqrt{-1}$
j	integer
J	Richardson number
k	integer
k, ℓ	horizontal wavenumber
L	Laplace transform
L	linear operator
n	integer
N	Brunt-Väisälä frequency
p	kinematic pressure

P_a	atmospheric pressure
q	function
Q( )	function
r	root of indicial equation; variable
s	Laplace transform variable
t	time
u_o	velocity scale
u, v	horizontal perturbation velocity components
U, V	horizontal mean velocity components
w	vertical perturbation velocity
W	function
$\mathbb{W}$	Wronskian
x, y	horizontal coordinates
X	function
z	vertical coordinate
α γ	non-dimensional horizontal wavenumbers
δ( )	Dirac delta function
ε	small parameter
ζ	integration variable
η	surface elevation
θ	non-dimensional density perturbation; angle
Θ	non-dimensional mean density
λ	standard deviation; parameter; function
Λ	function

ρ	density
ρ_o	density scale
σ	frequency
τ	coefficient of surface tension
ϕ	function
ψ	angle between wavefront normal and mean velocity; function
ω	non-dimensional frequency

Symbols:

$( )_o$	initial value; initial condition
$( )_*$	saddle point value; singular point
$( )_a$	particular solution a
$( )_b$	particular solution b
$( )_I$	profile I
$( )_{II}$	profile II
$( )_{III}$	profile III
$( )_j$	variable in j-th layer
$( )_n$	n-th mode
$(\_)$	dimensional variable
$(\_)'$	mean plus perturbation variable
$(\bar{})$	mean value
$( )'$	derivative with respect to z
$( )''$	second derivative with respect to z
$( )^*$	complex conjugate
$(\tilde{})$	Fourier transformed variable; Squire transformed variable

$\hat{(\,)}$ normal mode; Fourier-Laplace transformed variable

VITA

Name: Jerre Eugene Bradt

Born: February 23, 1941
Kimball, Nebraska

Parents: Gerald E. Bradt
Ida H. Bradt

Secondary Education: Kimball County High School
Kimball, Nebraska

College Education: Nebraska Wesleyan University
Lincoln, Nebraska

University of Nebraska
Lincoln, Nebraska
B.S. Physics 1963

University of Illinois
Champaign, Illinois
M.S. Physics 1965

University of Washington
Seattle, Washington
Ph.D. Oceanography 1979